# Exploring the universe in radio waves

Dom Pesce

BLACK HOLE INITIATIVE

***July 20, 2025***

***N3AS at UC Santa Cruz***

CENTER FOR ASTROPHYSICS
HARVARD & SMITHSONIAN

# Outline for today: radio highlights and looking ahead

A necessarily abbreviated list of radio highlights

Masers and cosmology

- NGC 4258
- the Megamaser Cosmology Project (MCP)

Near-horizon studies of supermassive black holes

- the Event Horizon Telescope (EHT)
- imaging the supermassive black hole in M87

Looking ahead

- next-generation radio facilities

# Some highlights of radio astronomy

1933 – Karl Jansky discovers extraterrestrial radio emission
1940 – Grote Reber builds first parabolic radio dish and confirms Jansky's discovery
1944 – Hendrik van de Hulst predicts the existence of the 21cm spin-flip transition of Hydrogen
1946 – Martin Ryle develops the first radio interferometer (Ryle & Vonberg 1946)
1951 – Edward Purcell and Doc Ewen observe the 21cm line (Ewan & Purcell 1951)
1965 – Bob Wilson and Arno Penzias discover the CMB radiation (Penzias & Wilson 1965)
1967 – Multiple groups (NRAO, DRAO, MIT) demonstrate VLBI for the first time
1968 – Irwin Shapiro and collaborators use radar to measure the "Shapiro effect" (Shapiro et al. 1968)
1968 – Anthony Hewish and Jocelyn Bell discover pulsars (Hewish et al. 1968)
1970 – Bob Wilson and collaborators detect astrophysical CO (Wilson et al. 1970)
1975 – Russell Hulse and Joe Taylor discover the first binary pulsar (Hulse & Taylor 1975)
1980 – The VLA is completed in New Mexico
1990 – The COBE/FIRAS team demonstrates that the CMB is a blackbody (Mather et al. 1990)
1992 – Aleksander Wolszczan and Dale Frail discover the first exoplanets (Wolszczan & Frail 1992)
1999 – Jim Herrnstein and collaborators measure the distance to NGC 4258 (Herrnstein et al. 1999)
2007 – Dunc Lorimer and collaborators discover the first FRB (Lorimer et al. 2007)
2011 – ALMA is completed in Chile
2019 – The Event Horizon Telescope resolves the "shadow" of a black hole (EHTC et al. 2019)
2023 – Multiple international groups report the first PTA detection of a gravitational-wave background

# Some highlights of radio astronomy

1933 – Karl Jansky discovers extraterrestrial radio emission
1940 – Grote Reber builds first parabolic radio dish and confirms Jansky's discovery
1944 – Hendrik van de Hulst predicts the existence of the 21cm spin-flip transition of Hydrogen
1946 – Martin Ryle develops the first radio interferometer (Ryle & Vonberg 1946)
1951 – Edward Purcell and Doc Ewen observe the 21cm line (Ewan & Purcell 1951)
1965 – Bob Wilson and Arno Penzias discover the CMB radiation (Penzias & Wilson 1965)
1967 – Multiple groups (NRAO, DRAO, MIT) demonstrate VLBI for the first time
1968 – Irwin Shapiro and collaborators use radar to measure the "Shapiro effect" (Shapiro et al. 1968)
1968 – Anthony Hewish and Jocelyn Bell discover pulsars (Hewish et al. 1968)
1970 – Bob Wilson and collaborators detect astrophysical CO (Wilson et al. 1970)
1975 – Russell Hulse and Joe Taylor discover the first binary pulsar (Hulse & Taylor 1975)
1980 – The VLA is completed in New Mexico
1990 – The COBE/FIRAS team demonstrates that the CMB is a blackbody (Mather et al. 1990)
1992 – Aleksander Wolszczan and Dale Frail discover the first exoplanets (Wolszczan & Frail 1992)
**1999 – Jim Herrnstein and collaborators measure the distance to NGC 4258 (Herrnstein et al. 1999)**
2007 – Dunc Lorimer and collaborators discover the first FRB (Lorimer et al. 2007)
2011 – ALMA is completed in Chile
**2019 – The Event Horizon Telescope resolves the "shadow" of a black hole (EHTC et al. 2019)**
2023 – Multiple international groups report the first PTA detection of a gravitational-wave background

# Megamaser Cosmology

# Masers in space?

The warm ($T \approx 1000$ K), dense ($n \approx 10^9$ cm$^{-3}$) gas in various astrophysical environments can contain water molecules

One rotational transition of the water molecule, with a rest frequency of ~22 GHz (wavelength of ~1.3 cm), can sustain maser emission under these physical conditions

The brightest of these masers are dubbed "megamasers" because of their large luminosities:

- Galactic (stellar) masers: $L \lesssim 10^{-4}\ L_\odot$
- extragalactic (AGN) megamasers: $L \gtrsim 10^{2}\ L_\odot$

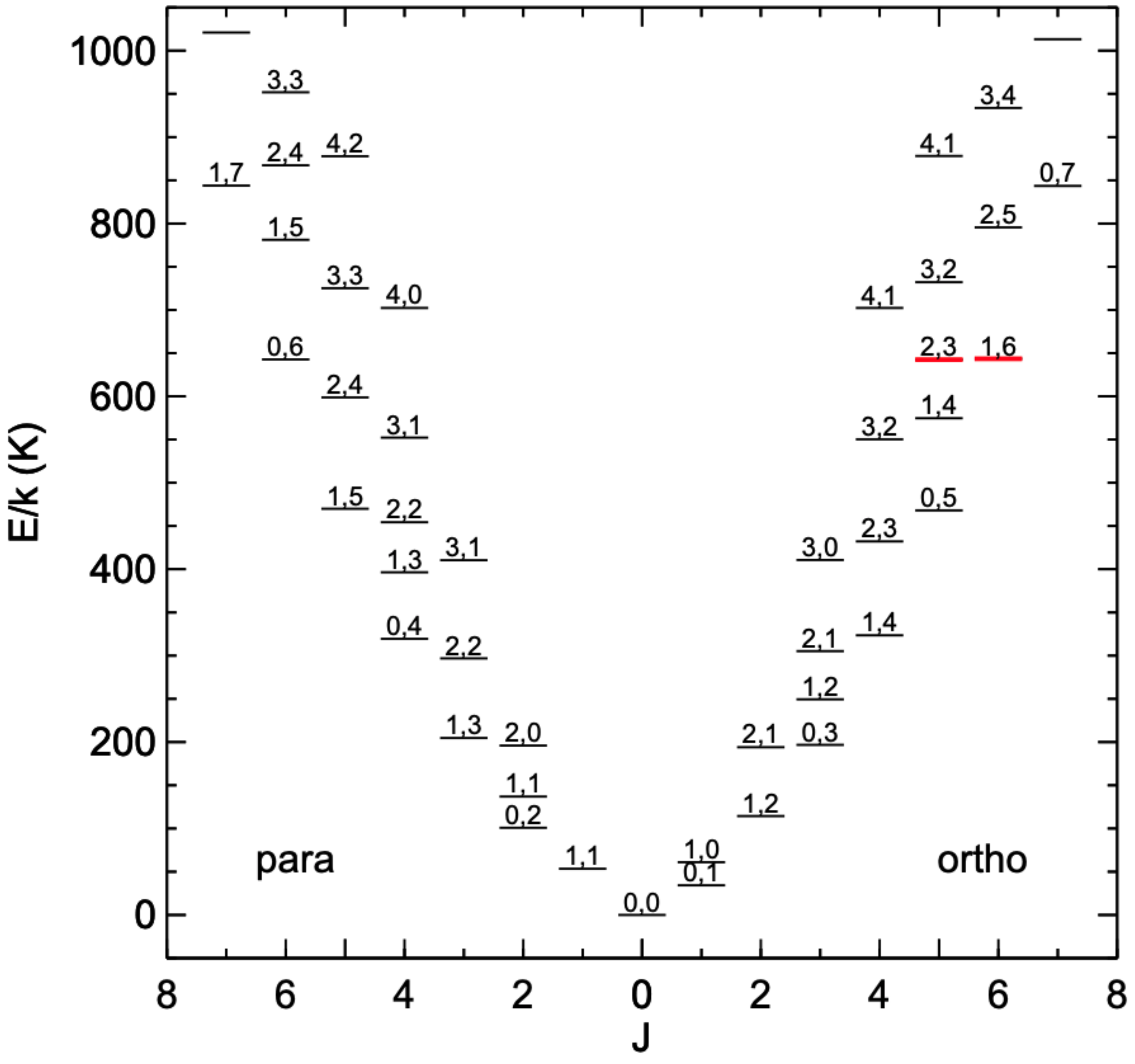

# Some history: the maser system in NGC 4258

The maser system in the galaxy NGC 4258 was first discovered by [Claussen, Heiligman, & Lo (1984)]

They observed the galaxy using the OVRO 40m dish
- beam size is ~100 arcseconds at 22 GHz (~3.7 kpc)
- the emission was attributed to a nuclear starburst

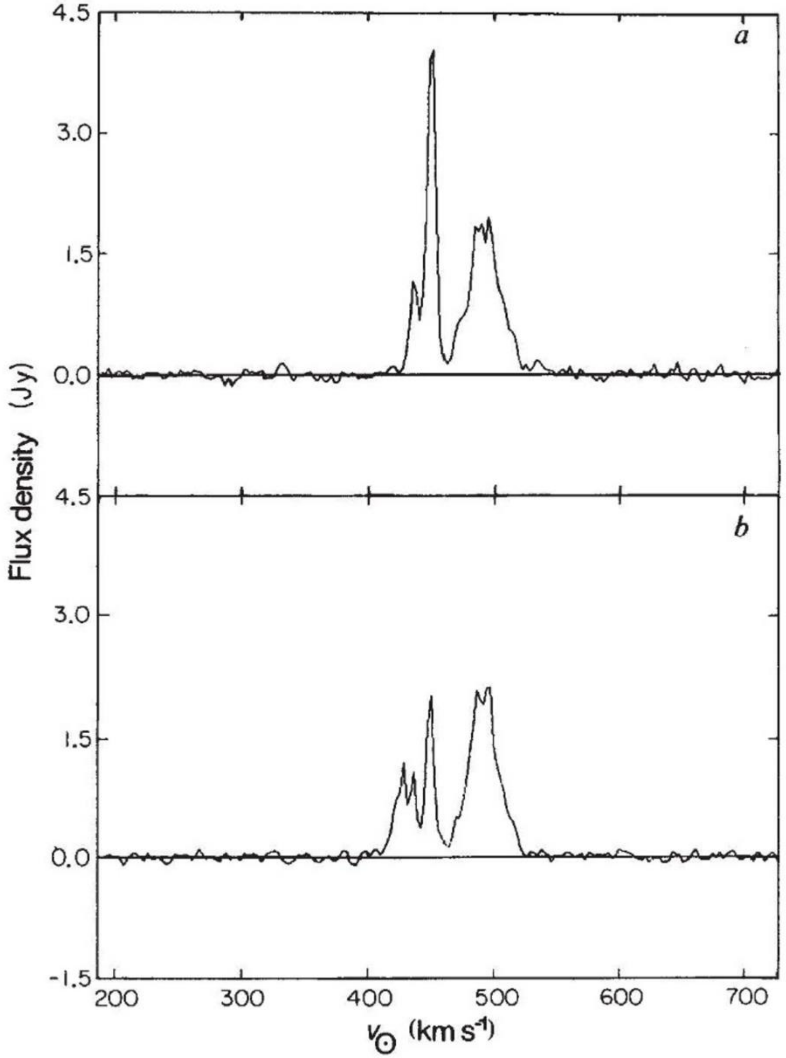


Claussen, Heiligman, & Lo (1984)

# Some history: the maser system in NGC 4258

The maser system in the galaxy NGC 4258 was first discovered by Claussen, Heiligman, & Lo (1984)

They observed the galaxy using the OVRO 40m dish

- beam size is ~100 arcseconds at 22 GHz (~3.7 kpc)
- the emission was attributed to a nuclear starburst

Followup observations with the VLA (Claussen & Lo 1986) confined the emission to a region ~1.3 pc across

VLBI observations by Claussen et al. (1988) solidified the circumnuclear association, showing that individual maser features are separated by only ~0.1-1 mas (~0.004-0.04 pc)

*"The maser emission in these nuclei is distributed in regions of circumstellar rather than interstellar sizes."*

– Claussen et al. (1988)

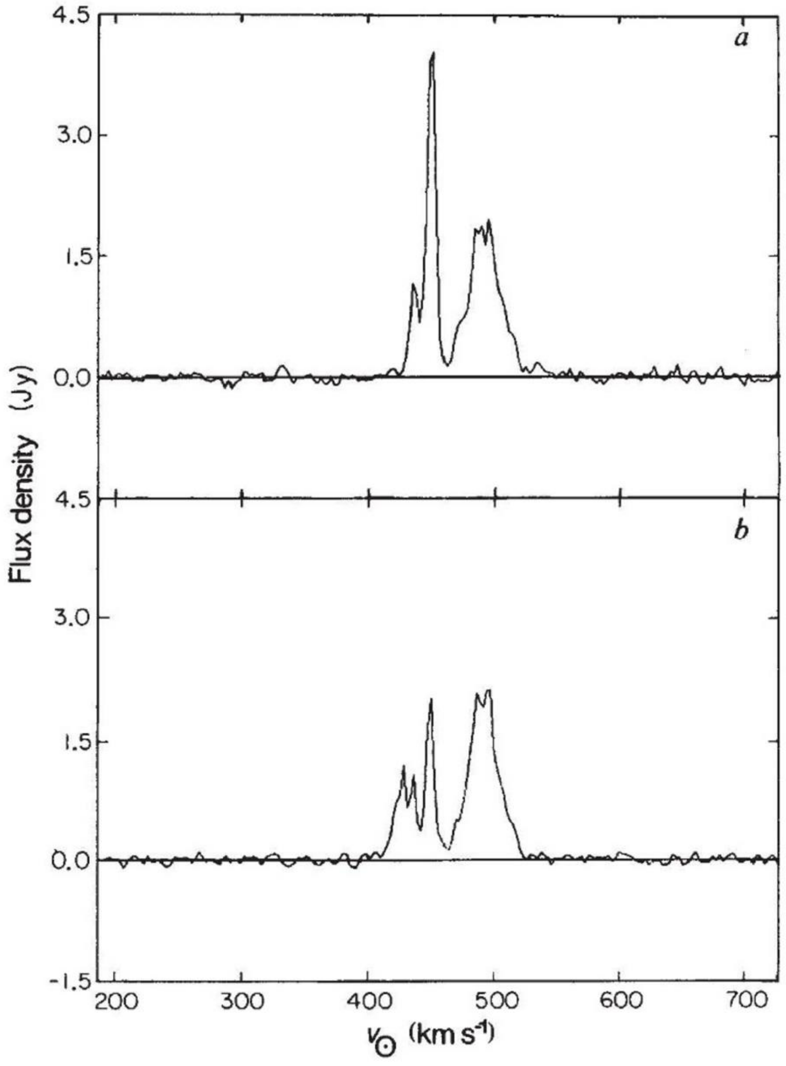


Claussen, Heiligman, & Lo (1984)

# Some history: the maser system in NGC 4258

A major breakthrough was enabled by a new wide-band spectrometer on the Nobeyama 45m dish

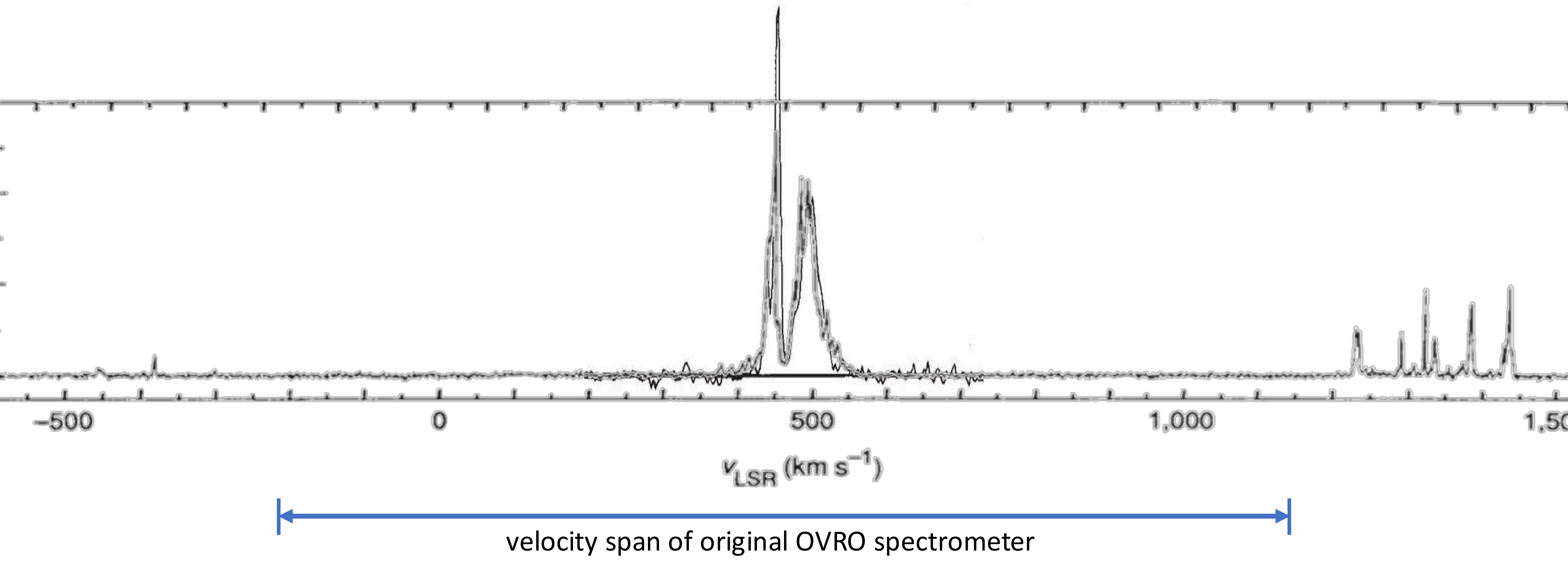


Nakai, Inoue, & Miyoshi (1993)

# Some history: the maser system in NGC 4258

A major breakthrough was enabled by a new wide-band spectrometer on the Nobeyama 45m dish

- VLBI with the Kashima 34m located the redshifted features to be within ~50 mas of the systemics
- blueshifted features also detected in the spectrum (though too weak to pick up with VLBI)

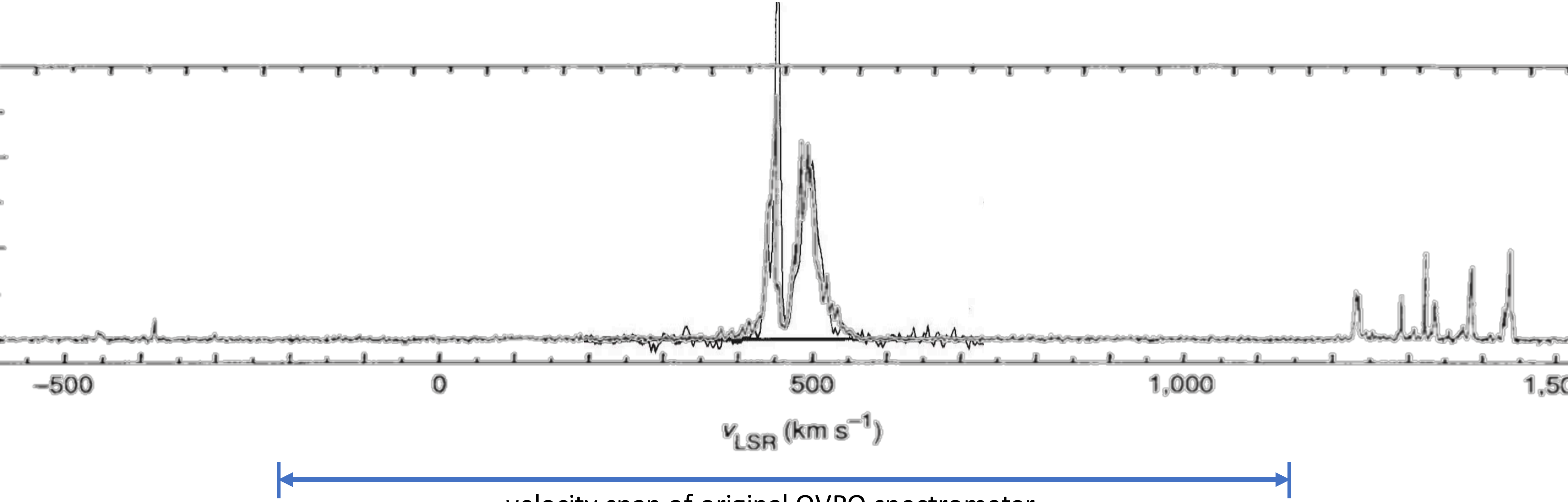


velocity span of original OVRO spectrometer

Nakai, Inoue, & Miyoshi (1993)

# Some history: the maser system in NGC 4258

Then, a flurry of activity:

- Makishima et al. (1994) observed NGC 4258 with ASCA (X-rays)
    - confirmed that it hosts a LLAGN

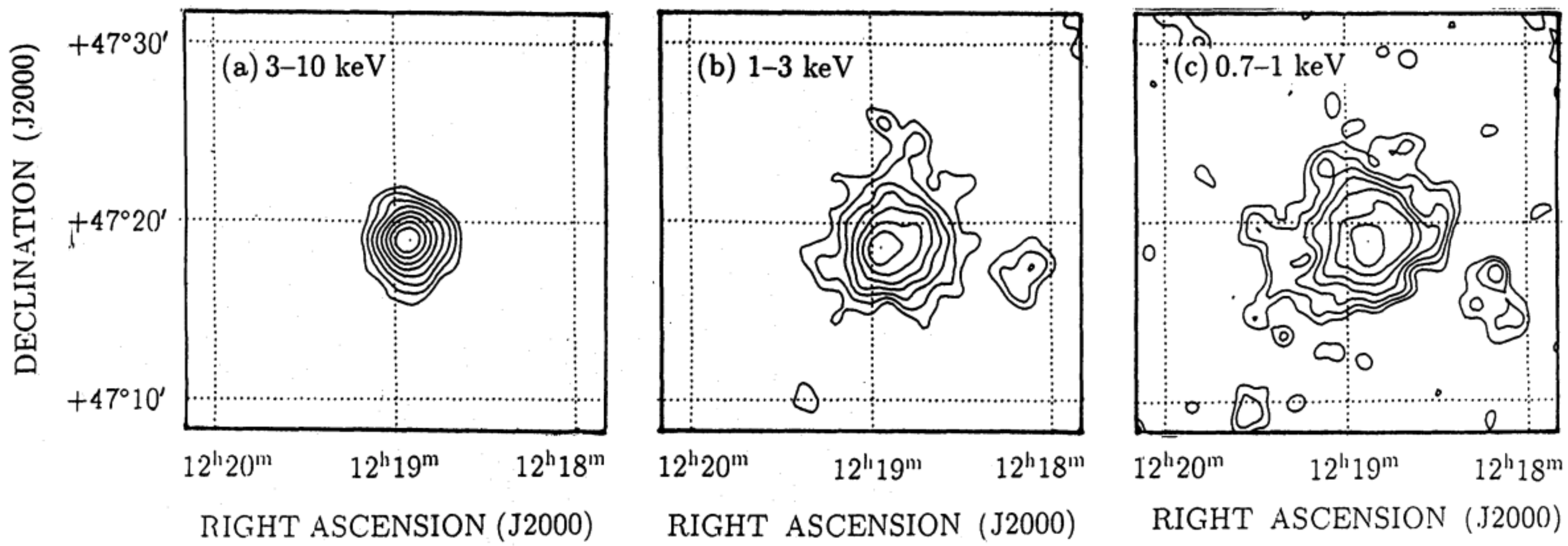


Makishima et al (1994)

# Some history: the maser system in NGC 4258

Then, a flurry of activity:

- Makishima et al. (1994) observed NGC 4258 with ASCA (X-rays)
    - confirmed that it hosts a LLAGN
- Haschick, Baan, & Peng (1994) presented 7 years of monitoring data on the systemic features using the Haystack 37m dish
    - measurement of a ~7.5 km/s/yr acceleration

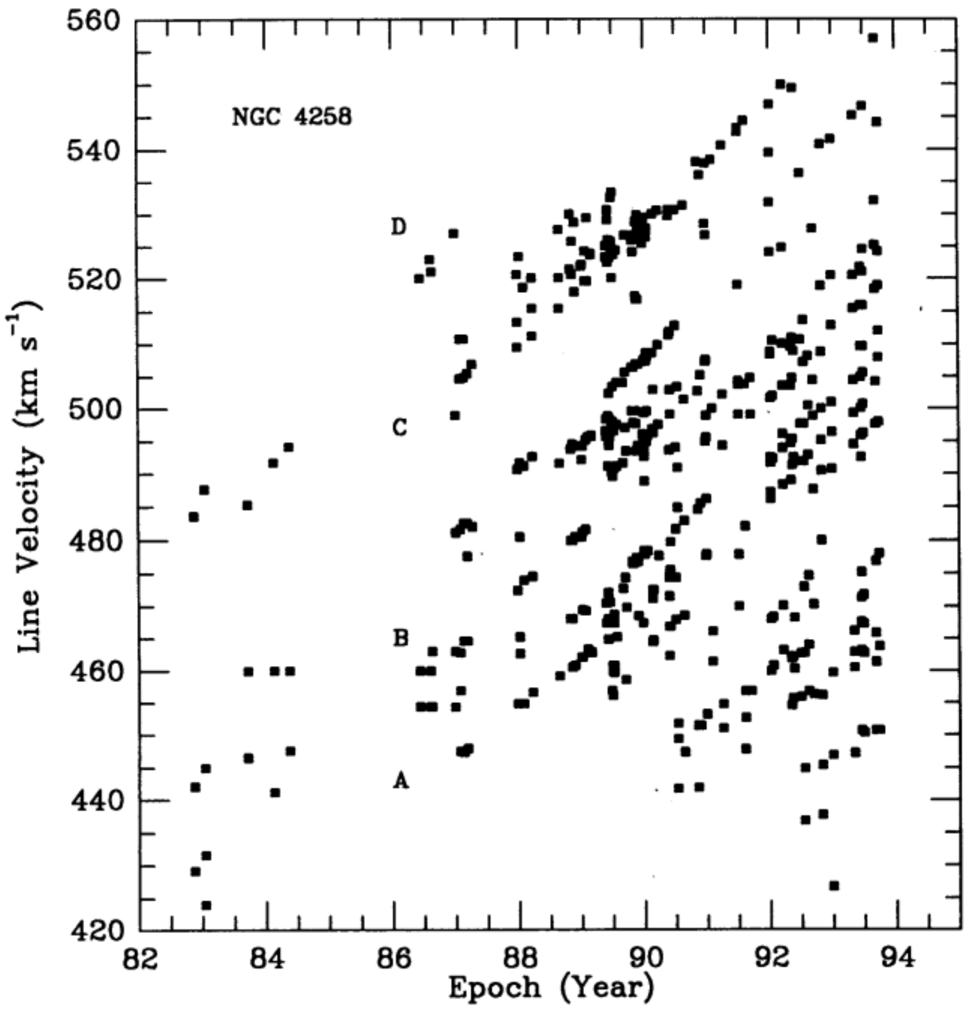


Haschick, Baan, & Peng (1994)

# Some history: the maser system in NGC 4258

Then, a flurry of activity:

- Makishima et al. (1994) observed NGC 4258 with ASCA (X-rays)
  - confirmed that it hosts a LLAGN
- Haschick, Baan, & Peng (1994) presented 7 years of monitoring data on the systemic features using the Haystack 37m dish
  - measurement of a ~7.5 km/s/yr acceleration
- Additional monitoring of the high-velocity features with the Effelsberg telescope between 1993-1994 (presented in Greenhill et al 1995b) did not identify any accelerations

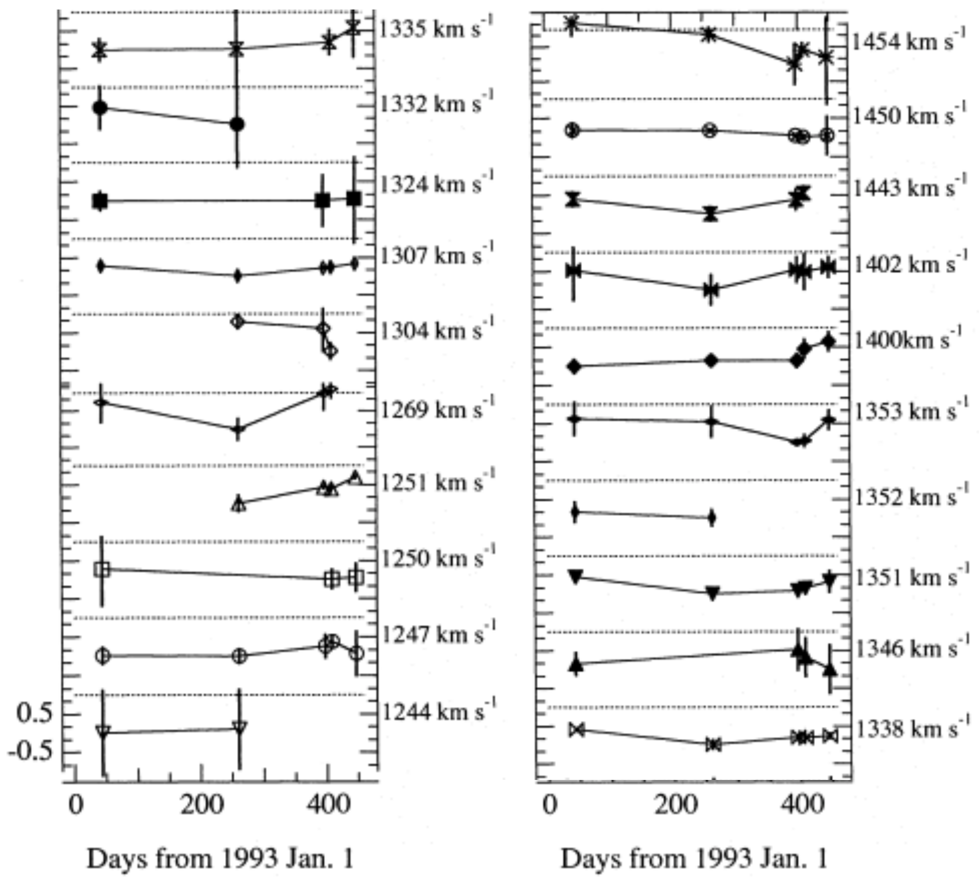


Greenhill et al. (1995b)

# Some history: the maser system in NGC 4258

Then, a flurry of activity:

- Makishima et al. (1994) observed NGC 4258 with ASCA (X-rays)
    - confirmed that it hosts a LLAGN
- Haschick, Baan, & Peng (1994) presented 7 years of monitoring data on the systemic features using the Haystack 37m dish
    - measurement of a ~7.5 km/s/yr acceleration
- Additional monitoring of the high-velocity features with the Effelsberg telescope between 1993-1994 (presented in Greenhill et al 1995b) did not identify any accelerations
- Watson & Wallin (1994) fit the many pieces together into a single cohesive picture of rotating, masing disk

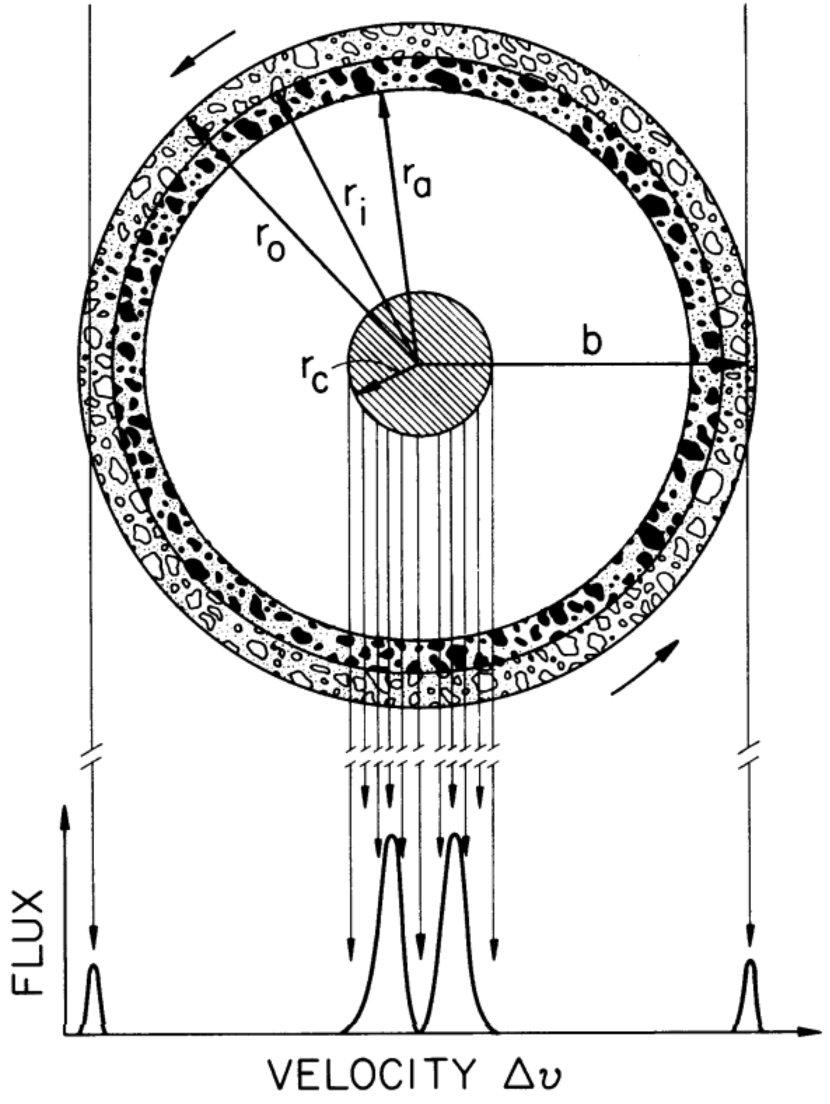


Watson & Wallin (1994)

# Some history: the maser system in NGC 4258

Then, a flurry of activity:

- Makishima et al. (1994) observed NGC 4258 with ASCA (X-rays)
  - confirmed that it hosts a LLAGN
- Haschick, Baan, & Peng (1994) presented 7 years of monitoring data on the systemic features using the Haystack 37m dish
  - measurement of a ~7.5 km/s/yr acceleration
- Additional monitoring of the high-velocity features with the Effelsberg telescope between 1993-1994 (presented in Greenhill et al 1995b) did not identify any accelerations
- Watson & Wallin (1994) fit the many pieces together into a single cohesive picture of rotating, masing disk

*"It is natural to suspect that other extragalactic water masers occur in circumnuclear disks and that those in NGC 4258 differ mostly in the clarity with which this is revealed."*

– Watson & Wallin (1994)

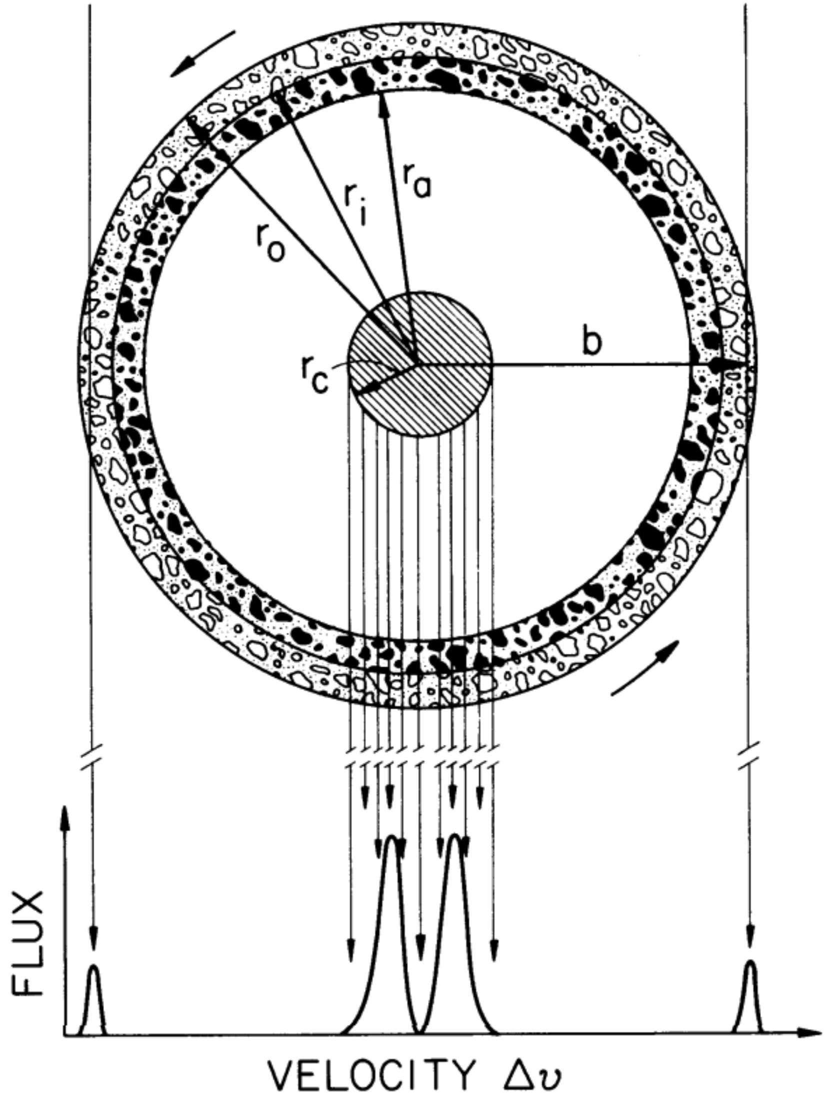


Watson & Wallin (1994)

# NGC 4258 history: initial VLBI results

Initial VLBI results:

- Greenhill et al (1994) presented the first VLBI map of the systemic features (see also Greenhill et al 1995a); same VLBI observations as in Claussen et al. (1988)

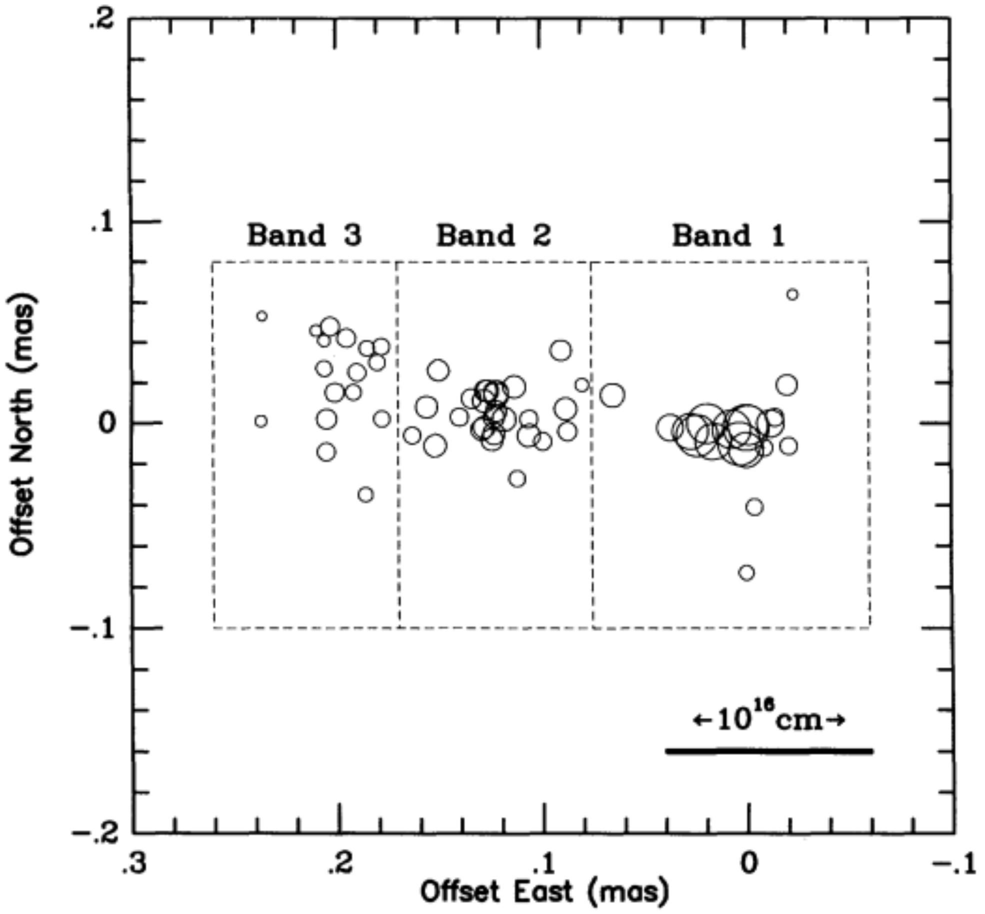


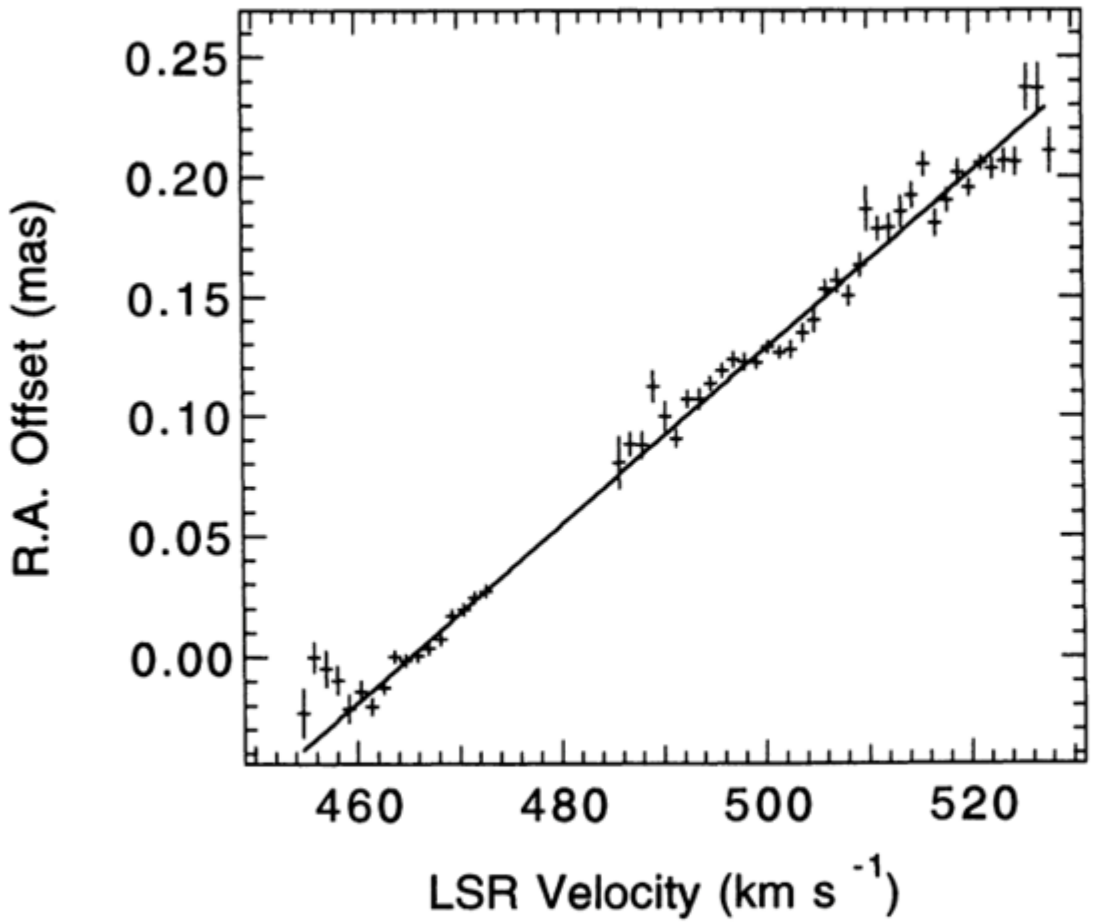


Greenhill et al (1995a)

# NGC 4258 history: initial VLBI results

Initial VLBI results:

- Greenhill et al (1994) presented the first VLBI map of the systemic features (see also Greenhill et al 1995a); same VLBI observations as in Claussen et al. (1988)
- Miyoshi et al (1995) presented the first VLBI map of the full system

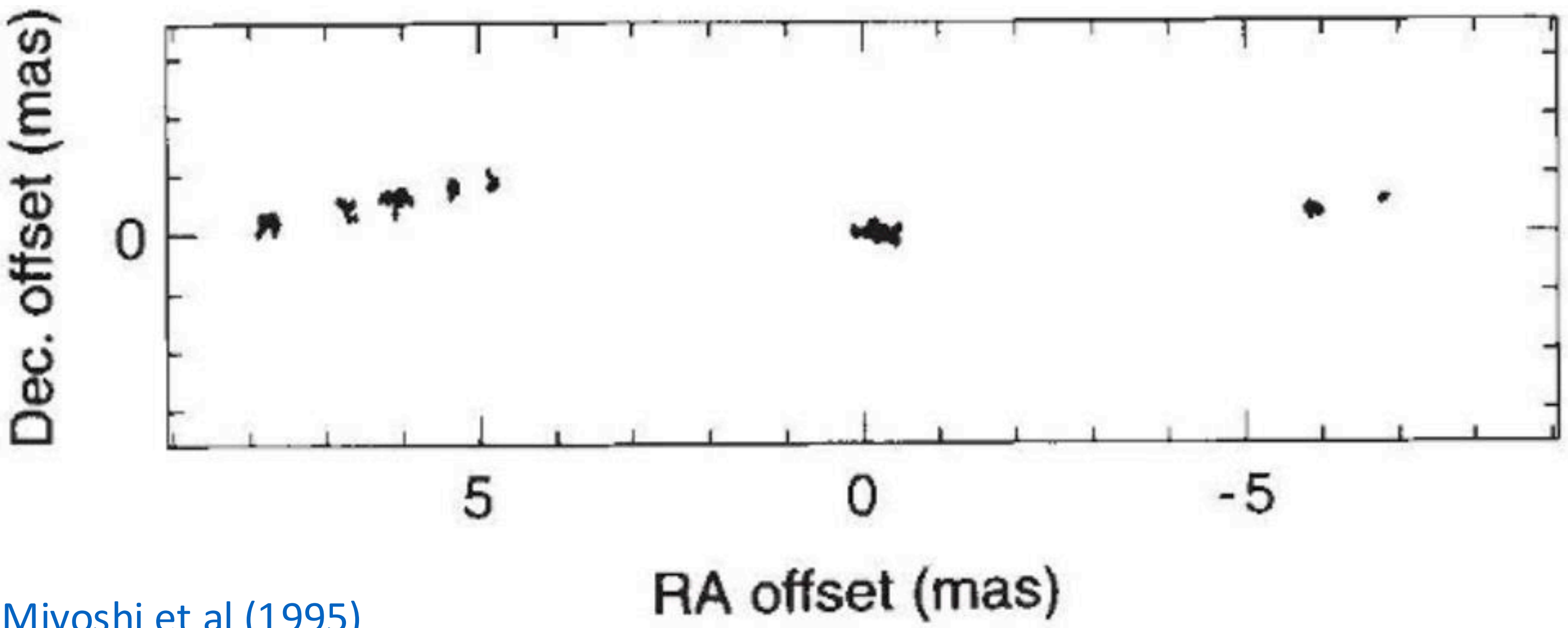


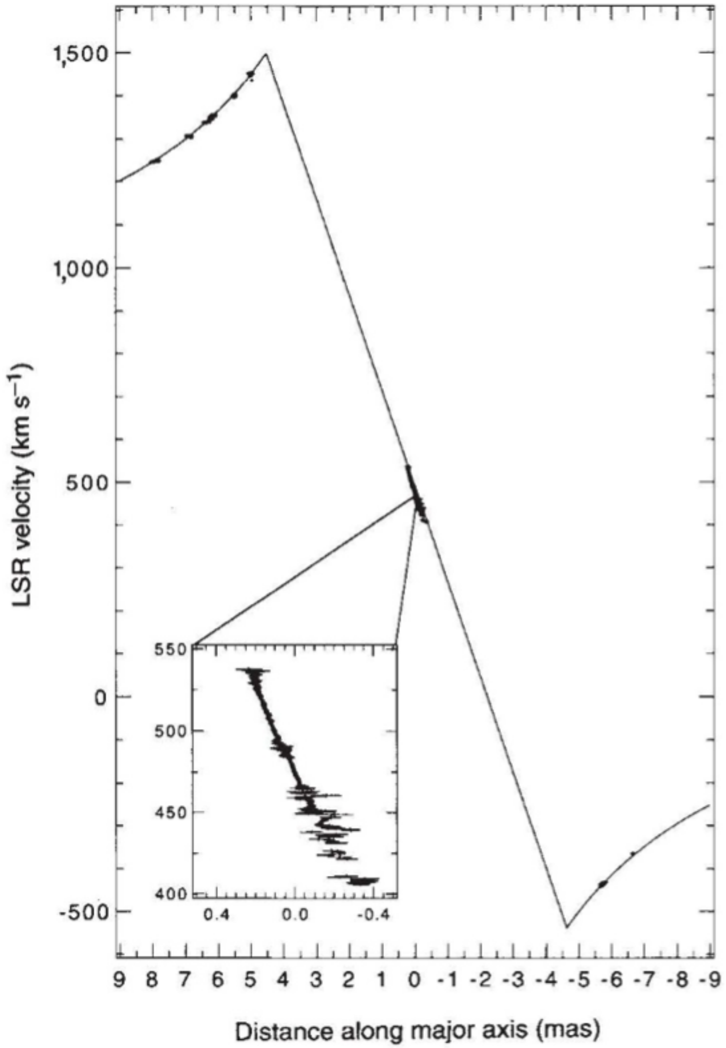


Miyoshi et al (1995)

# NGC 4258 history: initial VLBI results

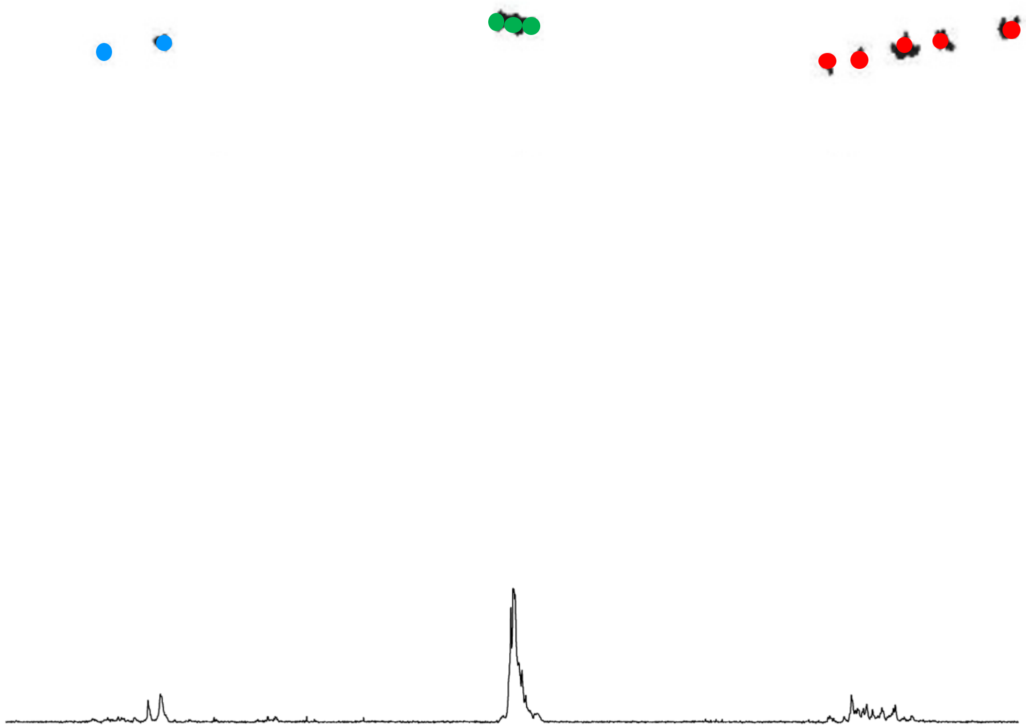

# NGC 4258 history: initial VLBI results

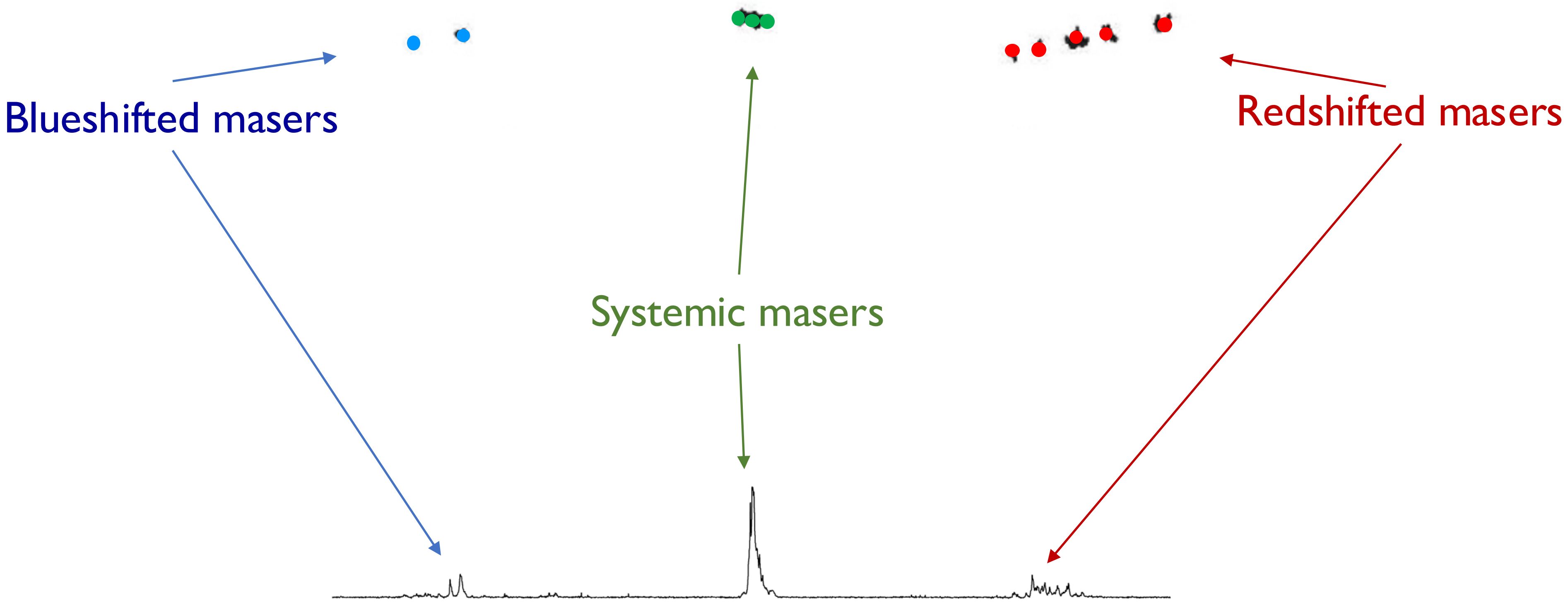

# NGC 4258 history: initial VLBI results

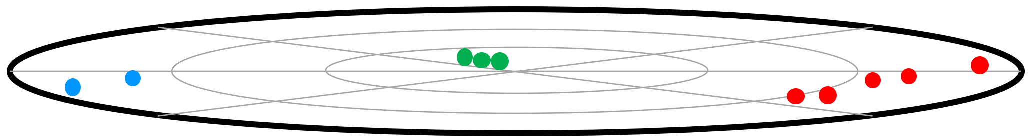

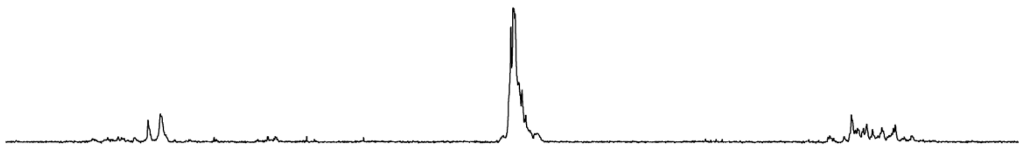

# NGC 4258 history: initial VLBI results

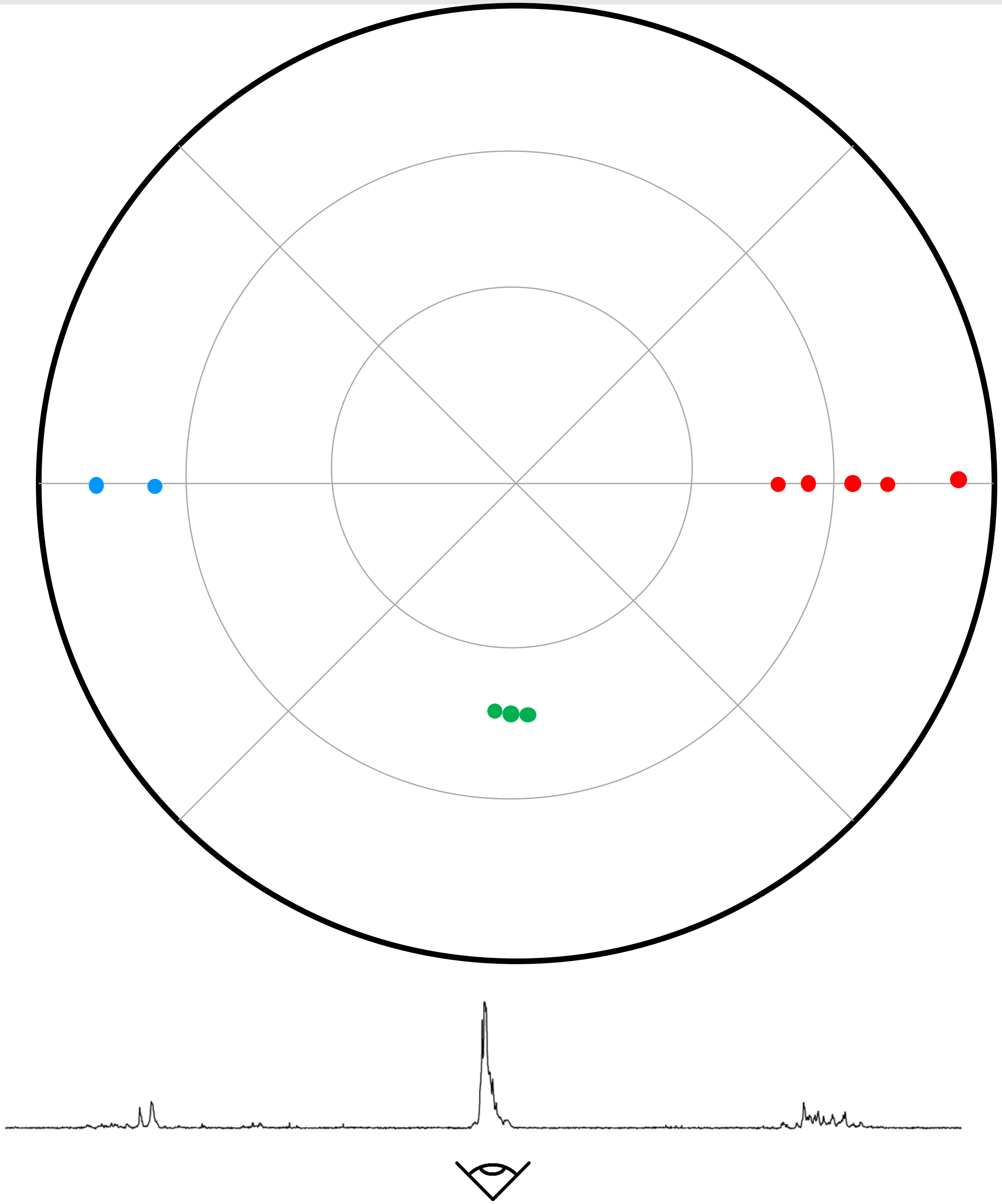

# NGC 4258 history: initial VLBI results

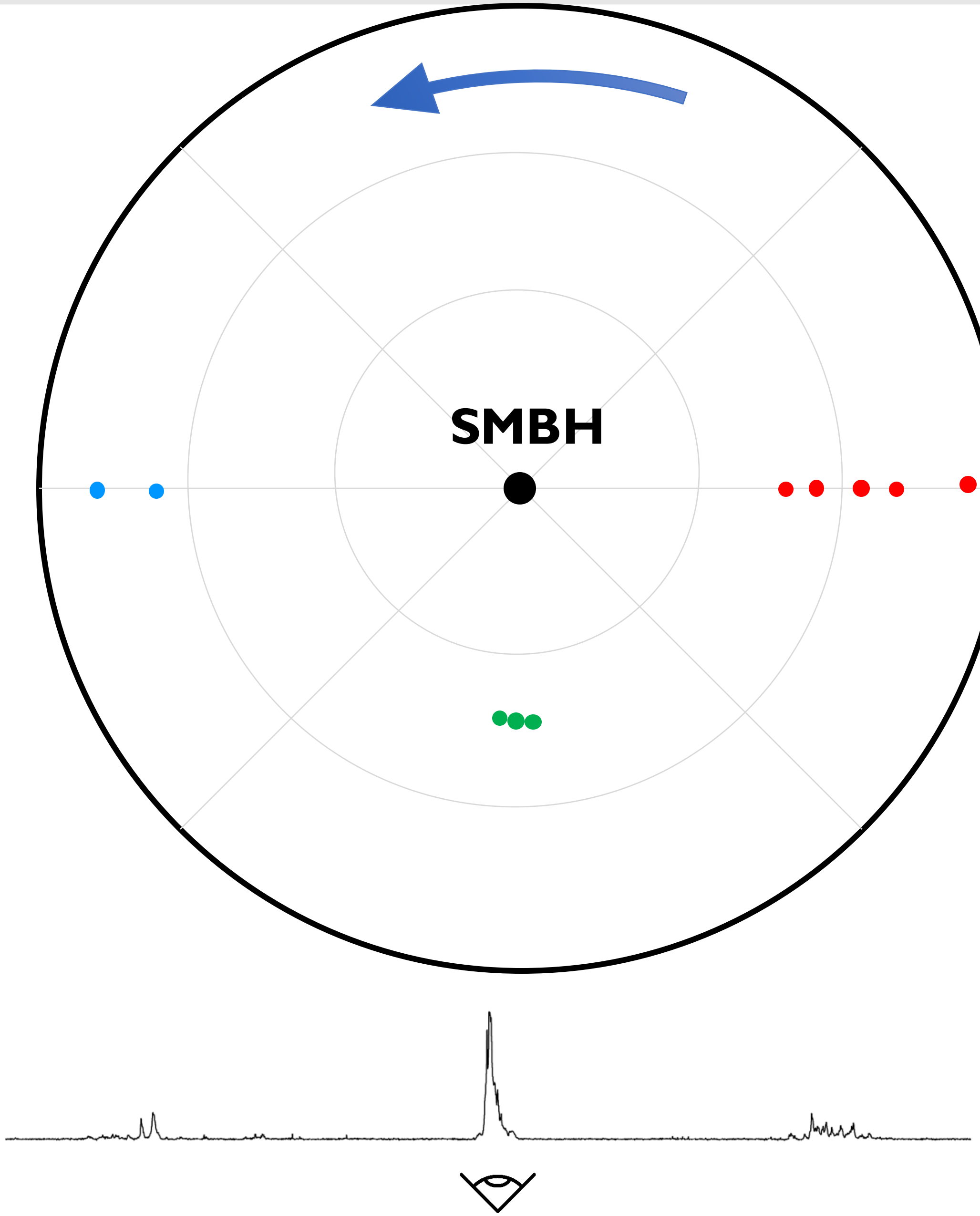

# NGC 4258 history: initial VLBI results

velocity
vectors

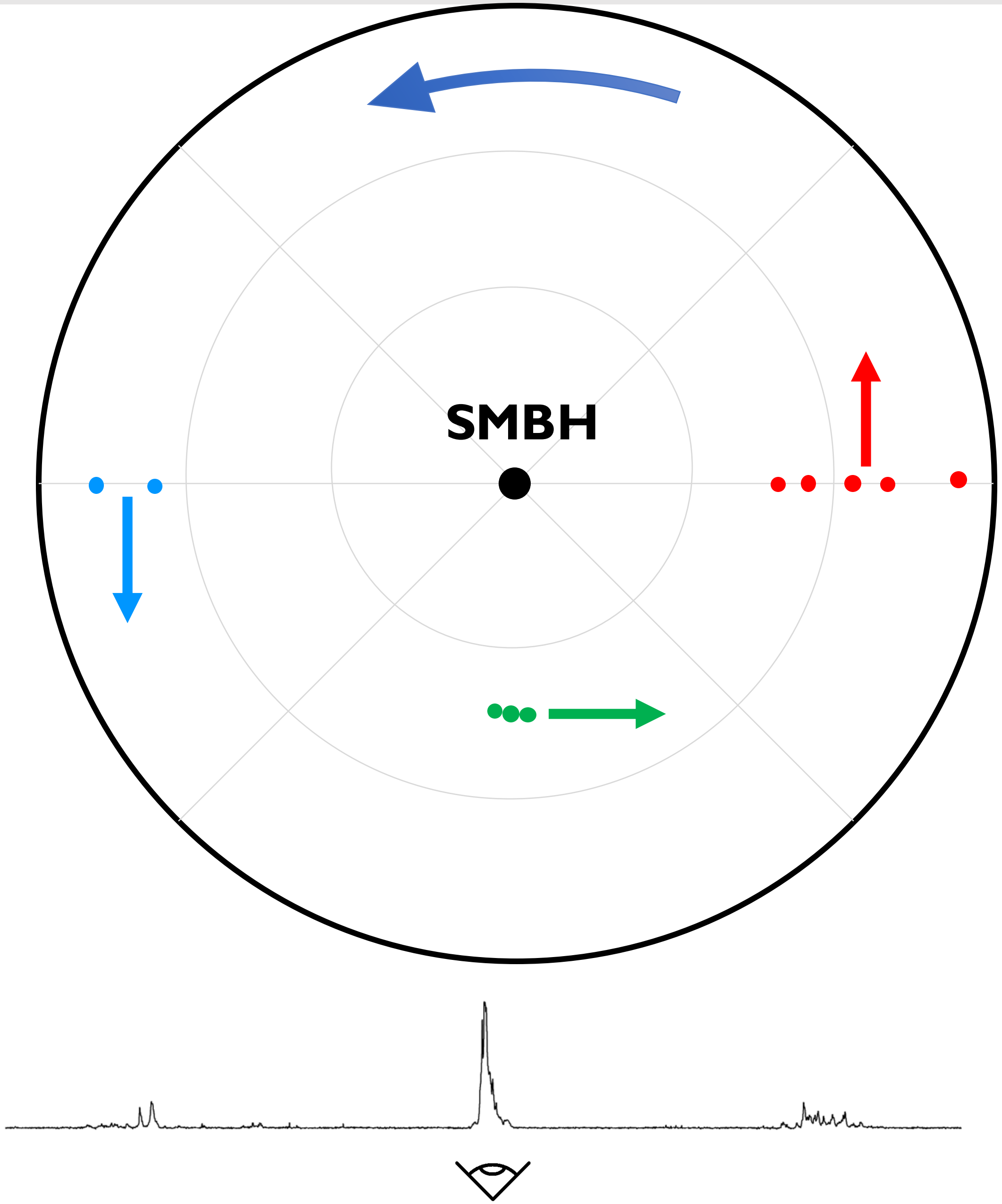

# NGC 4258 history: initial VLBI results

acceleration vectors

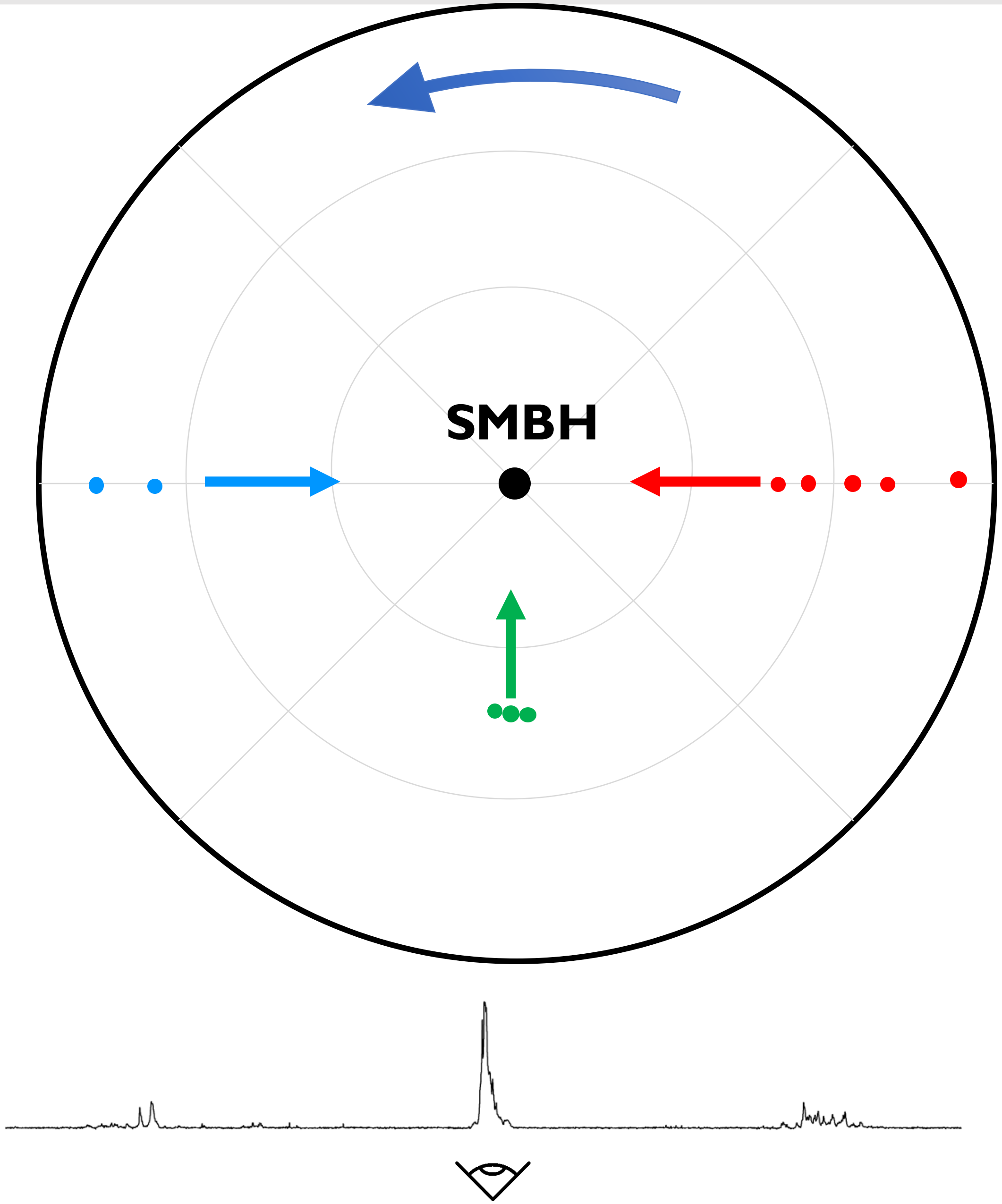

# Disk model

Consider a masing cloud on a circular orbit at radius r around a central SMBH of mass M and situated at an azimuthal angle ϕ with respect to the line of sight

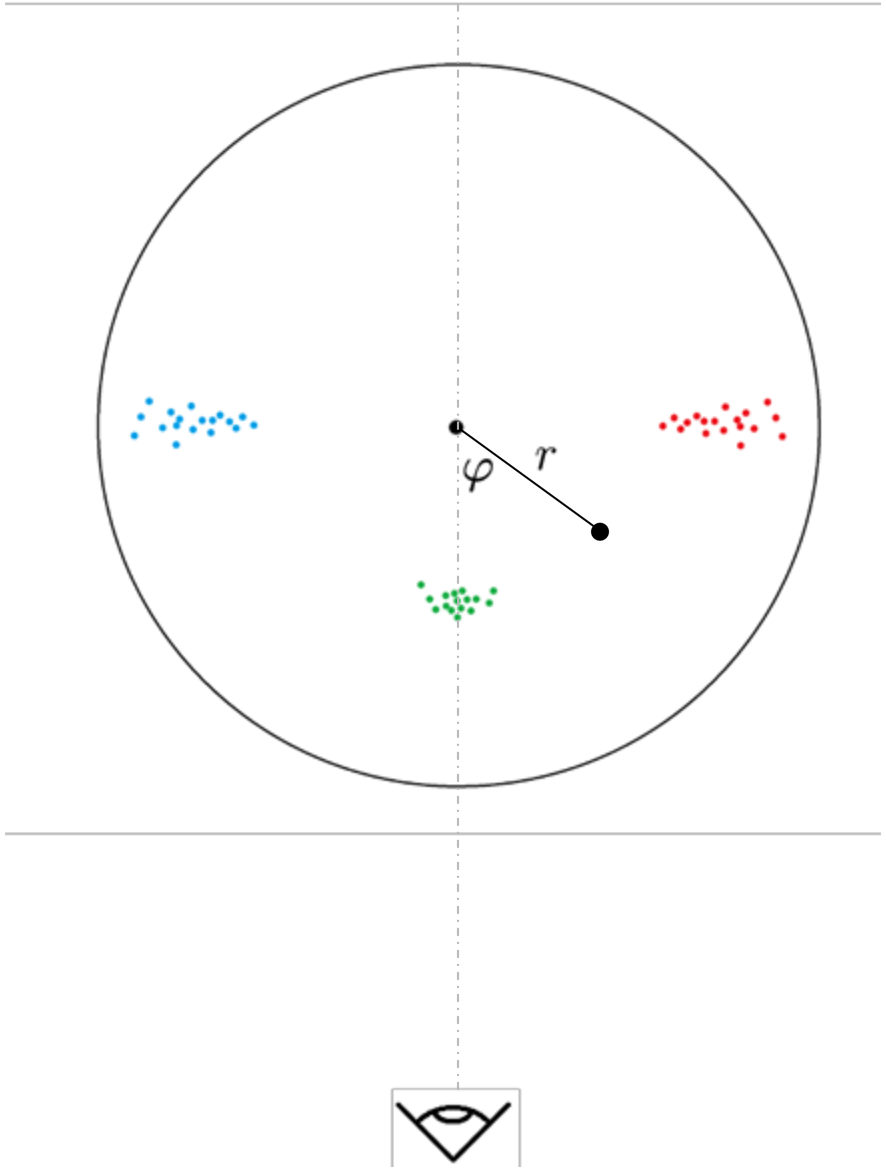

# Disk model

Consider a masing cloud on a circular orbit at radius r around a central SMBH of mass M and situated at an azimuthal angle ϕ with respect to the line of sight

Observed (on-sky) position: $\theta = \frac{r}{D}\sin(\varphi)$ ~0.1 mas

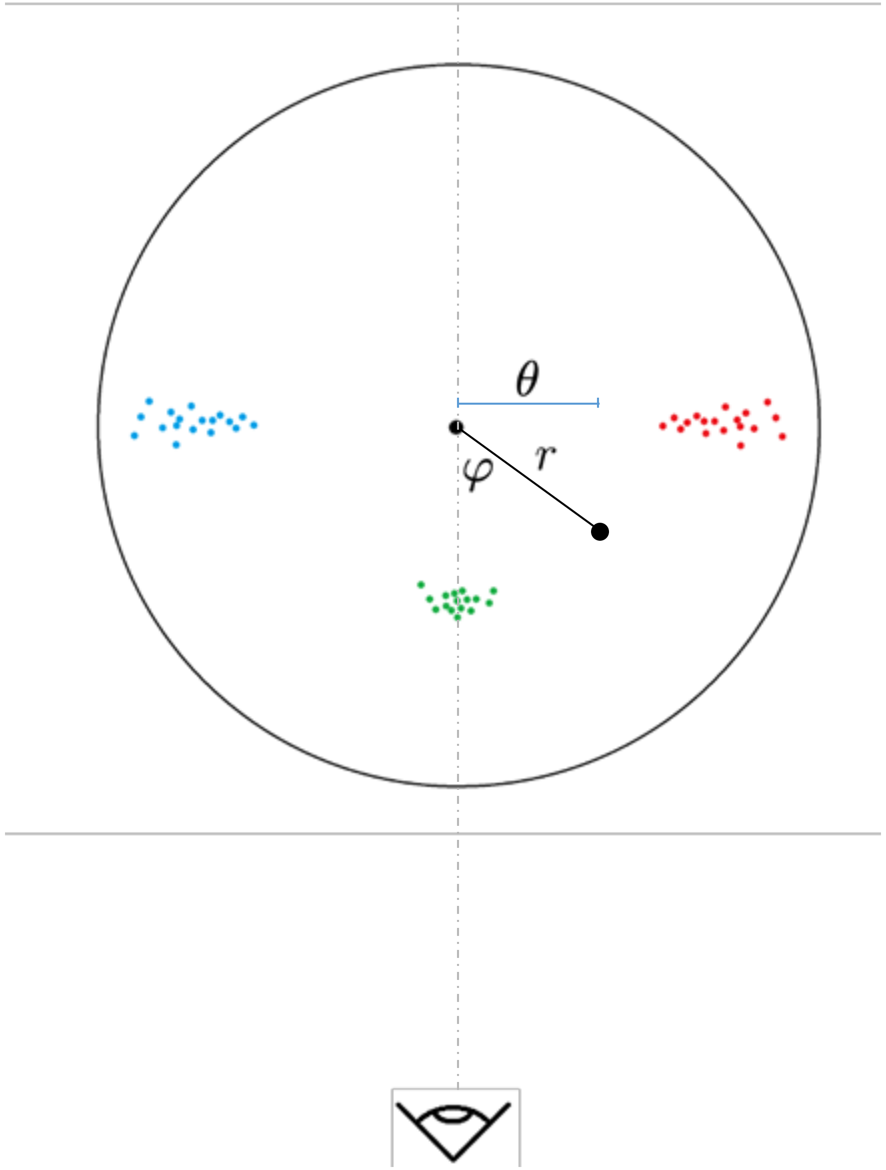

# Disk model

Consider a masing cloud on a circular orbit at radius r around a central SMBH of mass M and situated at an azimuthal angle ϕ with respect to the line of sight

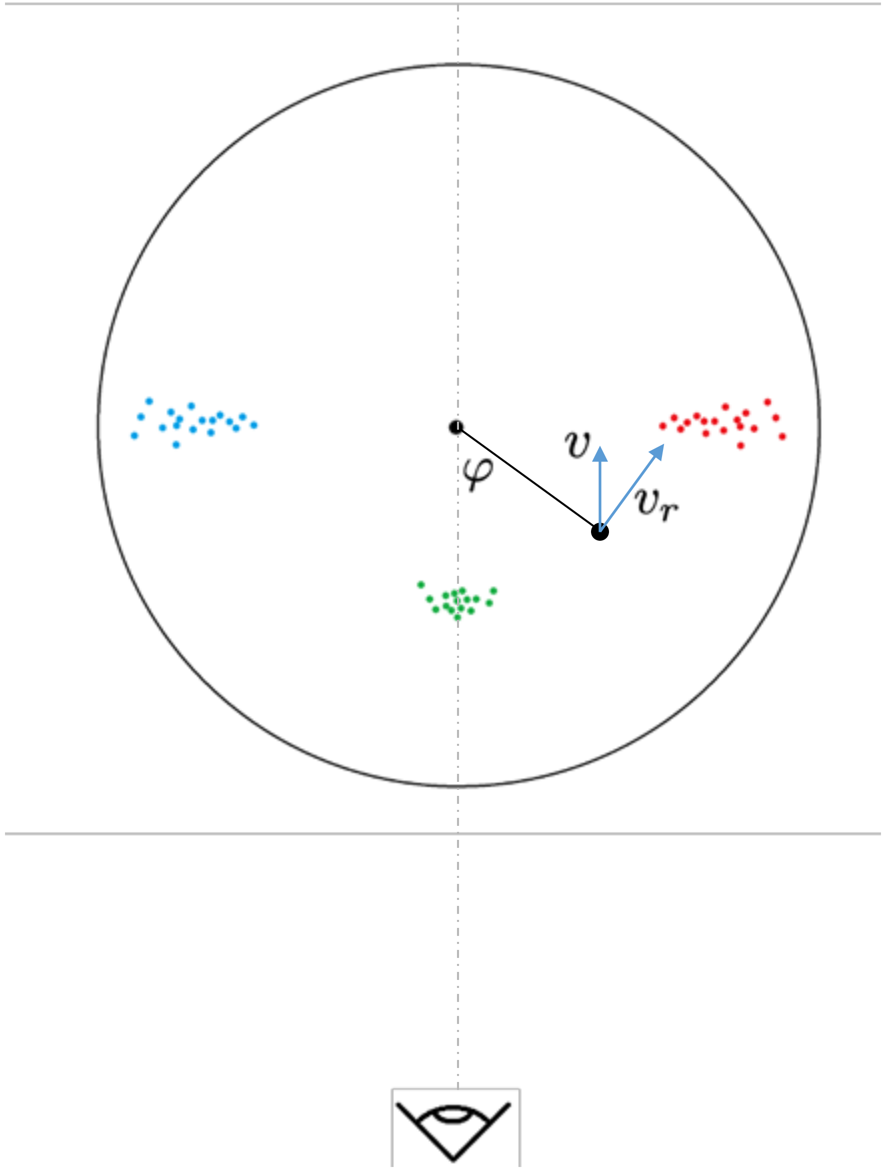


Observed (on-sky) position: $\theta = \frac{r}{D}\sin(\varphi)$ ~0.1 mas

Observed (line-of-sight) velocity: $v = v_r \sin(\varphi)$ ~100s km/s

$$v_r = \sqrt{\frac{GM}{r}}$$

# Disk model

Consider a masing cloud on a circular orbit at radius r around a central SMBH of mass M and situated at an azimuthal angle ϕ with respect to the line of sight

| | | |
|---|---|---|
| Observed (on-sky) position: | $\theta = \frac{r}{D}\sin(\varphi)$ | ~0.1 mas |
| Observed (line-of-sight) velocity: | $v = v_r \sin(\varphi)$ | ~100s km/s |
| Observed (line-of-sight) acceleration: | $a = a_r \sin(\varphi)$ | ~ km/s/yr |

$$v_r = \sqrt{\frac{GM}{r}} \qquad a_r = \frac{v_r^2}{r} = \frac{GM}{r^2}$$

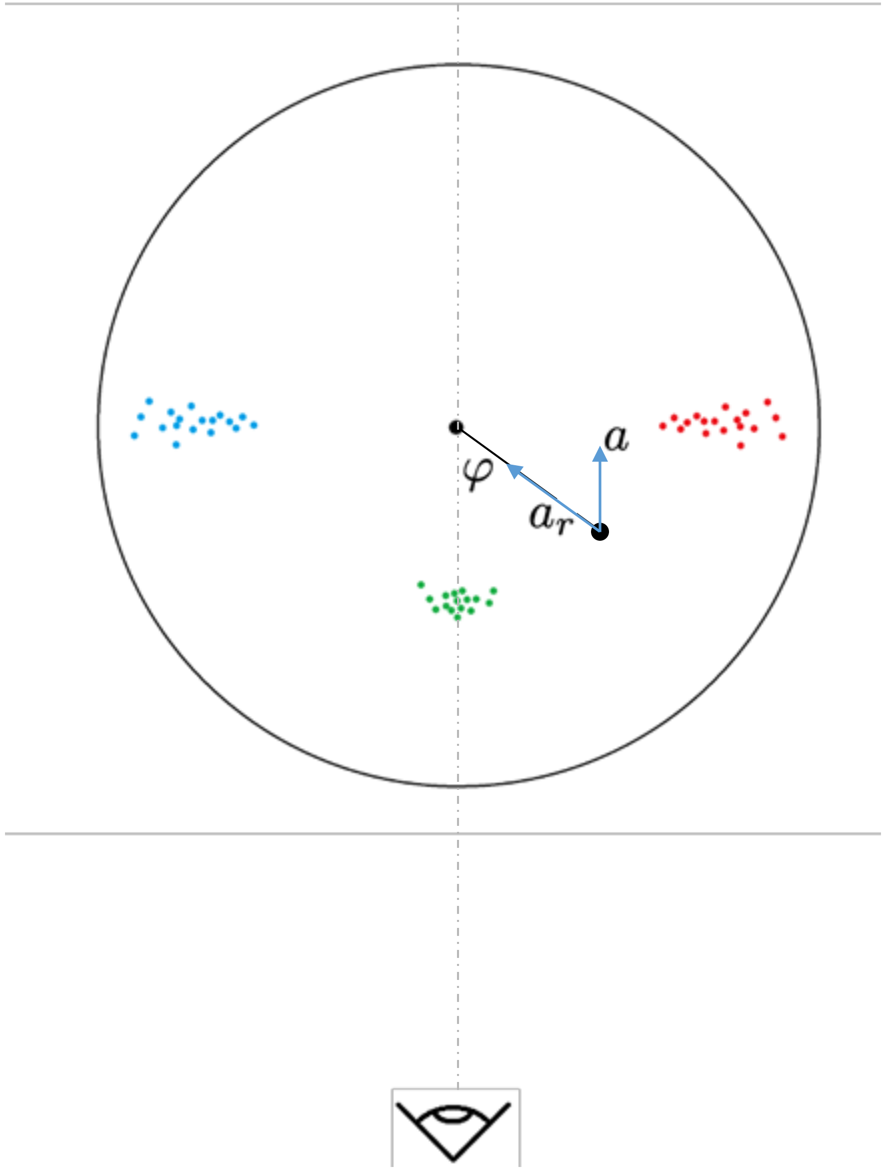

# Disk model

Consider a masing cloud on a circular orbit at radius r around a central SMBH of mass M and situated at an azimuthal angle ϕ with respect to the line of sight

Observed (on-sky) position: $\theta = \frac{r}{D}\sin(\varphi)$ ~0.1 mas

Observed (line-of-sight) velocity: $v = v_r \sin(\varphi)$ ~100s km/s

Observed (line-of-sight) acceleration: $a = a_r \sin(\varphi)$ ~ km/s/yr

$$v_r = \sqrt{\frac{GM}{r}} \qquad a_r = \frac{v_r^2}{r} = \frac{GM}{r^2}$$

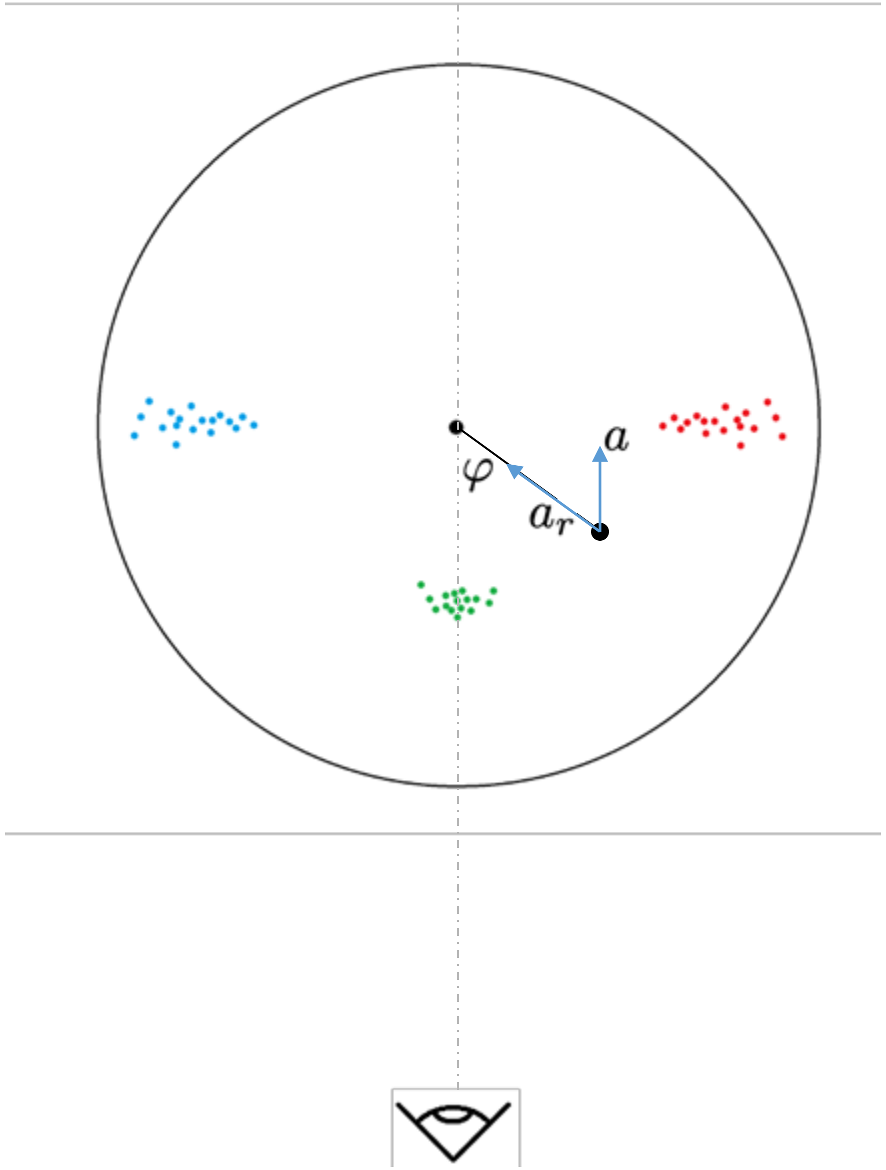

# NGC 4258 history: disk modeling

*"The new maser distance is particularly important because it is...completely independent of the Cepheid calibration. The geometric distance to NGC 4258 provides a unique and important confirmation of the Cepheid calibration. The confirmation will become even more direct and precise when Cepheids are measured in NGC 4258 itself in the coming years."*

– Herrnstein (1997)

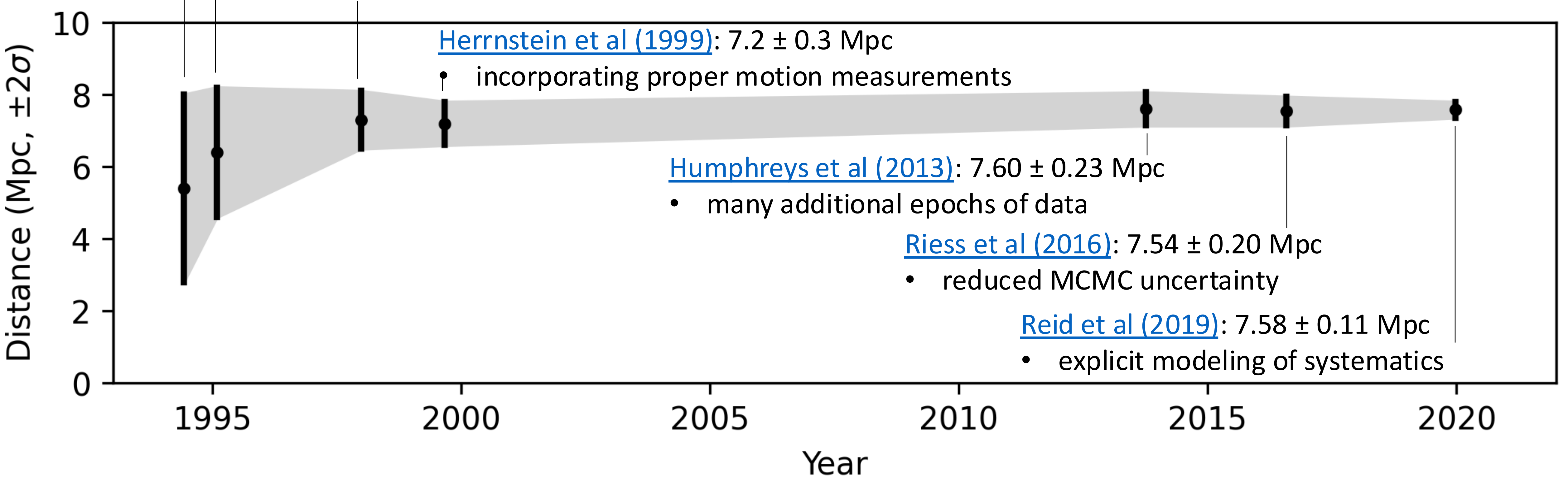

# NGC 4258 and cosmology: anchoring the distance ladder

Despite having a well-measured distance, NGC 4258 is ultimately just a single object. So how is it useful for cosmology?

- calibration “anchor” for other distance-measuring techniques

# NGC 4258 and cosmology: anchoring the distance ladder

Despite having a well-measured distance, NGC 4258 is ultimately just a single object. So how is it useful for cosmology?

- calibration “anchor” for other distance-measuring techniques

NGC 4258

absolute
distance scale

# NGC 4258 and cosmology: anchoring the distance ladder

Despite having a well-measured distance, NGC 4258 is ultimately just a single object. So how is it useful for cosmology?

- calibration “anchor” for other distance-measuring techniques

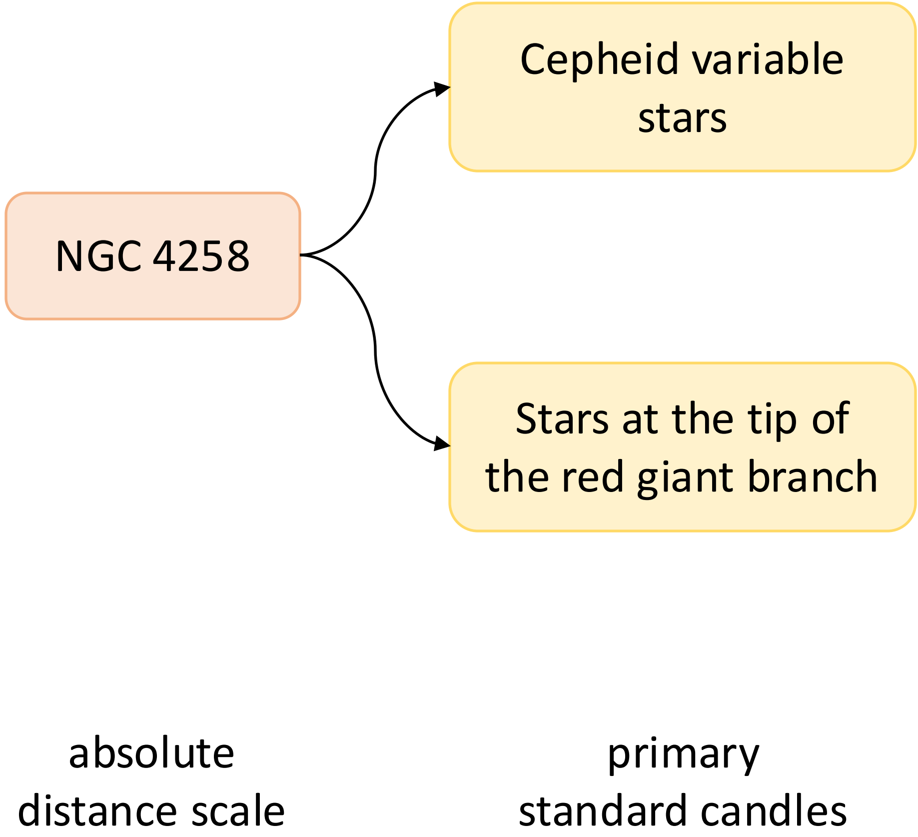

# NGC 4258 and cosmology: anchoring the distance ladder

Despite having a well-measured distance, NGC 4258 is ultimately just a single object. So how is it useful for cosmology?

- calibration "anchor" for other distance-measuring techniques

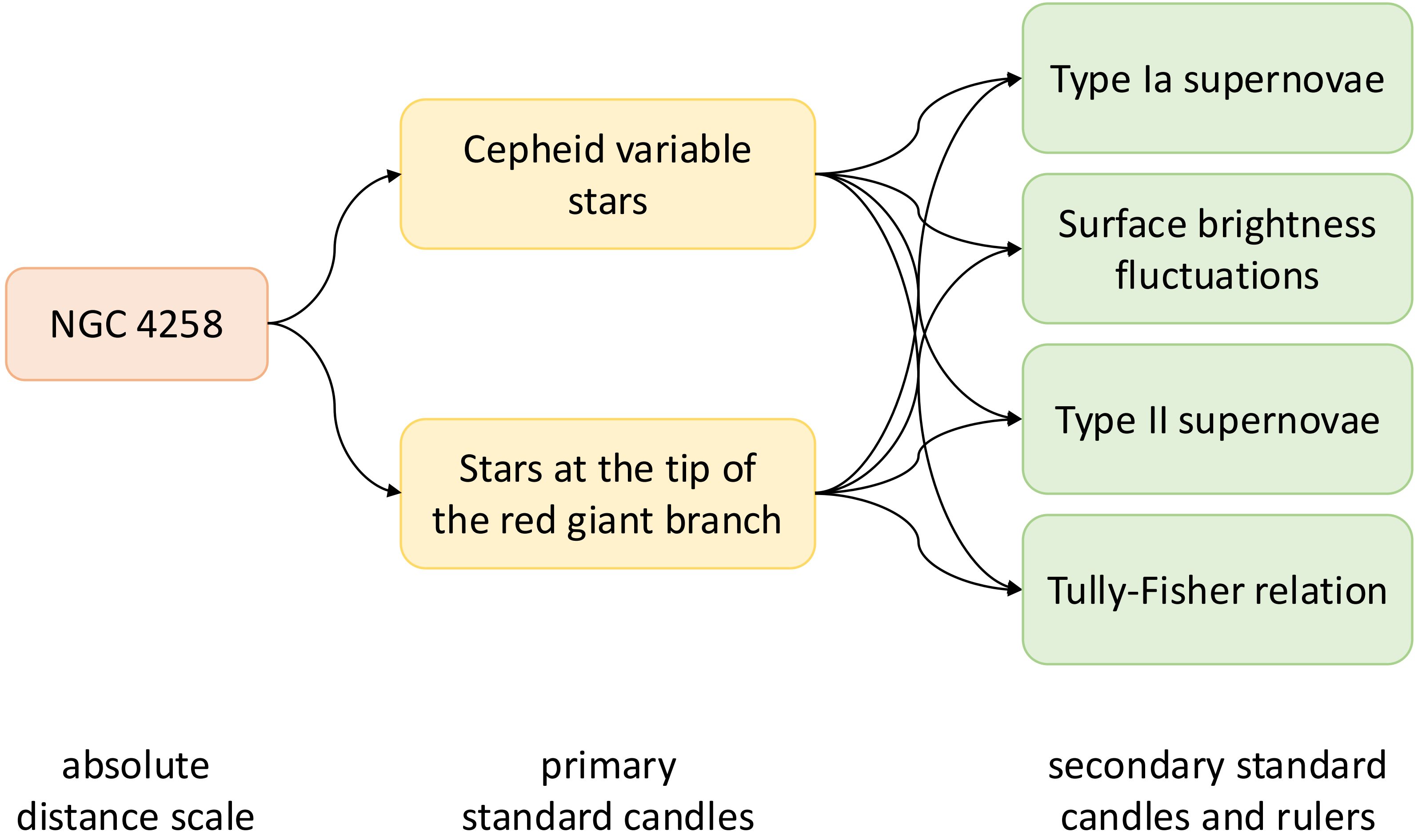

# NGC 4258 and cosmology: anchoring the distance ladder

Despite having a well-measured distance, NGC 4258 is ultimately just a single object. So how is it useful for cosmology?

- calibration "anchor" for other distance-measuring techniques

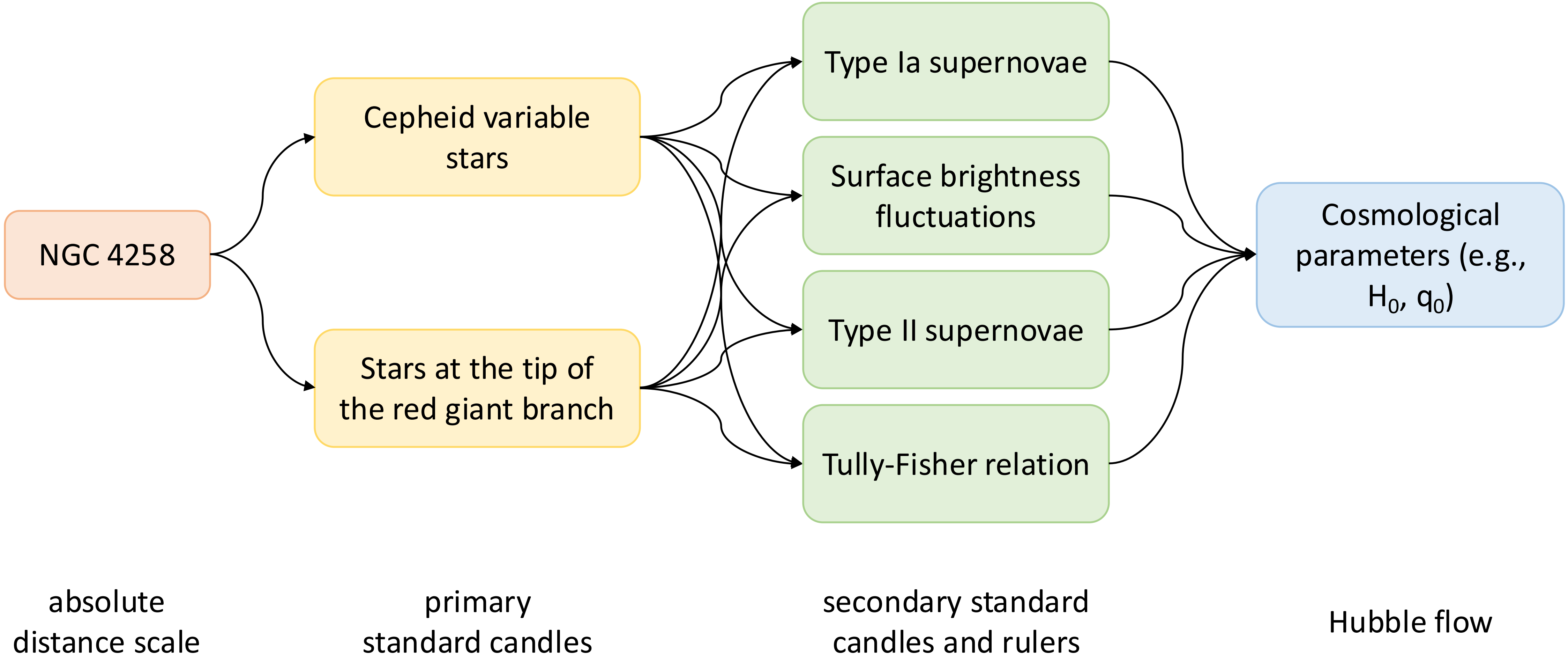

# NGC 4258 and cosmology: anchoring the distance ladder

Despite having a well-measured distance, NGC 4258 is ultimately just a single object. So how is it useful for cosmology?

- calibration “anchor” for other distance-measuring techniques

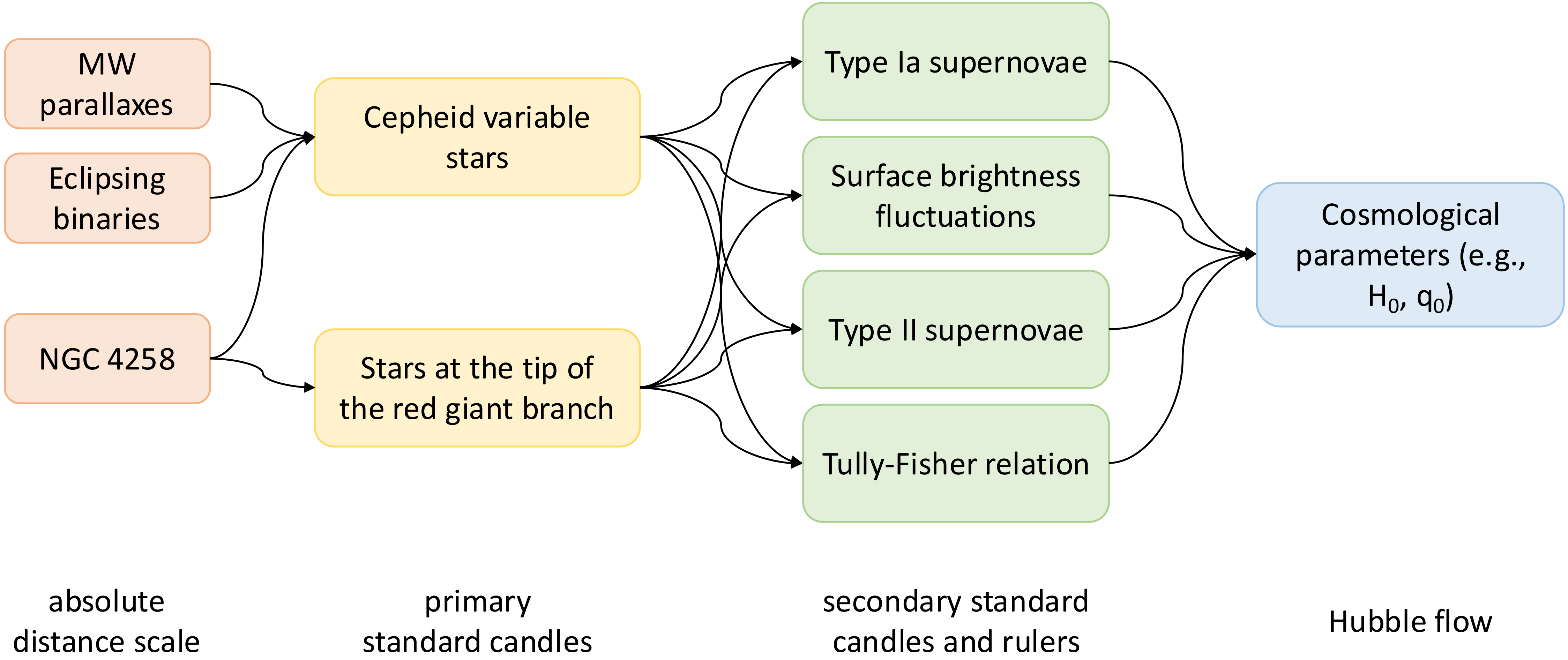

# What if there was more than one system like NGC 4258?

The importance and utility of NGC 4258 prompted searches for other $H_2O$ megamaser systems

# What if there was more than one system like NGC 4258?

The importance and utility of NGC 4258 prompted searches for other $H_2O$ megamaser systems

- Early maser surveys included Claussen, Heiligman, & Lo (1984) (NGC 4258, NGC 1068), Henkel et al (1984), and Haschick & Bann (1985) (both latter groups identified NGC 3079)
- Braatz et al (1994) presented results from the first large survey for megamaser systems in AGN rather than star-forming galaxies, discovering 5/120 new sources using the Effelsberg 100m
    - the count was brought up to 10/354 by Braatz et al (1996) using the Parkes 64m, with new sources including NGC 1052, NGC 1386, and IC 2560
- Other early searches include:
    - Greenhill et al (1997) discovered 1/29 (DSN)
    - Hagiwara et al (2002) discovered 1/15 (Effelsberg)
    - Greenhill et al (2003) discovered 7/160 (DSN)
        - along with Kondratko et al (2006), final count is 15/630 in total
- And many others:
    - Nakai et al (1995), Wilner et al (1999), Falcke et al (2000), Greenhill et al (2002), Hagiwara et al (2003), Sato et al (2005), etc.

By the early 2000's, the total number of known $H_2O$ megamaser sources was ~25

# The GBT era

With the completion of the Green Bank Telescope (GBT) K-band commissioning in spring of 2002, the megamaser discovery rate increased dramatically

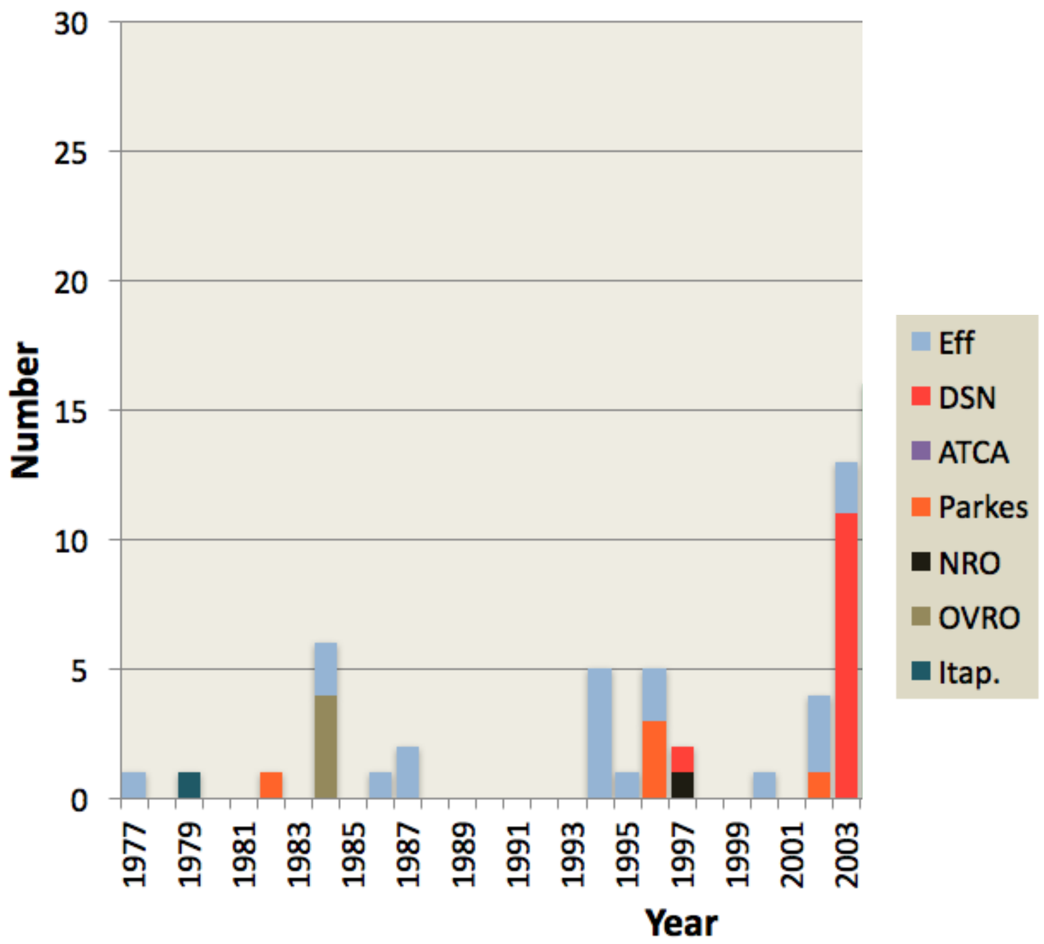


Figure credit: Jim Braatz

# The GBT era

With the completion of the Green Bank Telescope (GBT) K-band commissioning in spring of 2002, the megamaser discovery rate increased dramatically

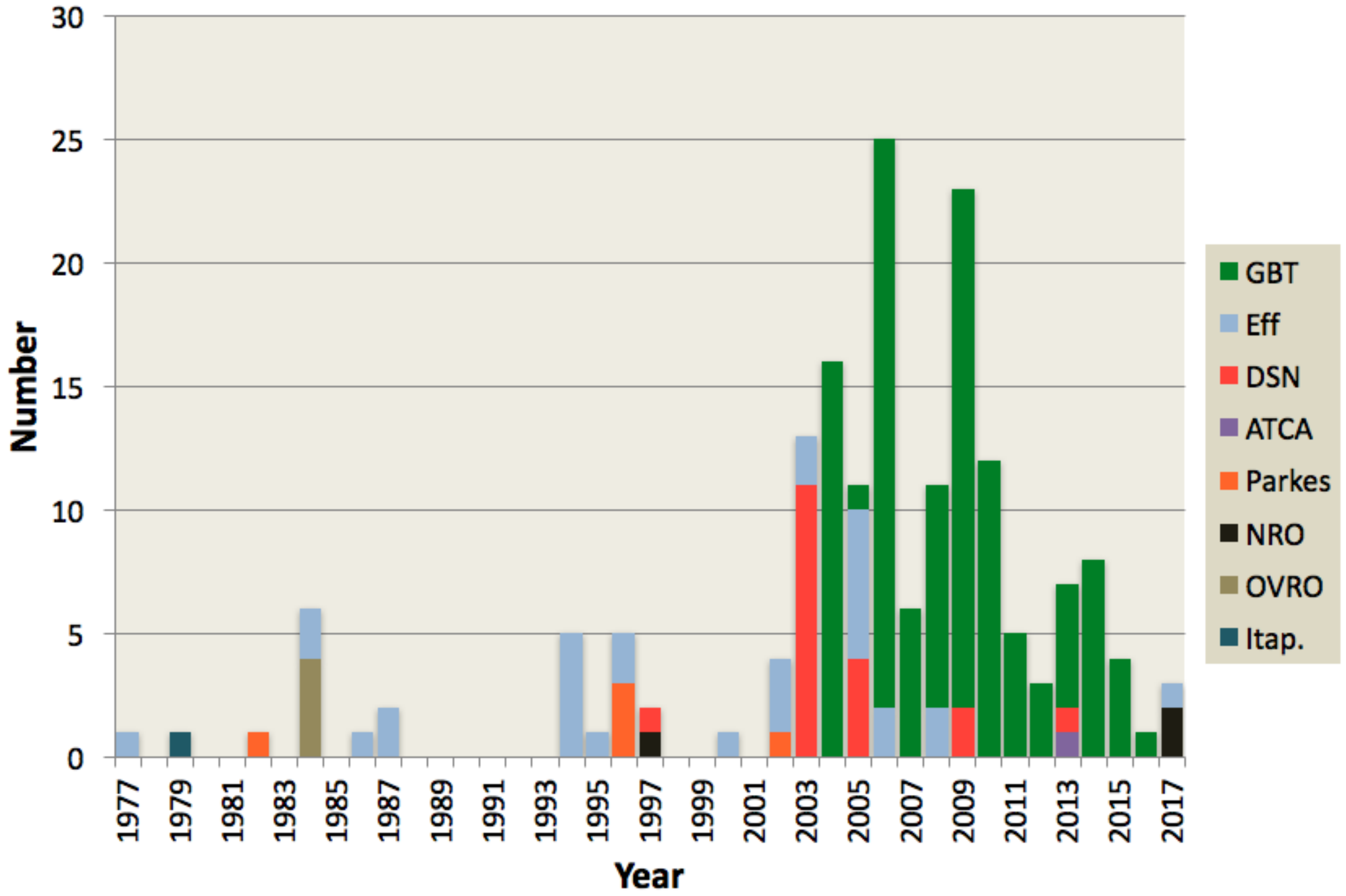


As of today, roughly ~200 $H_2O$ megamaser systems are known, out of nearly 5000 galaxies that have been surveyed. The majority of these systems have been discovered using the GBT.

Figure credit: Jim Braatz

# The GBT era

With the completion of the Green Bank Telescope (GBT) K-band commissioning in spring of 2002, the megamaser discovery rate increased dramatically

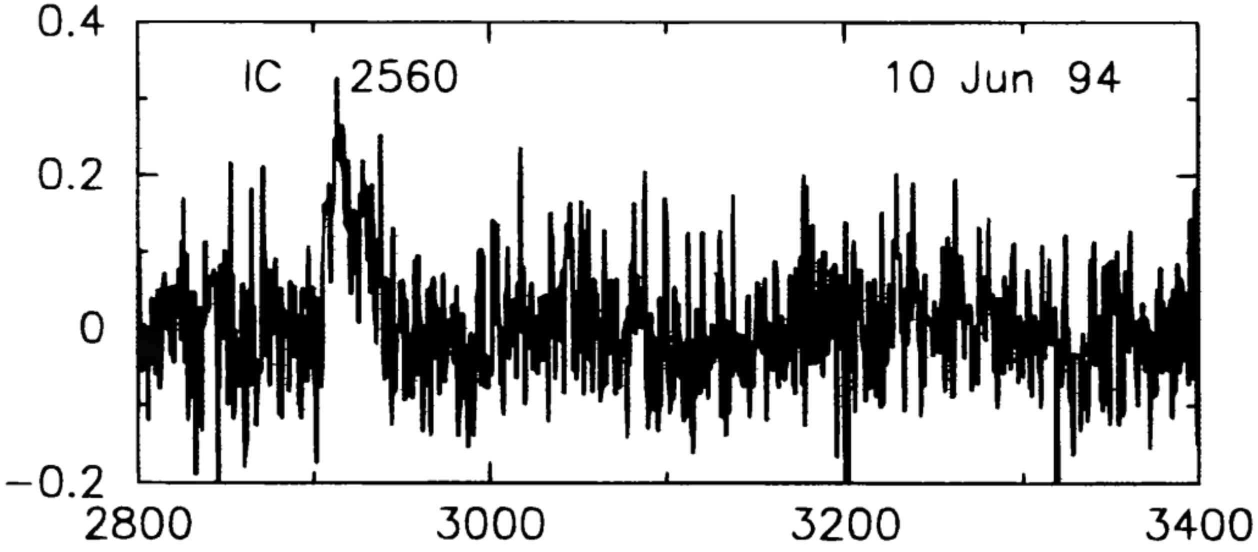


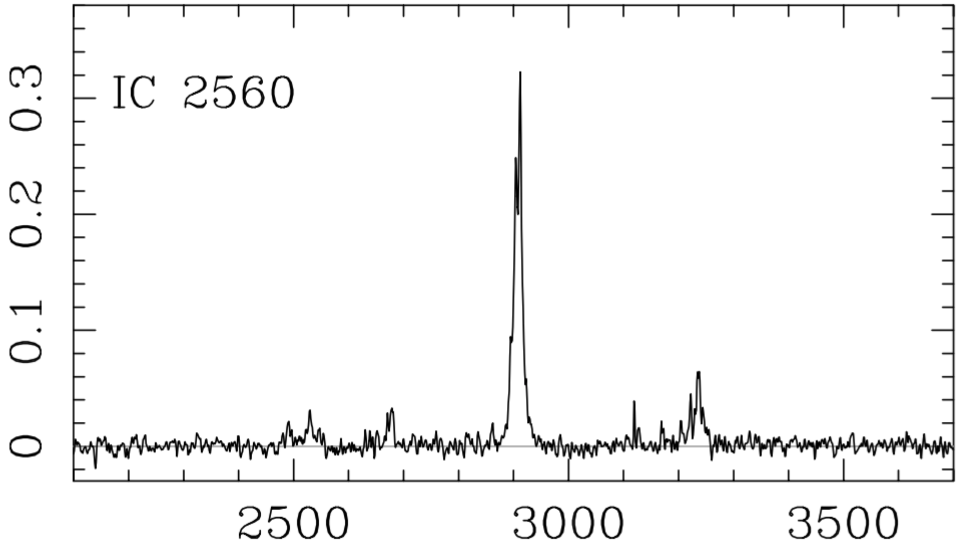


Braatz et al (1996)

Braatz et al (2003)

# Megamaser Cosmology Project

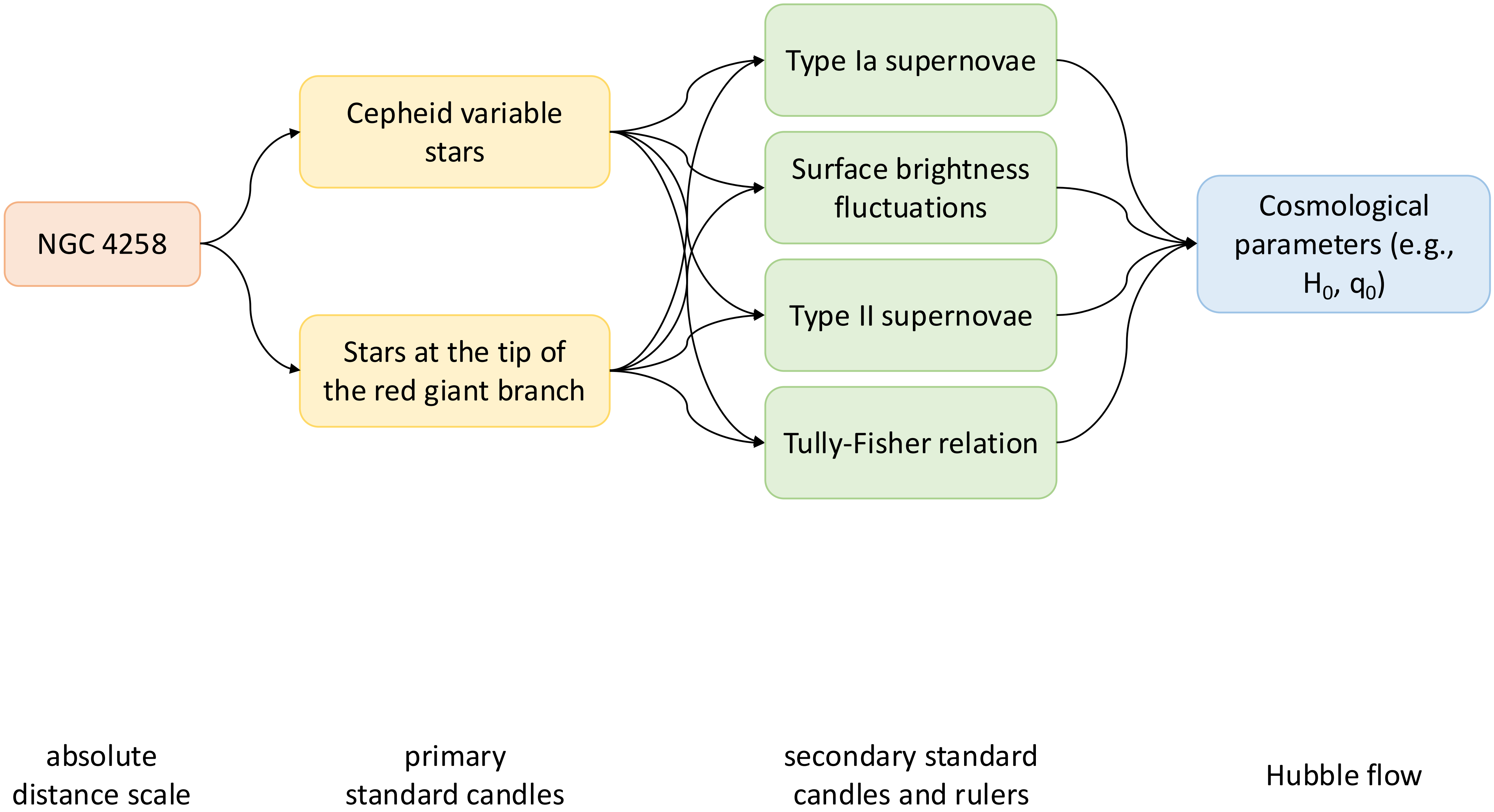

# Megamaser Cosmology Project

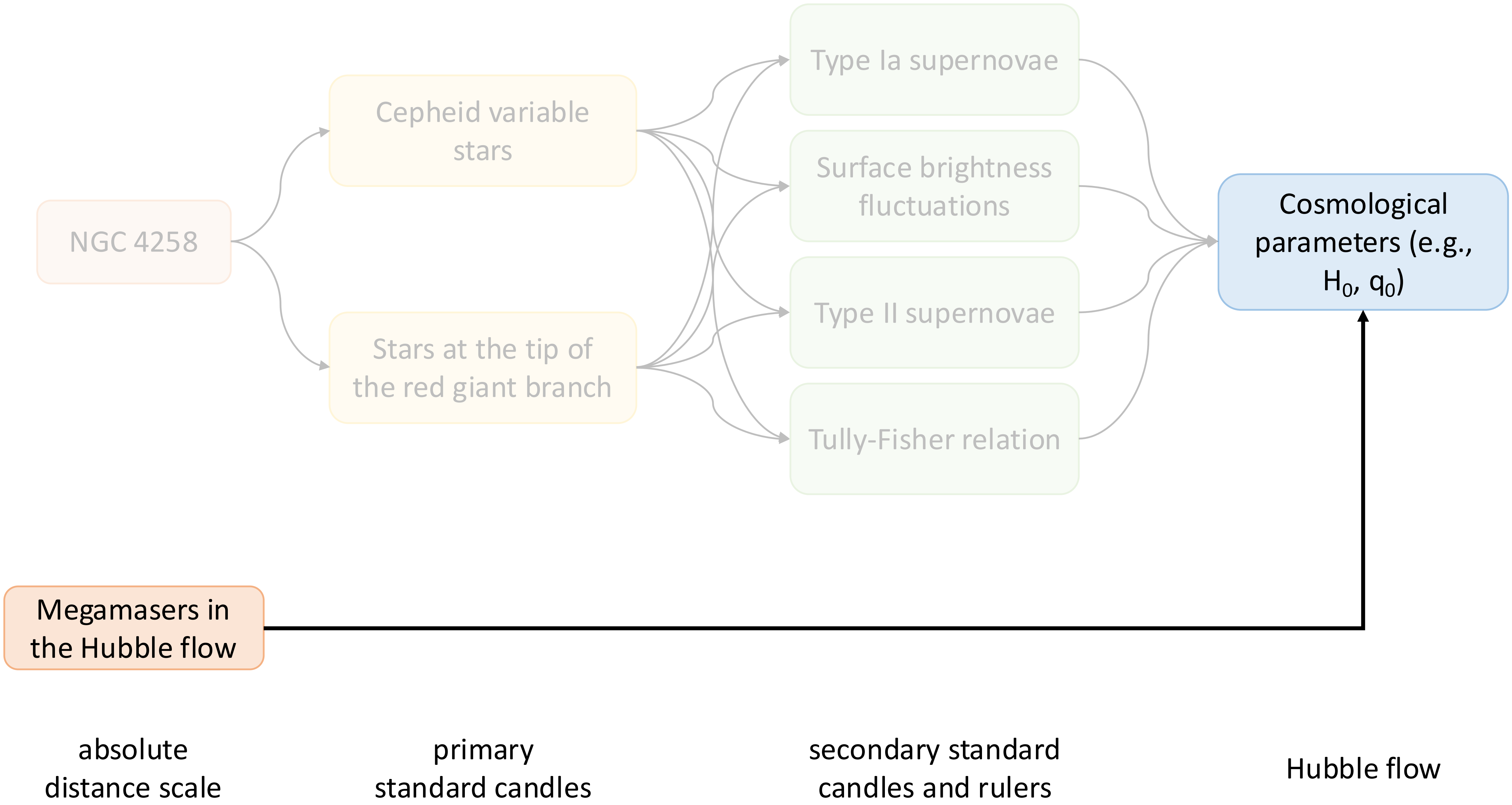

# Megamaser Cosmology Project

NGC 4258 is useful for anchoring the distance ladder, but it is too nearby to provide strong constraints on $H_0$ by itself

- peculiar velocity uncertainty is large (i.e., comparable in magnitude to the recession velocity)

To determine single-step $H_0$ constraints using the megamaser technique, we require objects that are participating in the Hubble flow (i.e., peculiar velocity << recession velocity)

The vast increase in sensitivity provided by the GBT permits detection of faint (~mJy-level) maser features in short (<1 hour) integration times, enabling:

- efficient surveying of AGN for the identification of new maser systems
- regular monitoring of disk megamaser systems to measure accelerations

The discovery of multiple new megamaser disk systems circa 2010 led to the formation of the **Megamaser Cosmology Project** (MCP), with the goal of directly measuring $H_0$ using megamasers

# Megamaser Cosmology Project

The MCP is a multi-year, international effort to find megamaser-hosting galaxies in the Hubble flow and measure their distances, with the primary goal of constraining $H_0$ to a 3% precision independent of standard candles, distance ladders, or the CMB.

To date, the MCP has determined distances to 5 megamaser-hosting AGN:

- UGC 3789 (Reid et al. 2009, Braatz et al. 2010, Reid et al. 2013)
- NGC 6264 (Kuo et al. 2013)
- NGC 6323 (Kuo et al. 2015)
- NGC 5765b (Gao et al. 2016)
- CGCG 074-064 (Pesce et al. 2020a)

Individual MCP distance measurements have a ~10% measurement precision, compared to the ~1.5% precision of the measurement to NGC 4258

# Megamaser Cosmology Project

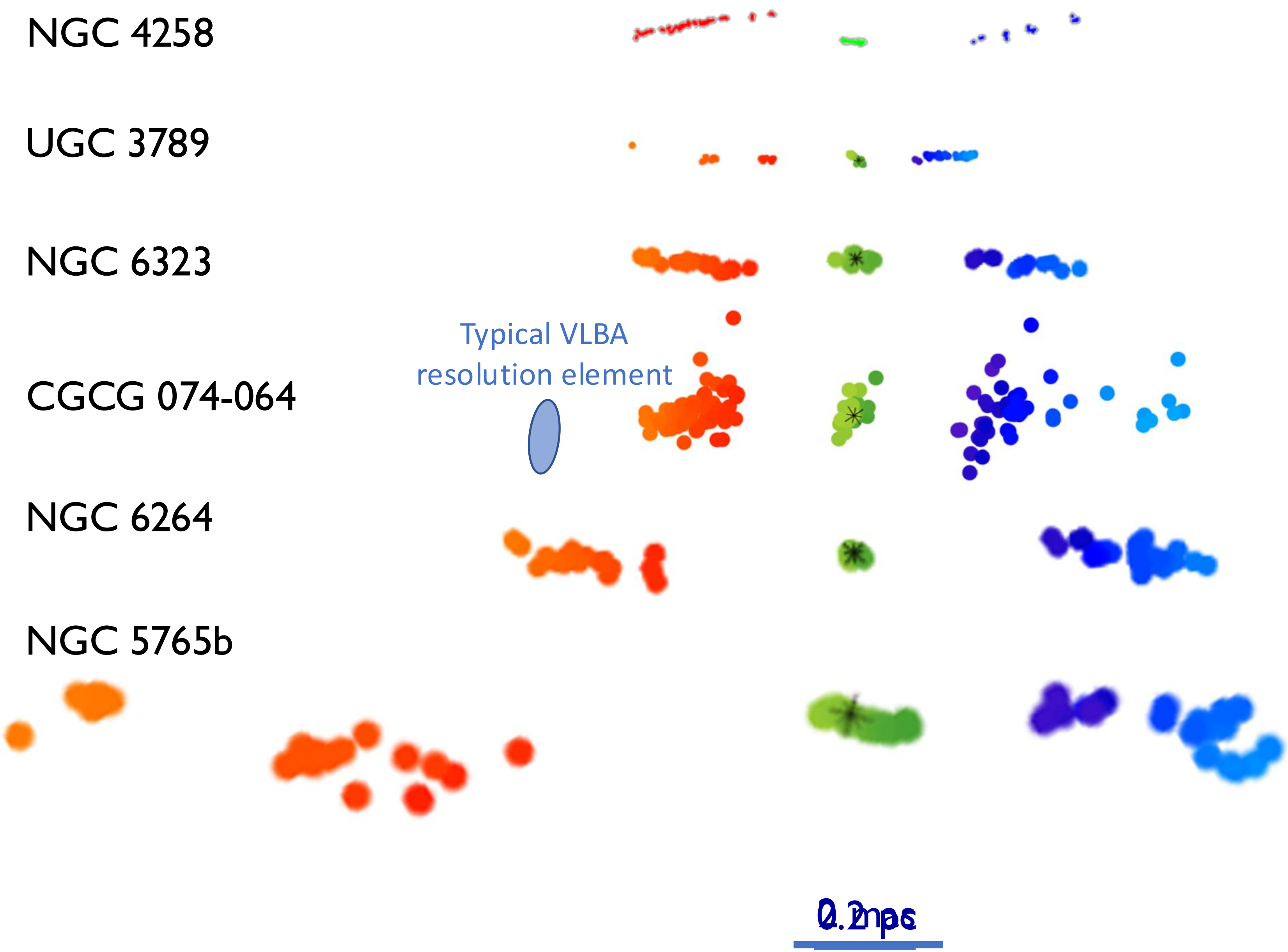


Maser galaxies in the Hubble flow have distance measurements that are individually much less precise than that of NGC 4258. So to obtain the best constraint on the Hubble constant, we need to combine measurements from multiple galaxies.

# MCP $H_0$ constraints

The MCP has combined the distance measurements to NGC 4258 and 5 other megamaser galaxies in the Hubble flow to produce a maser-only constraint on $H_0$ of 73.9 ± 3.0 km/s/Mpc

The MCP measurement is independent of standard candles and other distance-measuring techniques, making it a "single-rung" distance ladder

The value measured by the MCP is consistent with that produced by other low-z methods

- see "Hubble tension" for lots of extra excitement

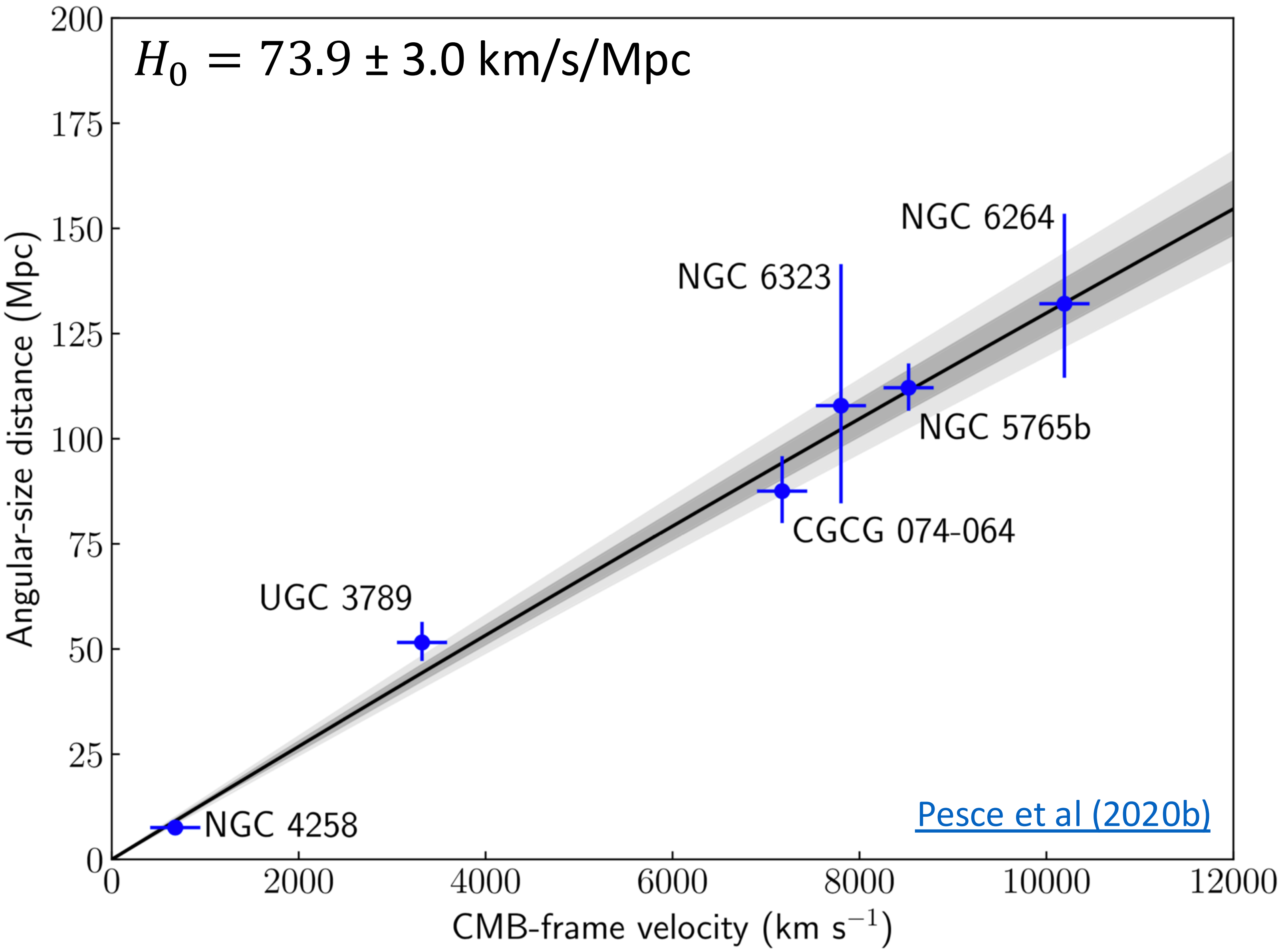

# Event Horizon Telescope

# What should a black hole look like?

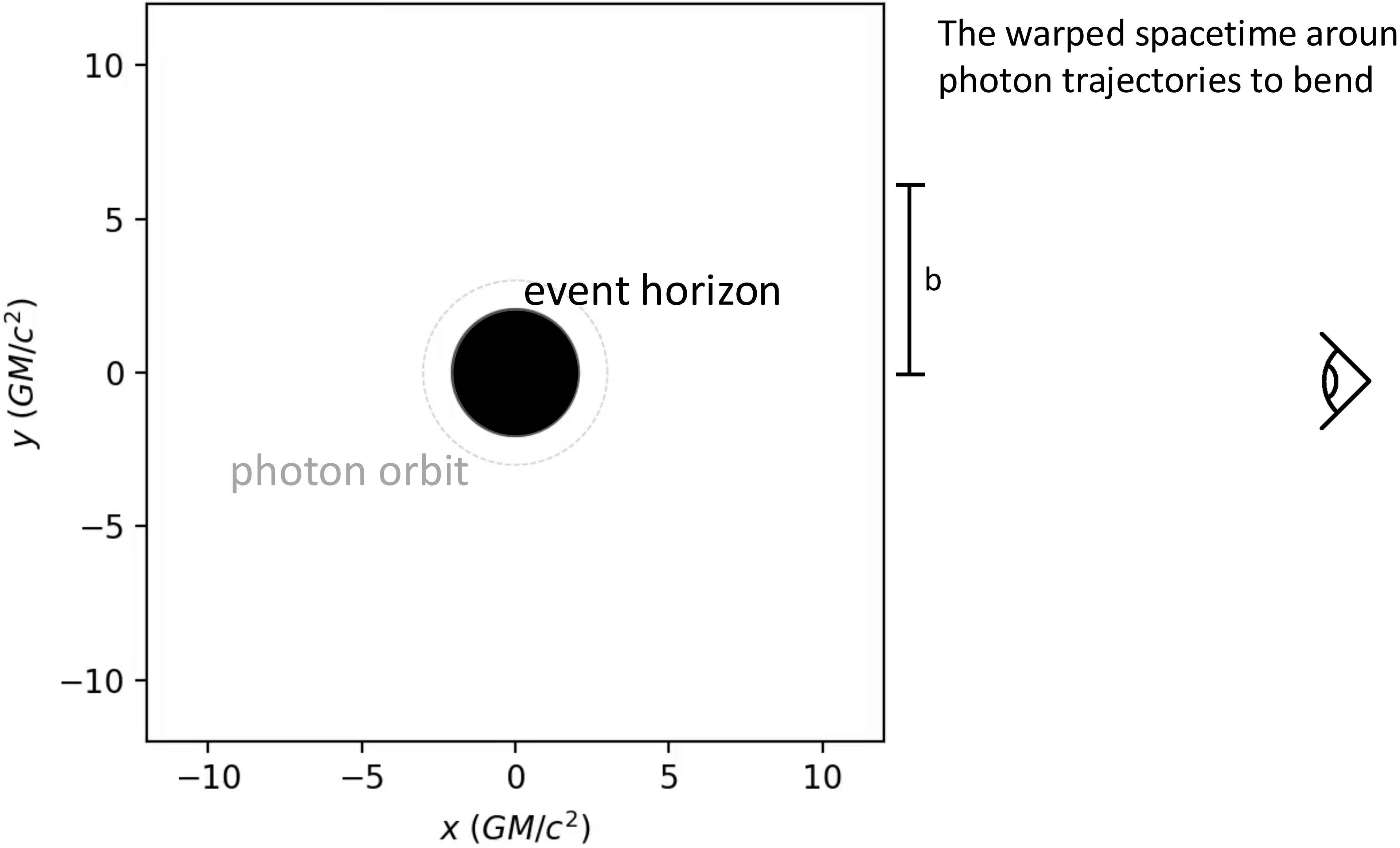


The warped spacetime around a black hole causes photon trajectories to bend

# What should a black hole look like?

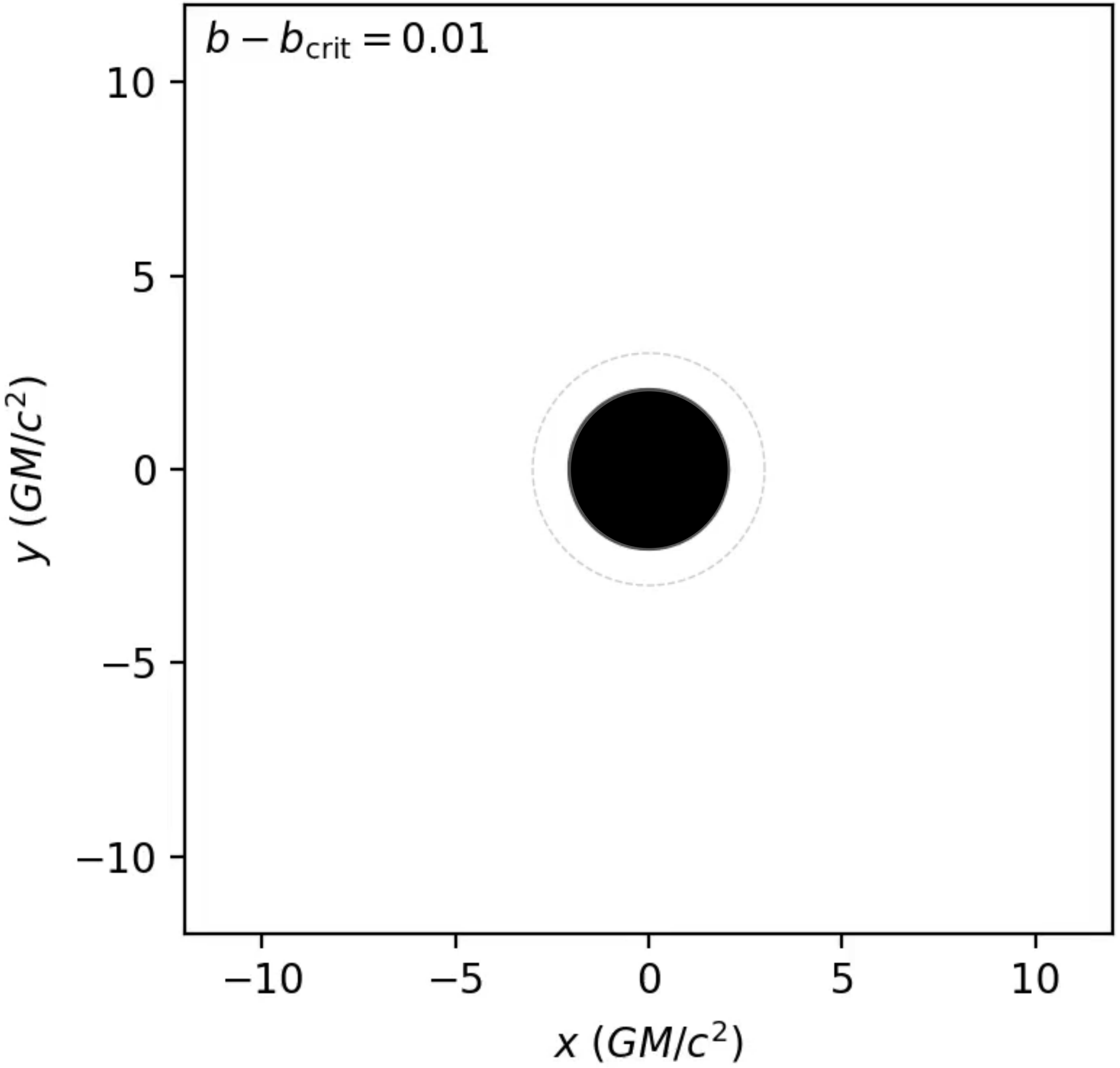


The warped spacetime around a black hole causes photon trajectories to bend

The closer these trajectories get to a critical impact parameter, the more tightly wound they become

# What should a black hole look like?

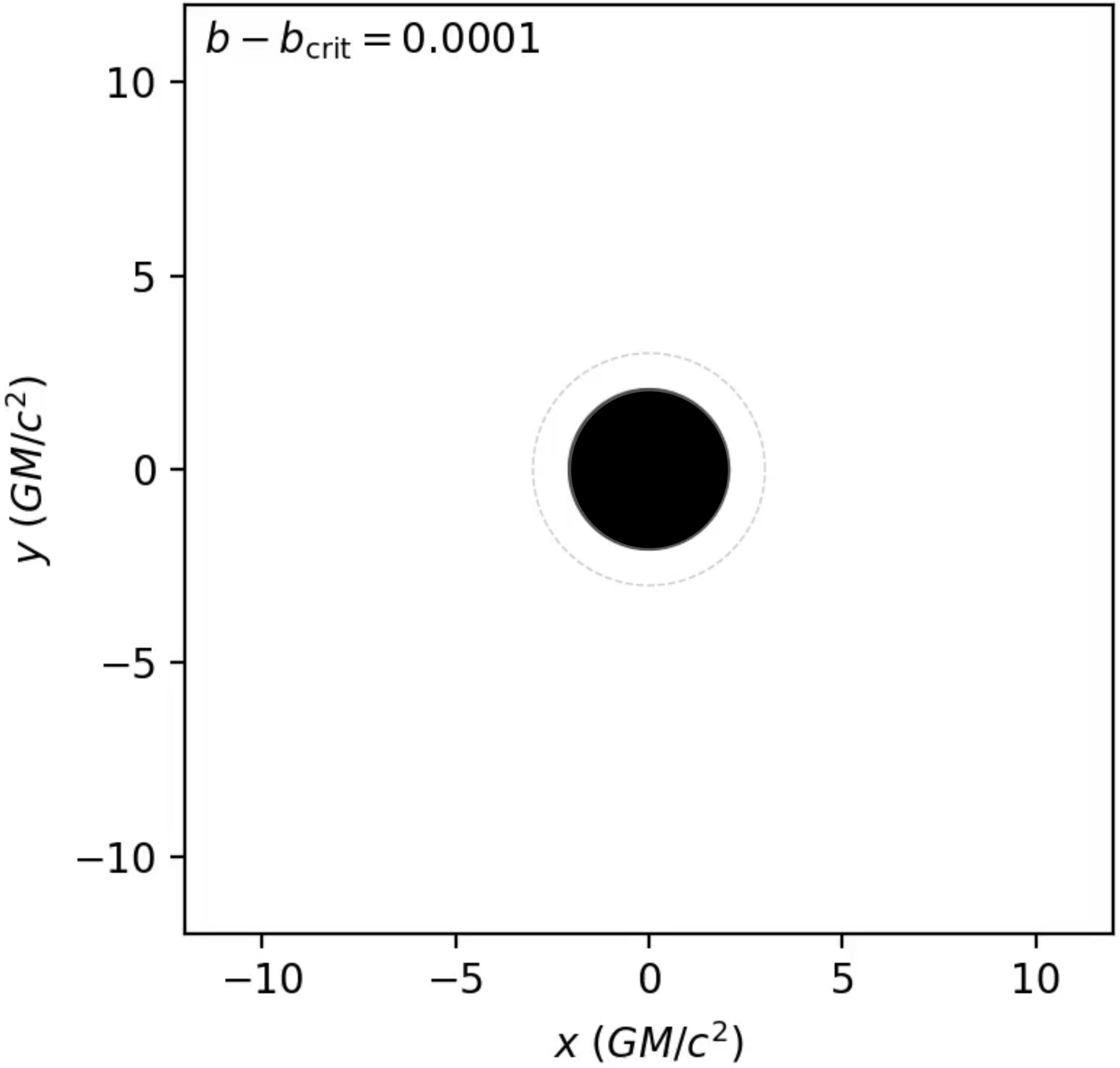


The warped spacetime around a black hole causes photon trajectories to bend

The closer these trajectories get to a critical impact parameter, the more tightly wound they become

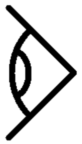

# What should a black hole look like?

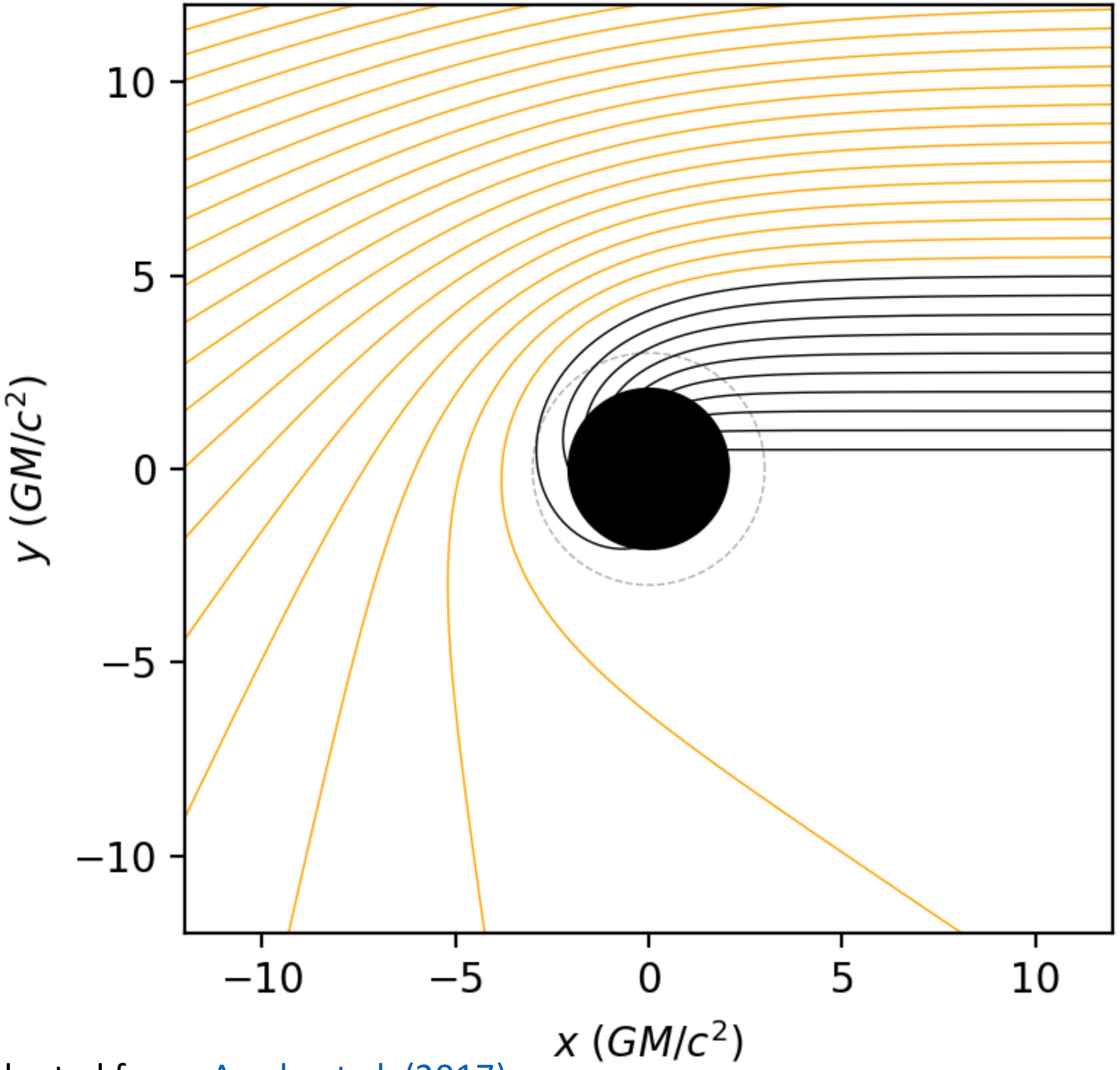


The warped spacetime around a black hole causes photon trajectories to bend

The closer these trajectories get to a critical impact parameter, the more tightly wound they become

The trajectories interior to this critical impact parameter intersect the horizon, and these collectively form the black hole "**shadow**"

Adapted from: Asada et al. (2017)

# Photon ring and black hole shadow

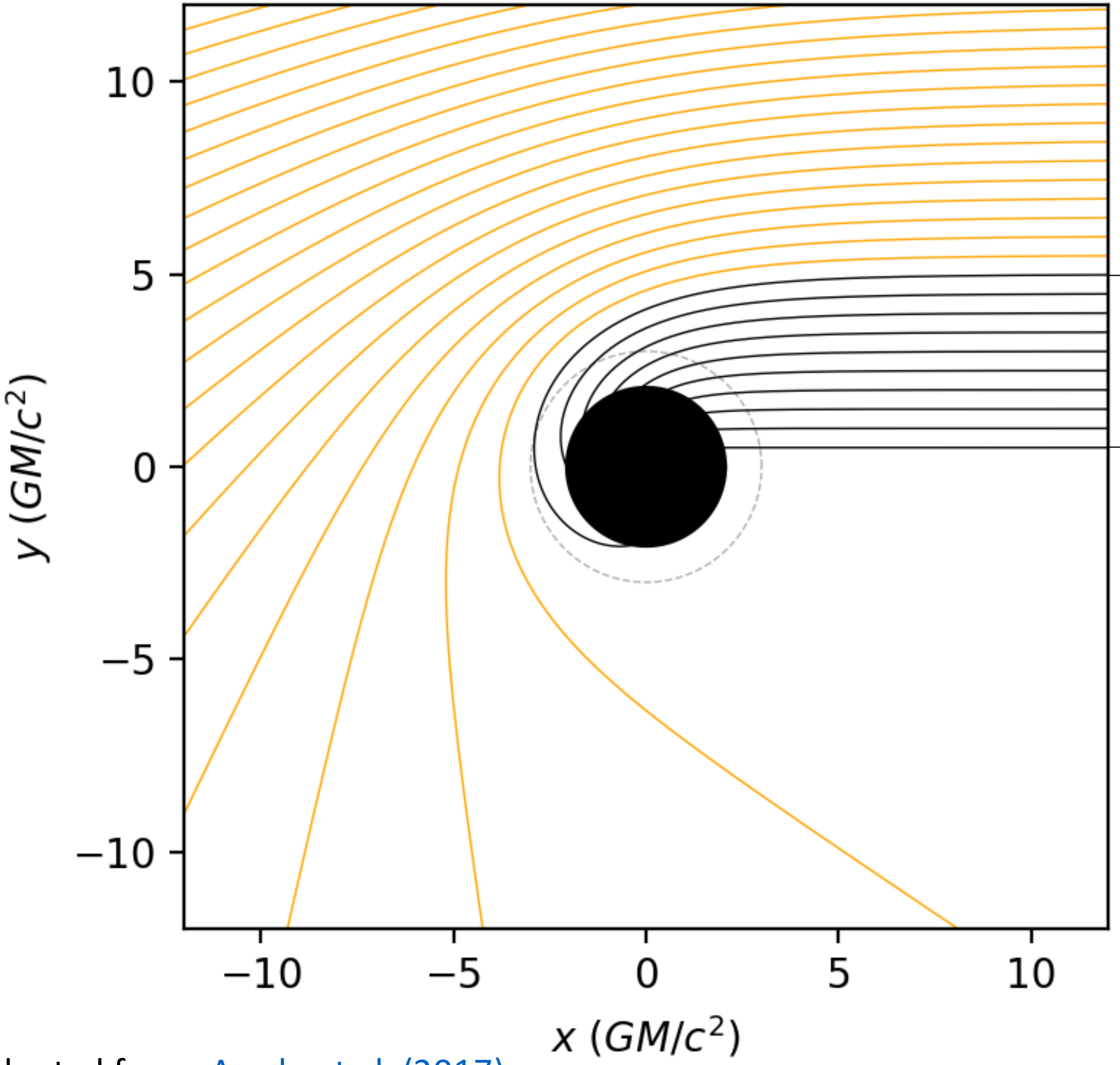


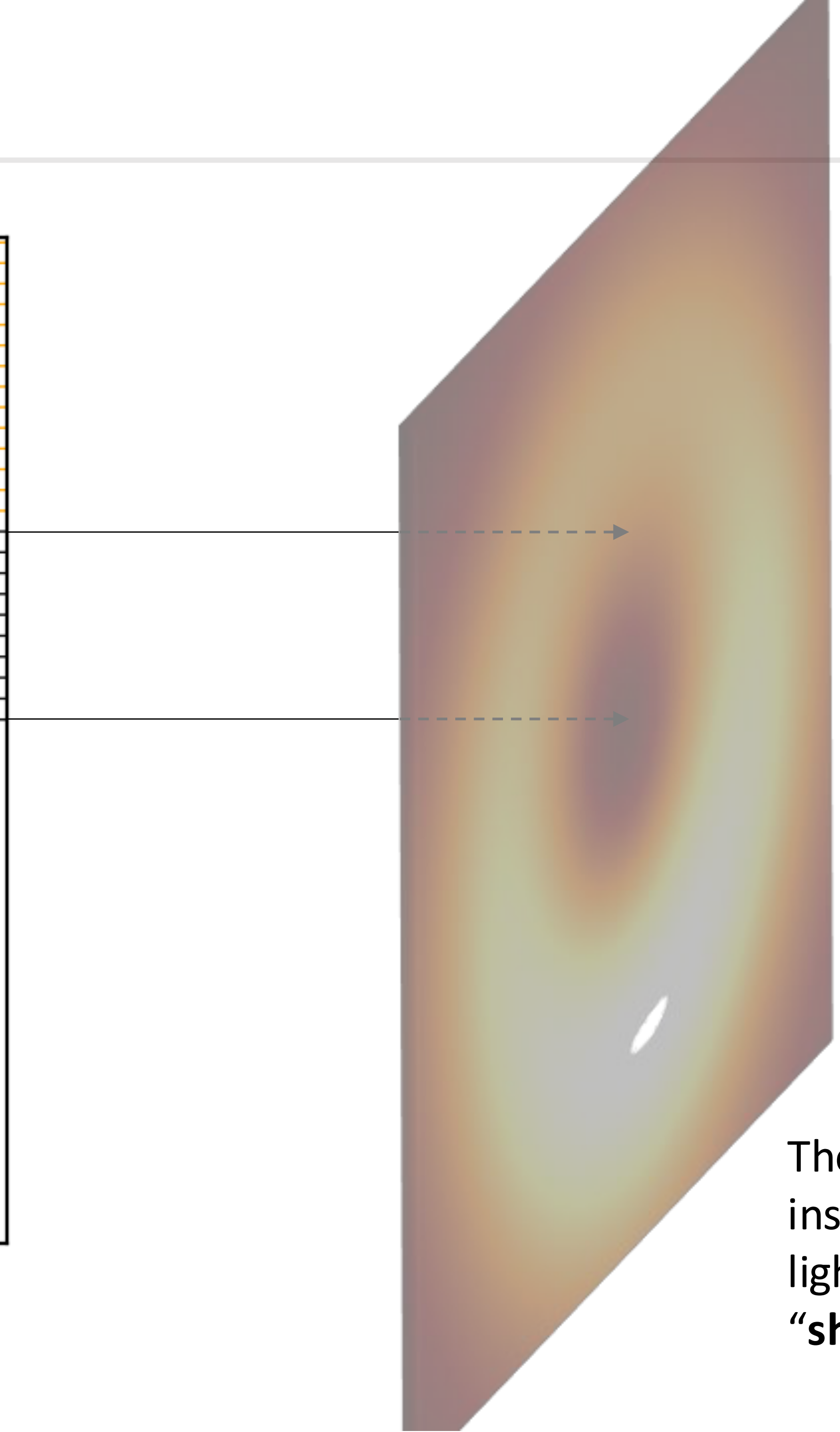

The dark region inside the ring of light is the black hole "**shadow**"

Adapted from: Asada et al. (2017)

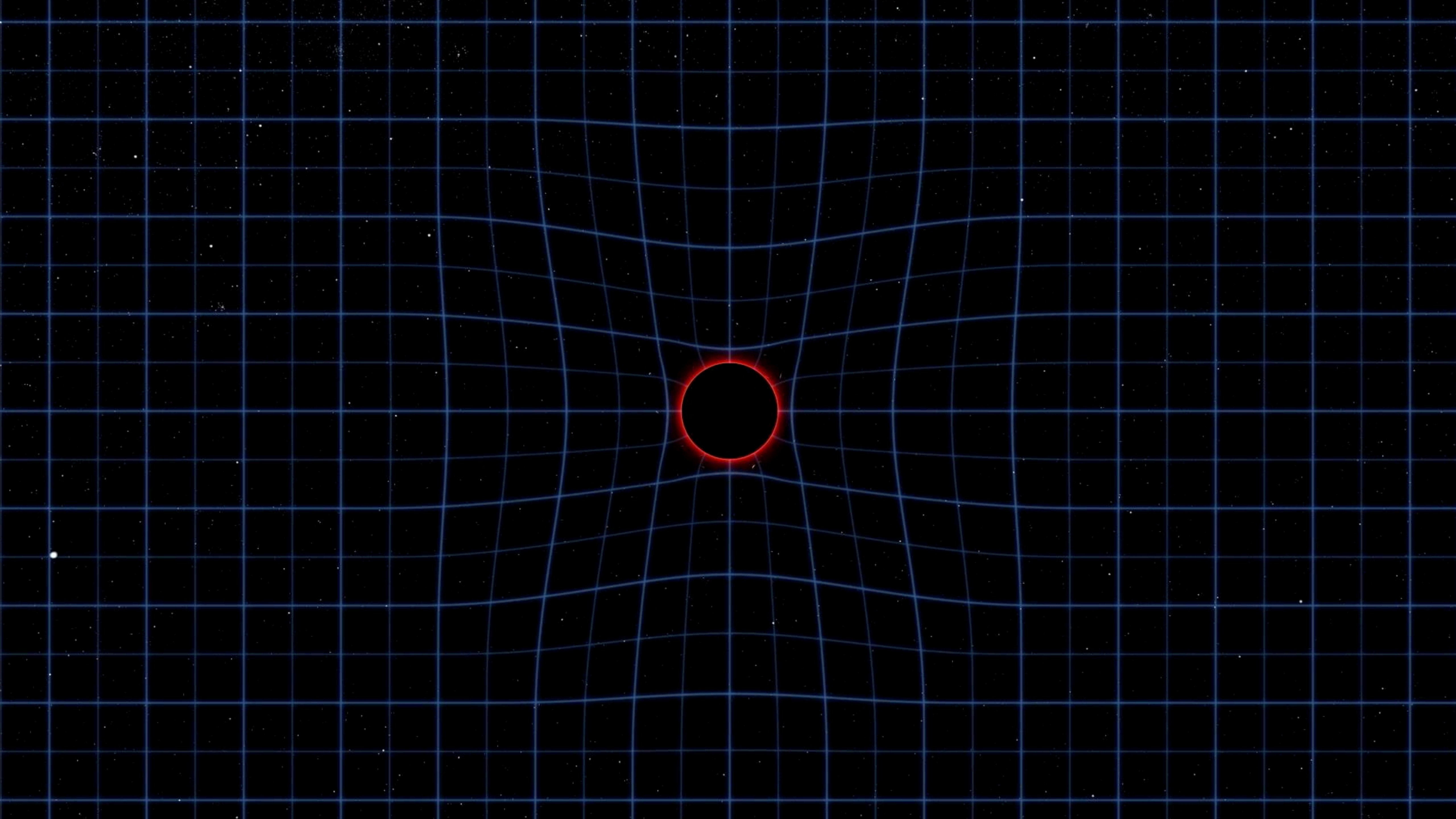

# The challenge

The primary challenge is one of angular resolution: even the largest black holes subtend tiny angles

- e.g., the shadow of the supermassive black hole in the galaxy M87 is only ~40 $\mu$as across

# The challenge

The primary challenge is one of angular resolution: even the largest black holes subtend tiny angles

- e.g., the shadow of the supermassive black hole in the galaxy M87 is only ~40 $\mu$as across

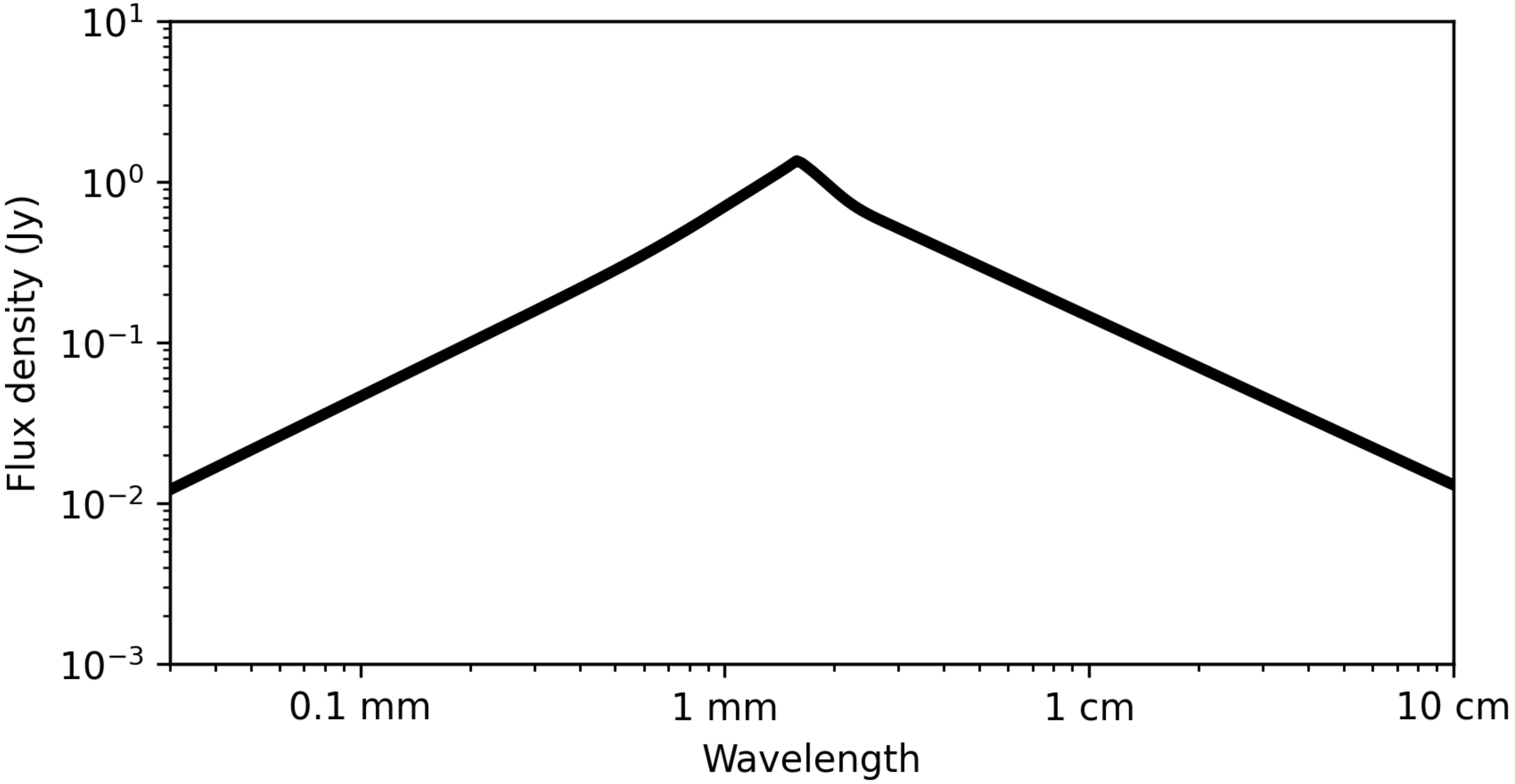

# The challenge

The primary challenge is one of angular resolution: even the largest black holes subtend tiny angles

- e.g., the shadow of the supermassive black hole in the galaxy M87 is only ~40 $\mu$as across

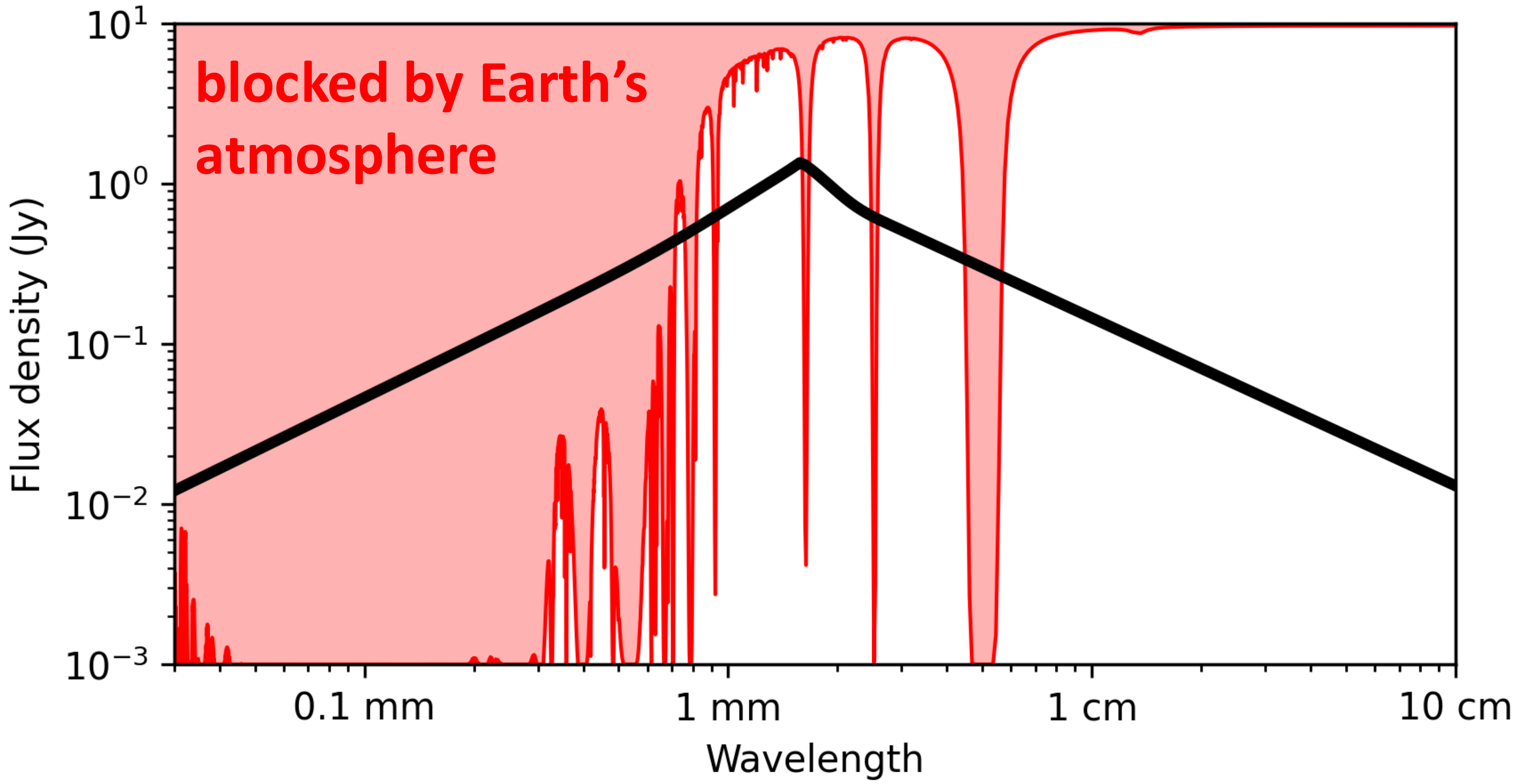

# The challenge

The primary challenge is one of angular resolution: even the largest black holes subtend tiny angles

- e.g., the shadow of the supermassive black hole in the galaxy M87 is only ~40 $\mu$as across

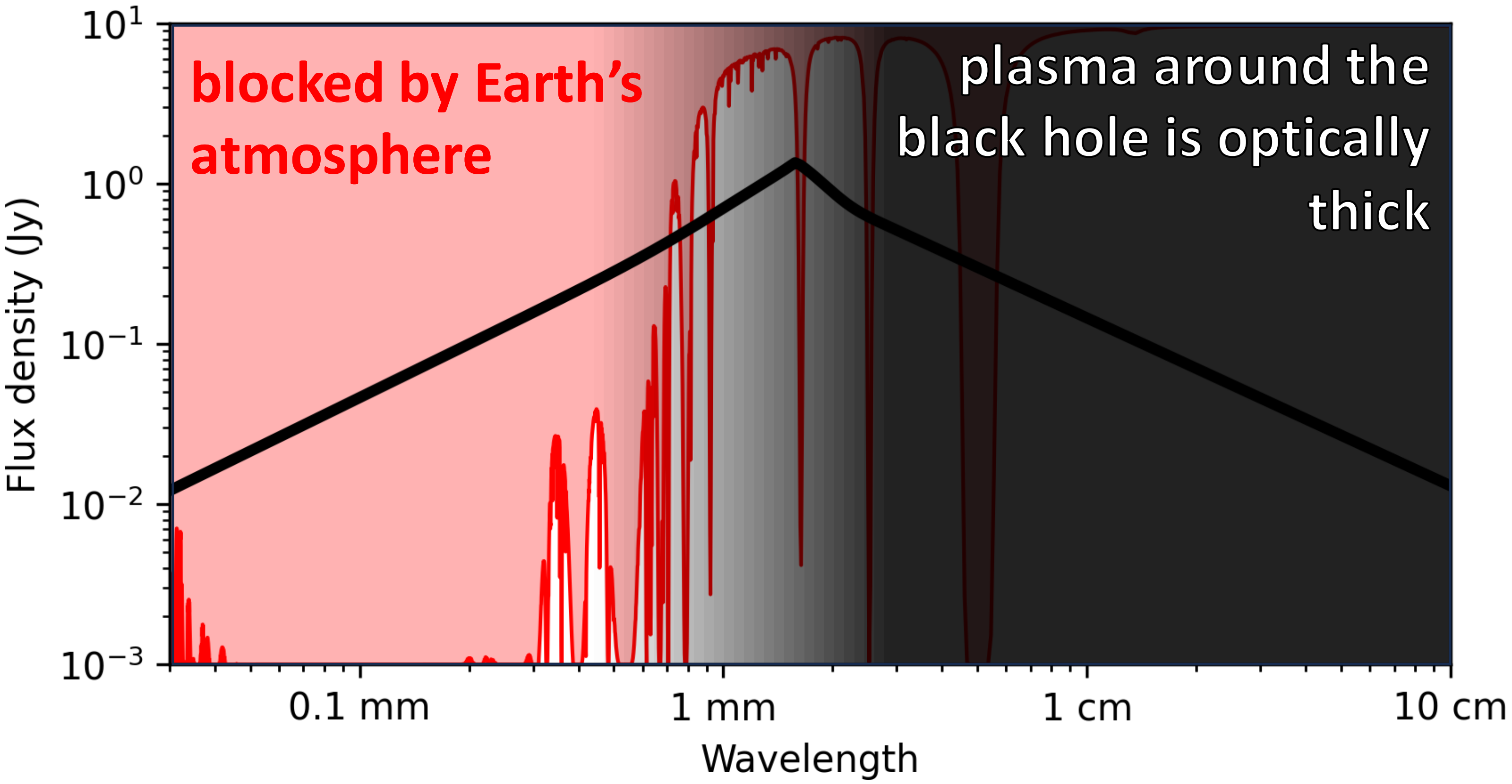

# The challenge

The primary challenge is one of angular resolution: even the largest black holes subtend tiny angles

- e.g., the shadow of the supermassive black hole in the galaxy M87 is only ~40 $\mu$as across

The best wavelength to observe at is ~1 mm

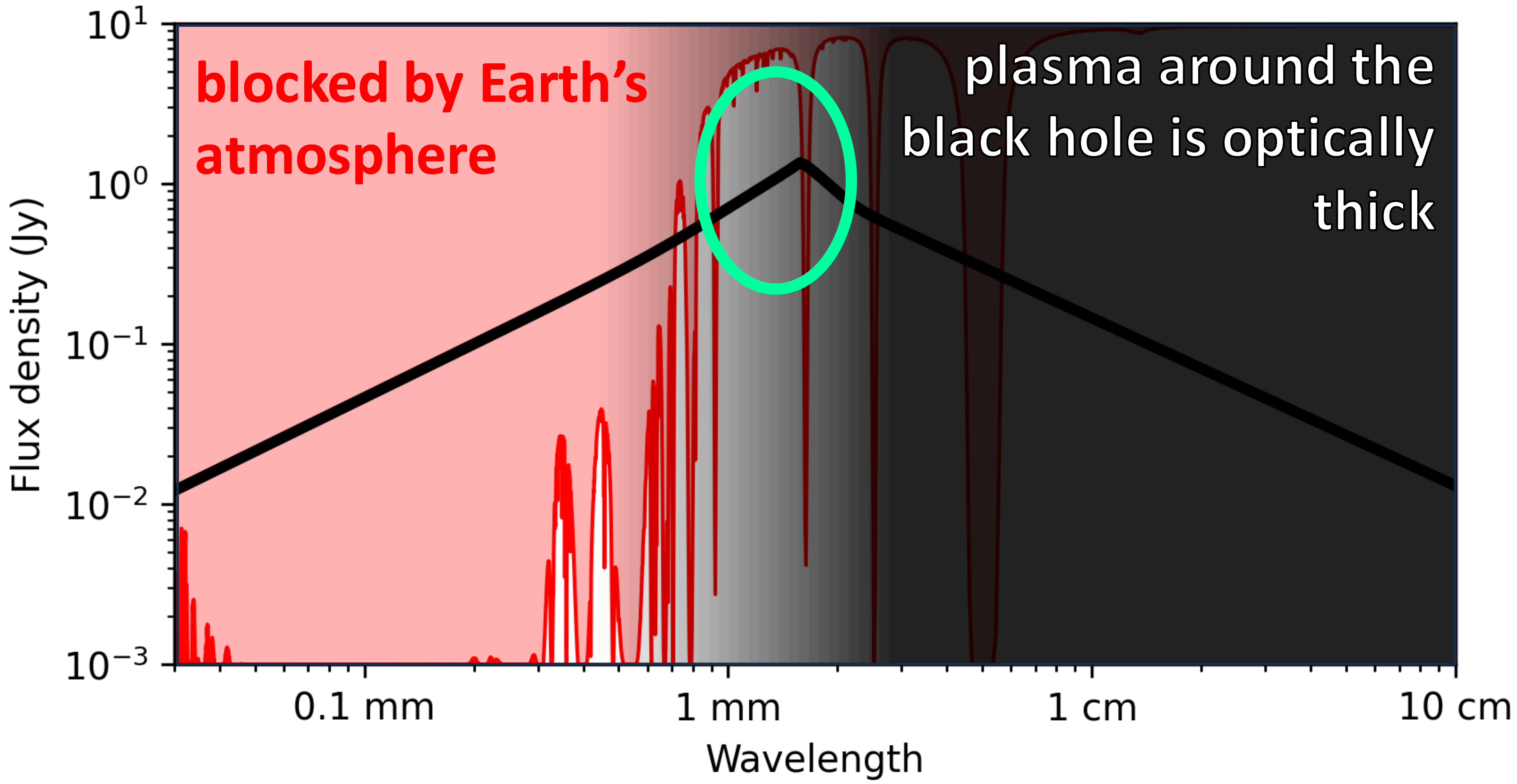

# The challenge

The primary challenge is one of angular resolution: even the largest black holes subtend tiny angles

- e.g., the shadow of the supermassive black hole in the galaxy M87 is only ~40 $\mu$as across

The best wavelength to observe at is ~1 mm

It turns out that the diffraction-limited angular resolution achievable at an observing wavelength of 1mm and using a telescope with a diameter equal to that of the Earth is about 20 $\mu$as

# The challenge

The primary challenge is one of angular resolution: even the largest black holes subtend tiny angles

- e.g., the shadow of the supermassive black hole in the galaxy M87 is only ~40 $\mu$as across

The best wavelength to observe at is ~1 mm

It turns out that the diffraction-limited angular resolution achievable at an observing wavelength of 1mm and using a telescope with a diameter equal to that of the Earth is about 20 $\mu$as

- a “cosmic conspiracy”

# The challenge

The primary challenge is one of angular resolution: even the largest black holes subtend tiny angles

- e.g., the shadow of the supermassive black hole in the galaxy M87 is only ~40 $\mu$as across

The best wavelength to observe at is ~1 mm

It turns out that the diffraction-limited angular resolution achievable at an observing wavelength of 1mm and using a telescope with a diameter equal to that of the Earth is about 20 $\mu$as

- a “cosmic conspiracy”

Enter: the Event Horizon Telescope

# The Event Horizon Telescope: 2017 edition

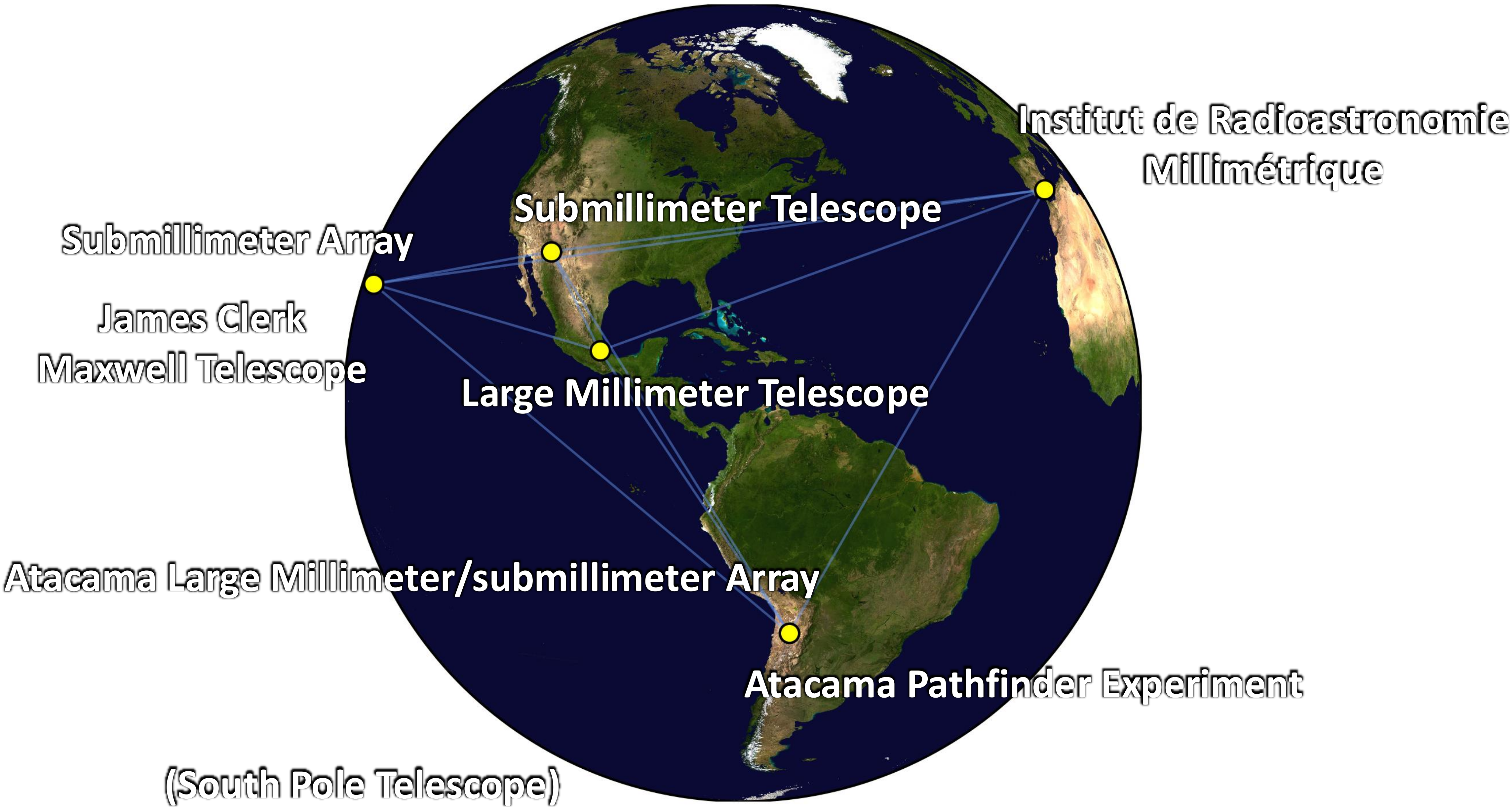

# Data journey at a glance


Raw signals
[PB]

Correlation
[TB]

Calibration
[MB]

Image
[kB]

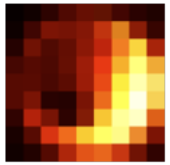

Credit: Lindy Blackburn

# Calibration: decoherence

Water vapor in the atmosphere introduces time-variable delays in wavefront arrival that manifest as phase wander in the recorded signal

Coherent integration time is limited to several seconds by atmospheric turbulence

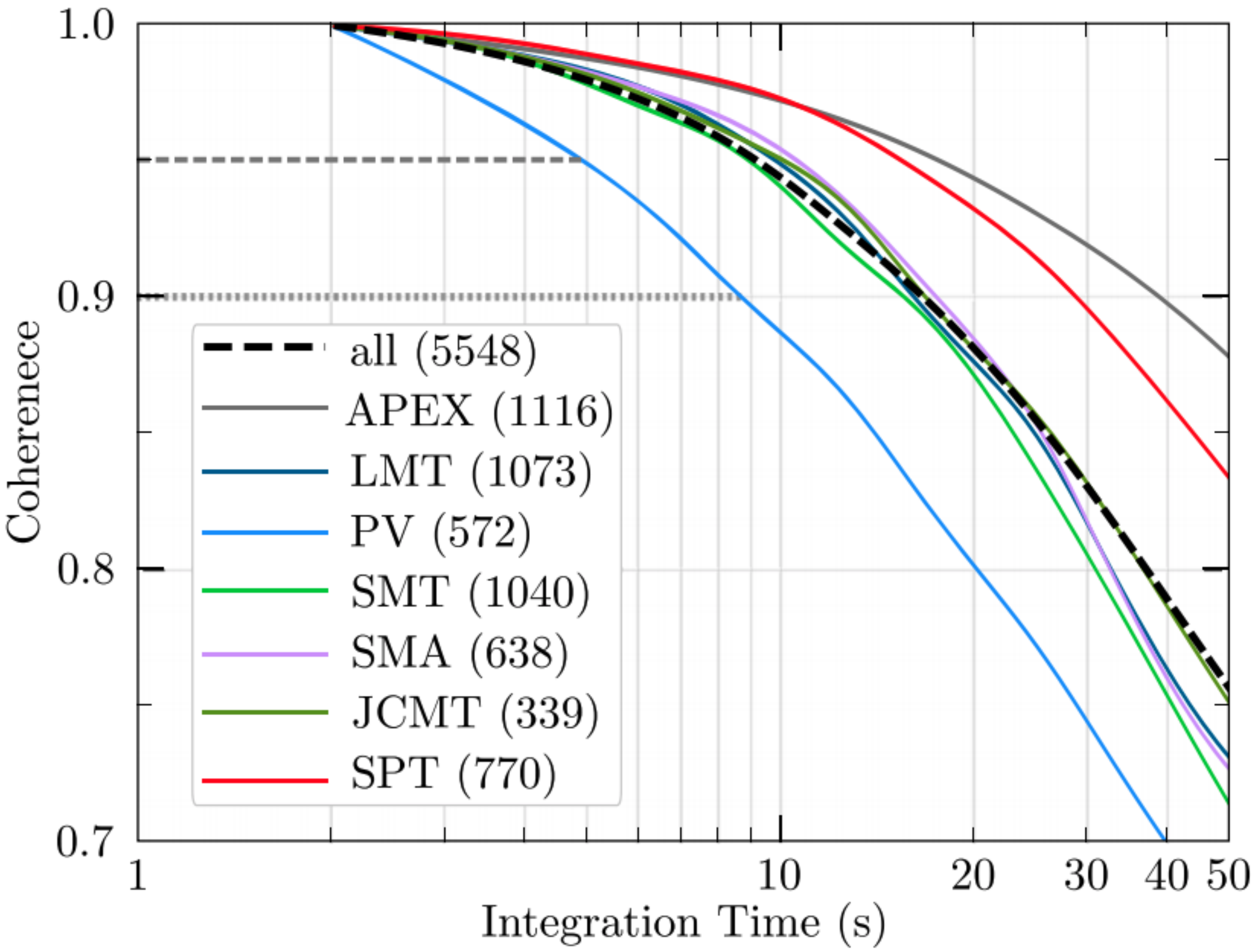


EHTC et al. (2019b)

# Calibration: closure phases

Each measurement is made on a baseline between two stations

Corruptions typically occur at individual stations

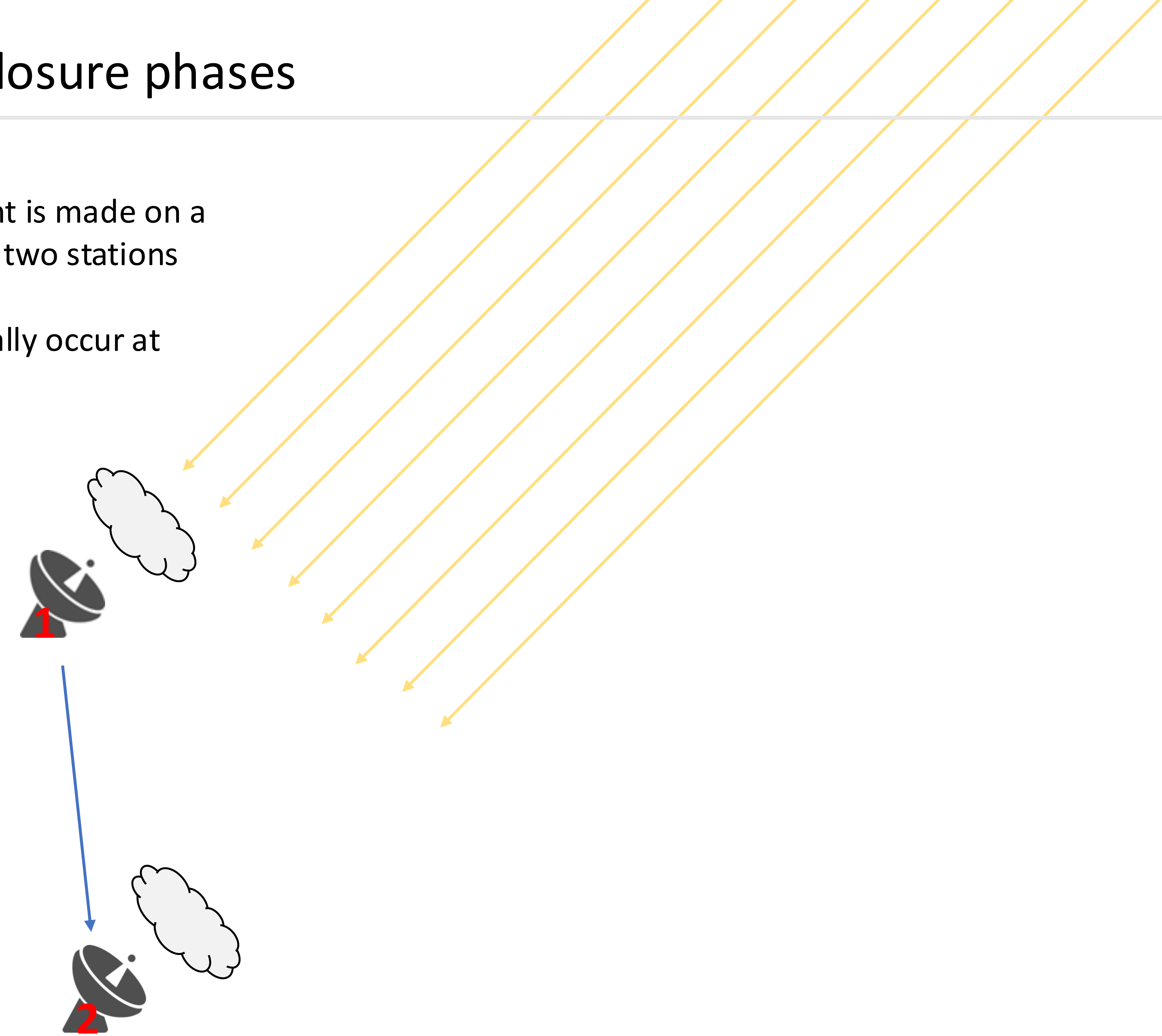

# Calibration: closure phases

Each measurement is made on a baseline between two stations

Corruptions typically occur at individual stations

$$V_{12} = \langle E_1 E_2^* \rangle = A_{12} e^{i\phi_{12}}$$

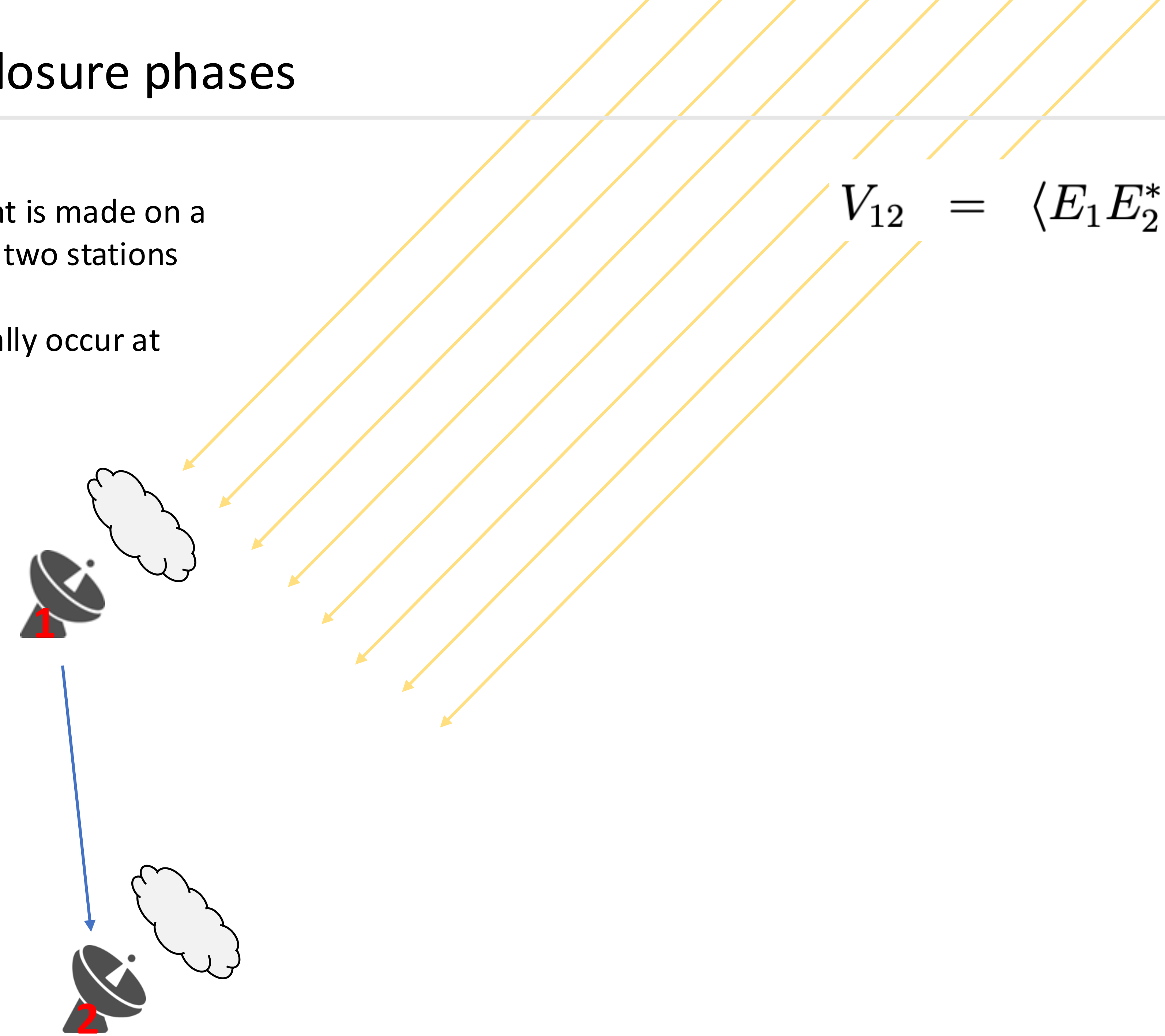

# Calibration: closure phases

Each measurement is made on a baseline between two stations

Corruptions typically occur at individual stations

$$
\begin{aligned}
V_{12} &= \langle E_1 E_2^* \rangle = A_{12} e^{i\phi_{12}} \\
\hat{V}_{12} &= \langle (G_1 E_1)(G_2 E_2)^* \rangle \\
&= G_1 \langle E_1 E_2^* \rangle G_2^* \\
&= G_1 V_{12} G_2^*
\end{aligned}
$$

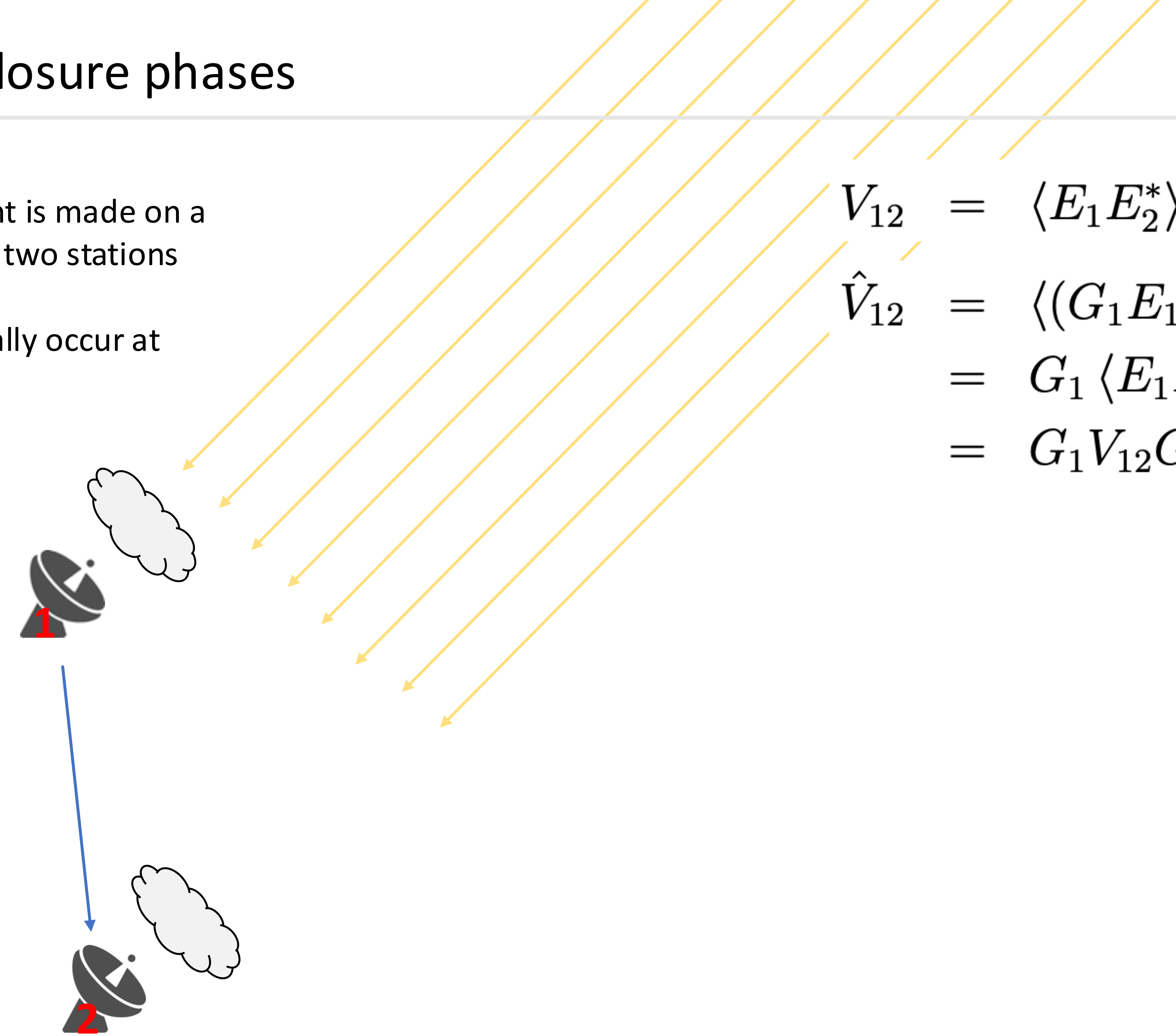

# Calibration: closure phases

Each measurement is made on a baseline between two stations

Corruptions typically occur at individual stations

$$
\begin{aligned}
V_{12} &= \langle E_1 E_2^* \rangle = A_{12} e^{i\phi_{12}} \\
\hat{V}_{12} &= \langle (G_1 E_1)(G_2 E_2)^* \rangle \\
&= G_1 \langle E_1 E_2^* \rangle G_2^* \\
&= G_1 V_{12} G_2^*
\end{aligned}
$$

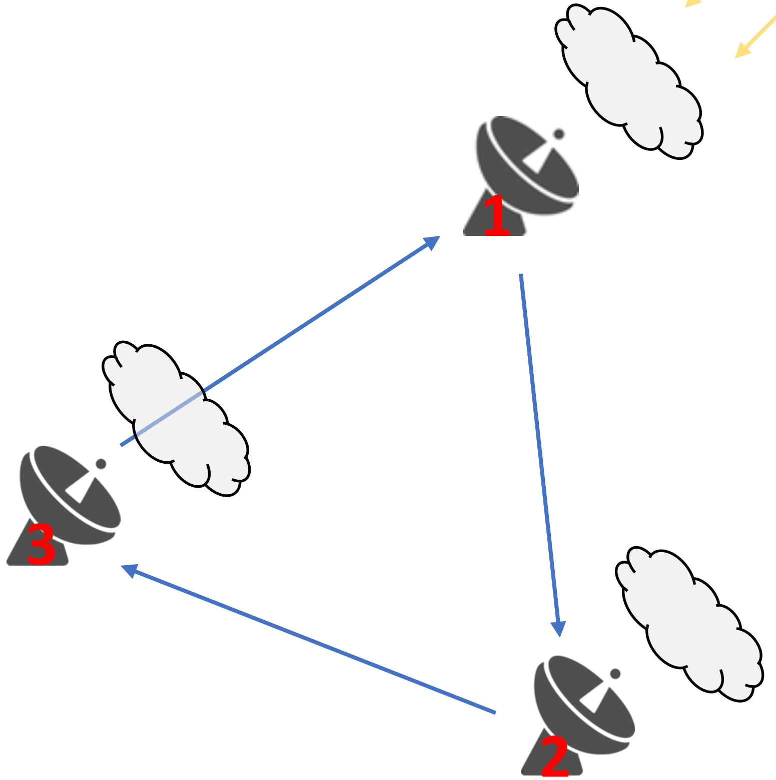


$$
\begin{aligned}
\hat{V}_{12}\hat{V}_{23}\hat{V}_{31} &= (G_1 V_{12} G_2^*)(G_2 V_{23} G_3^*)(G_3 V_{31} G_1^*) \\
&= (G_1 G_1^*)(G_2 G_2^*)(G_3 G_3^*) V_{12} V_{23} V_{31}
\end{aligned}
$$

# Calibration: closure phases

Each measurement is made on a baseline between two stations

Corruptions typically occur at individual stations

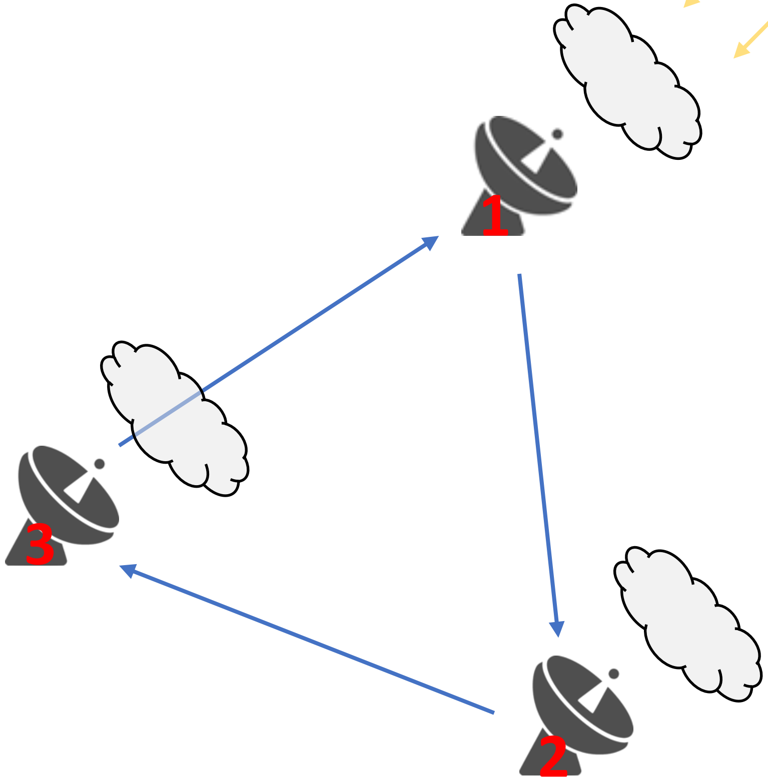


$$
\begin{aligned}
V_{12} &= \langle E_1 E_2^* \rangle = A_{12} e^{i\phi_{12}} \\
\hat{V}_{12} &= \langle (G_1 E_1)(G_2 E_2)^* \rangle \\
&= G_1 \langle E_1 E_2^* \rangle G_2^* \\
&= G_1 V_{12} G_2^*
\end{aligned}
$$

$$
\begin{aligned}
\hat{V}_{12}\hat{V}_{23}\hat{V}_{31} &= (G_1 V_{12} G_2^*)(G_2 V_{23} G_3^*)(G_3 V_{31} G_1^*) \\
&= (G_1 G_1^*)(G_2 G_2^*)(G_3 G_3^*) V_{12} V_{23} V_{31}
\end{aligned}
$$

$$
\arg\left(\hat{V}_{12}\hat{V}_{23}\hat{V}_{31}\right) = \arg\left(V_{12}V_{23}V_{31}\right)
$$

$$
\hat{\phi}_{12} + \hat{\phi}_{23} + \hat{\phi}_{31} = \phi_{12} + \phi_{23} + \phi_{31}
$$

# Calibration: phase steering

Combining closure phases with visibility phases on sensitive baselines allows us to recover the visibility phase values on weaker baselines

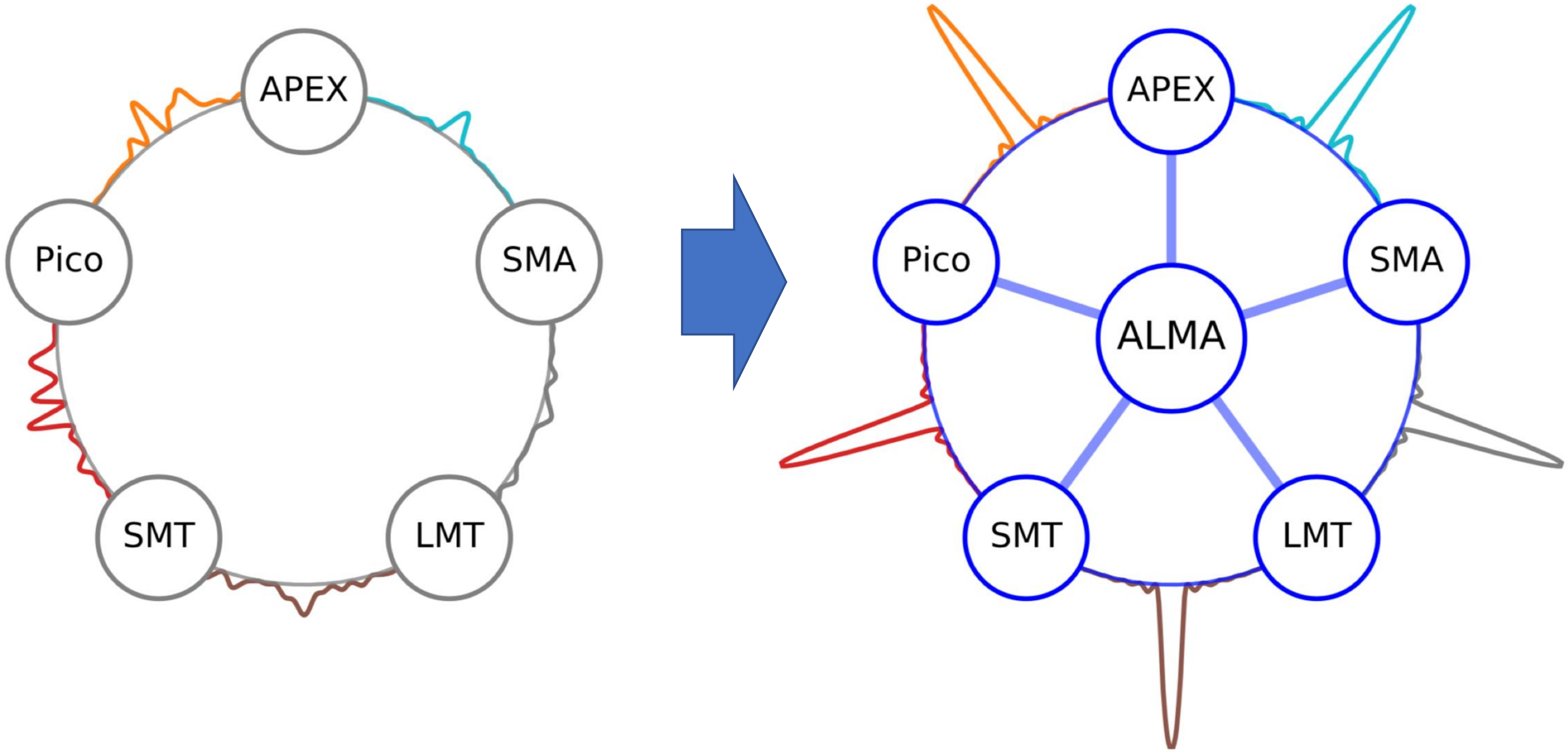


Credit: Lindy Blackburn

# Calibration: phase steering

Combining closure phases with visibility phases on sensitive baselines allows us to recover the visibility phase values on weaker baselines

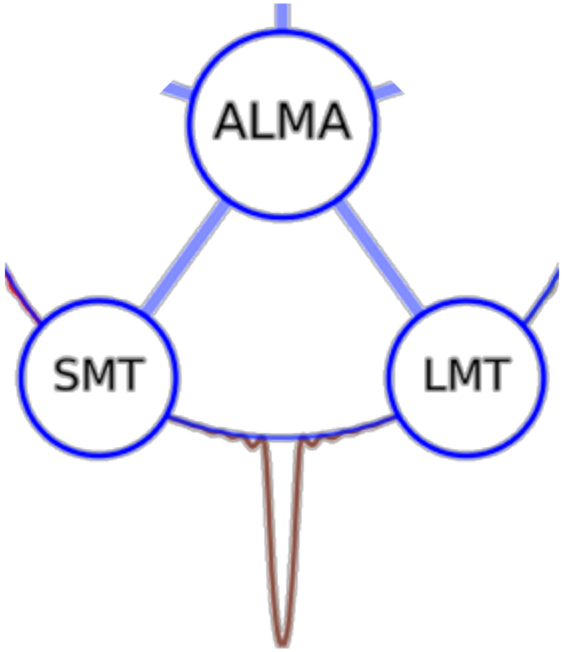


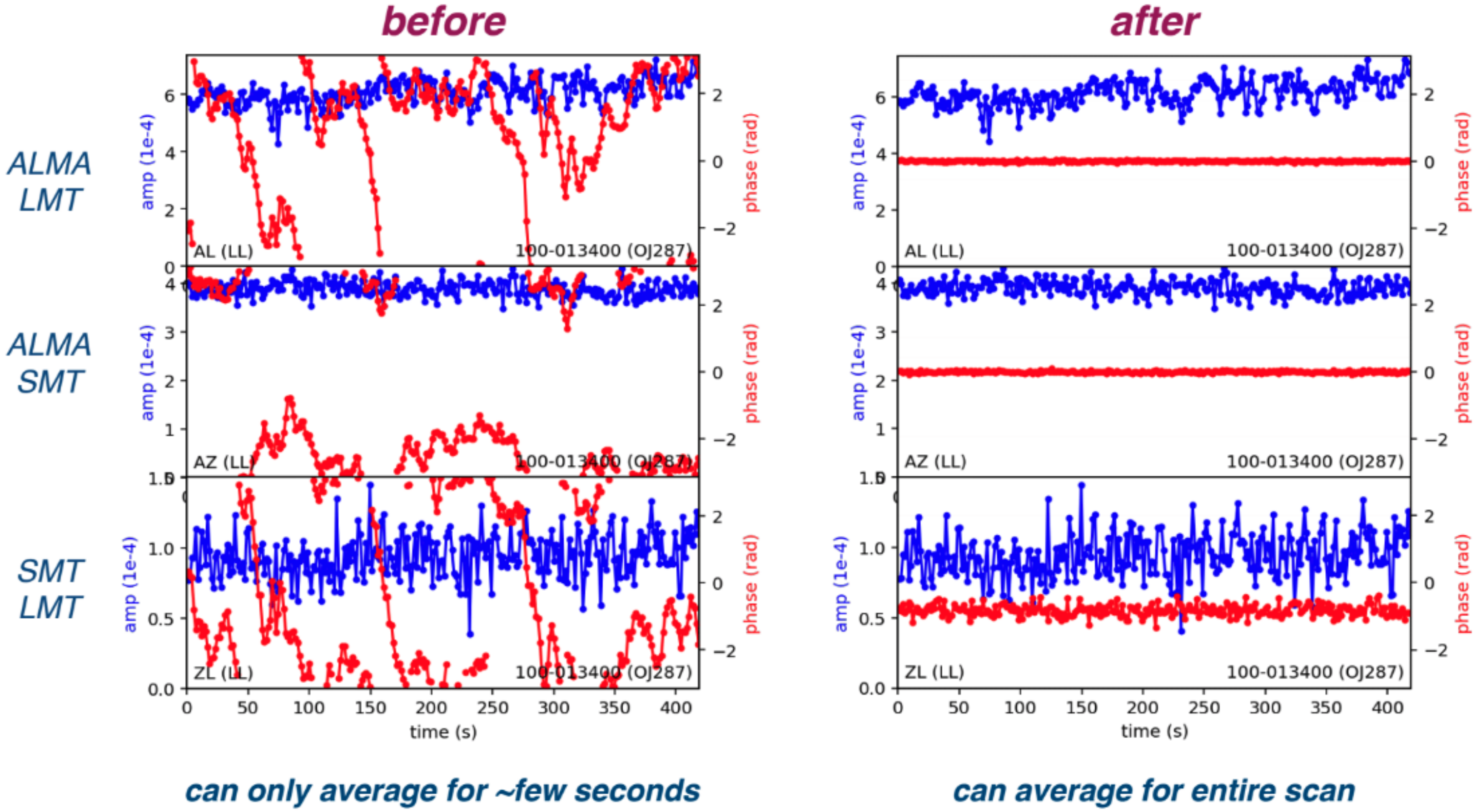


EHTC et al. (2019); Blackburn et al. (2019)

# What do the data tell us?

The visibility amplitudes show a clear “bounce,” characteristic of things like double sources

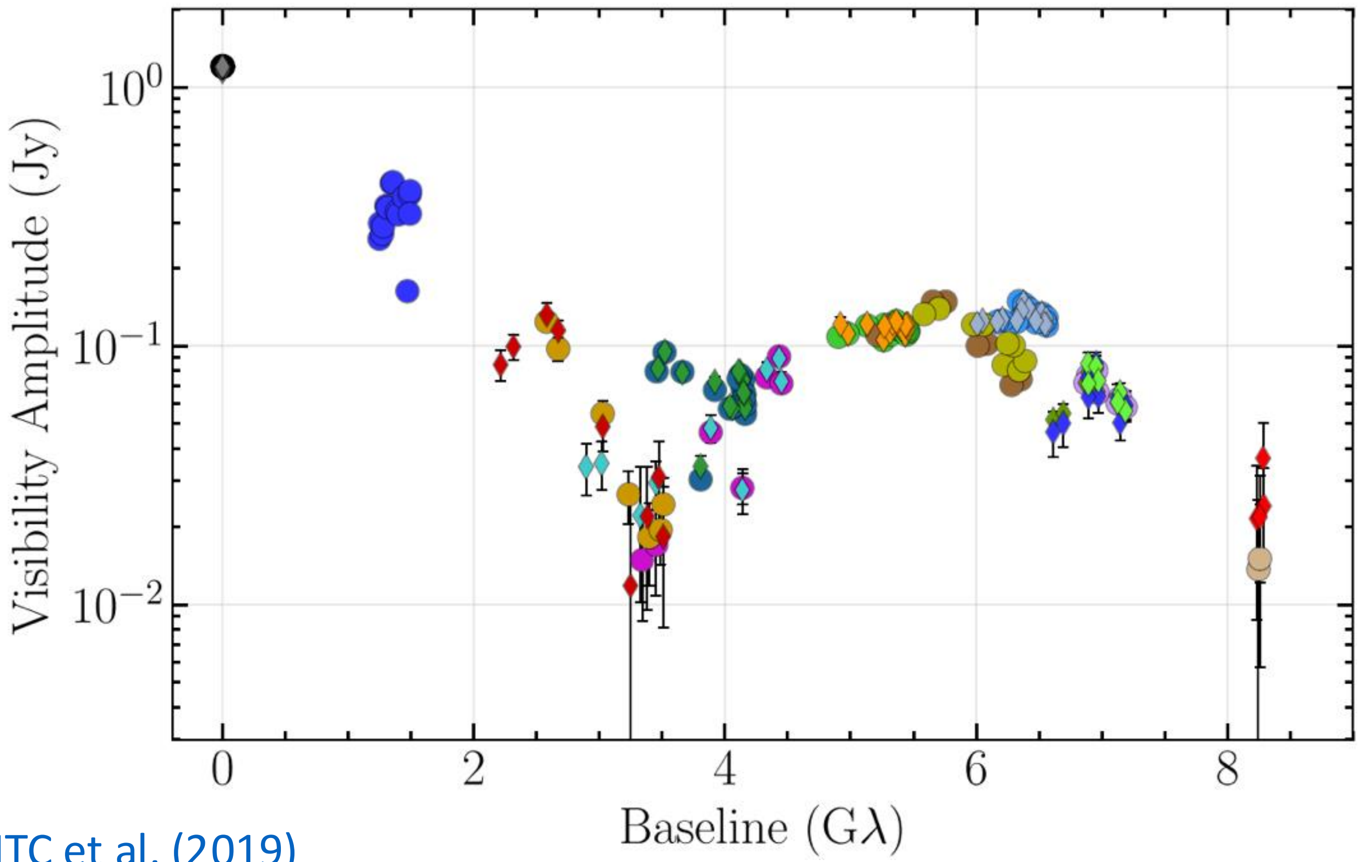


EHTC et al. (2019)

# What do the data tell us?

The visibility amplitudes show a clear “bounce,” characteristic of things like double sources

The envelope changes amplitude with orientation, but it never quite goes to zero

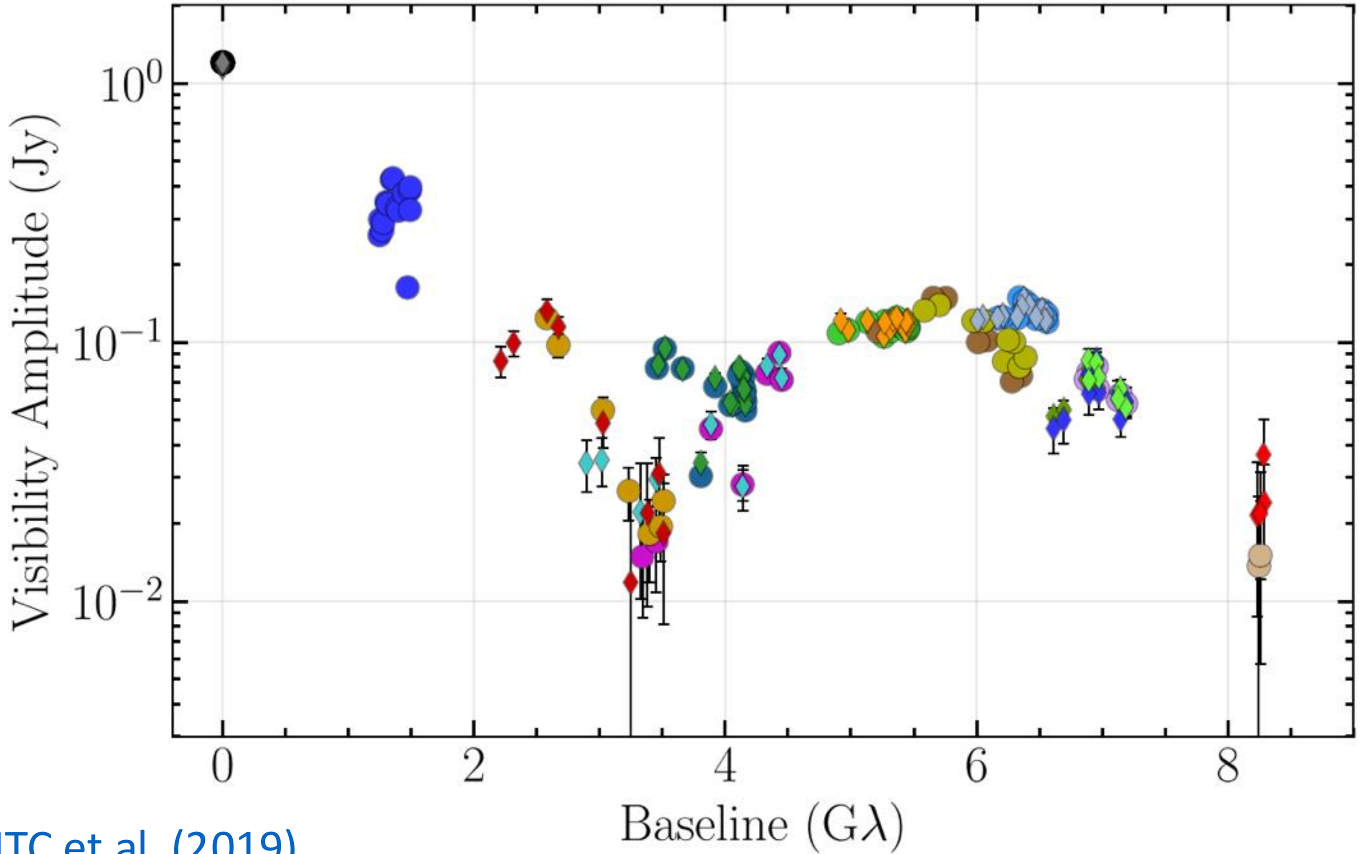


EHTC et al. (2019)

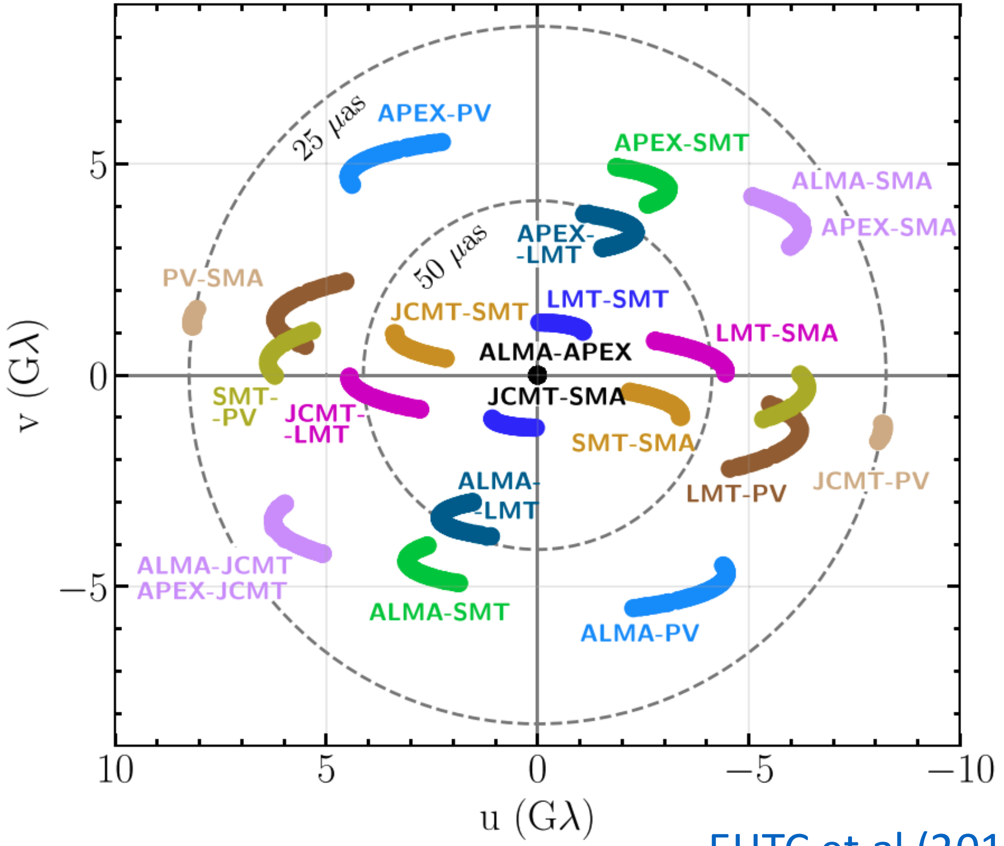


EHTC et al (2019)

# What do the data tell us?

The visibility amplitudes show a clear “bounce,” characteristic of things like double sources

The envelope changes amplitude with orientation, but it never quite goes to zero

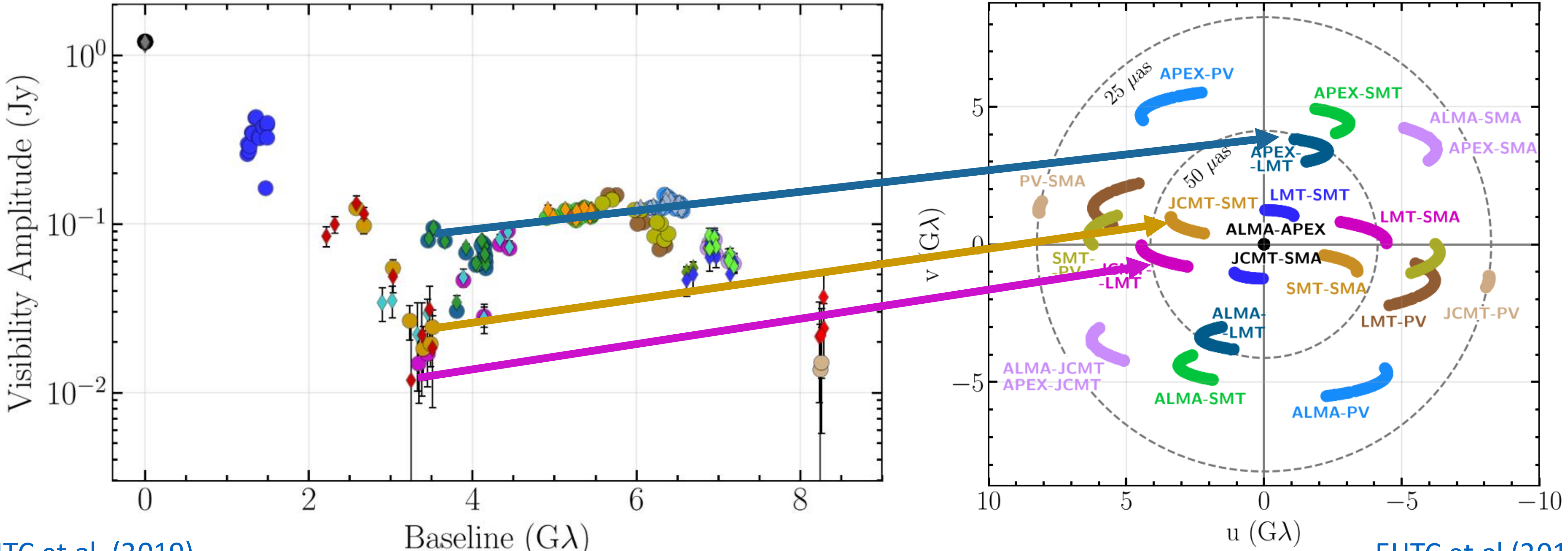


EHTC et al. (2019)

EHTC et al (2019)

# What do the data tell us?

The visibility amplitudes show a clear "bounce," characteristic of things like double sources

The envelope changes amplitude with orientation, but it never quite goes to zero

- a "double source" at all orientations?

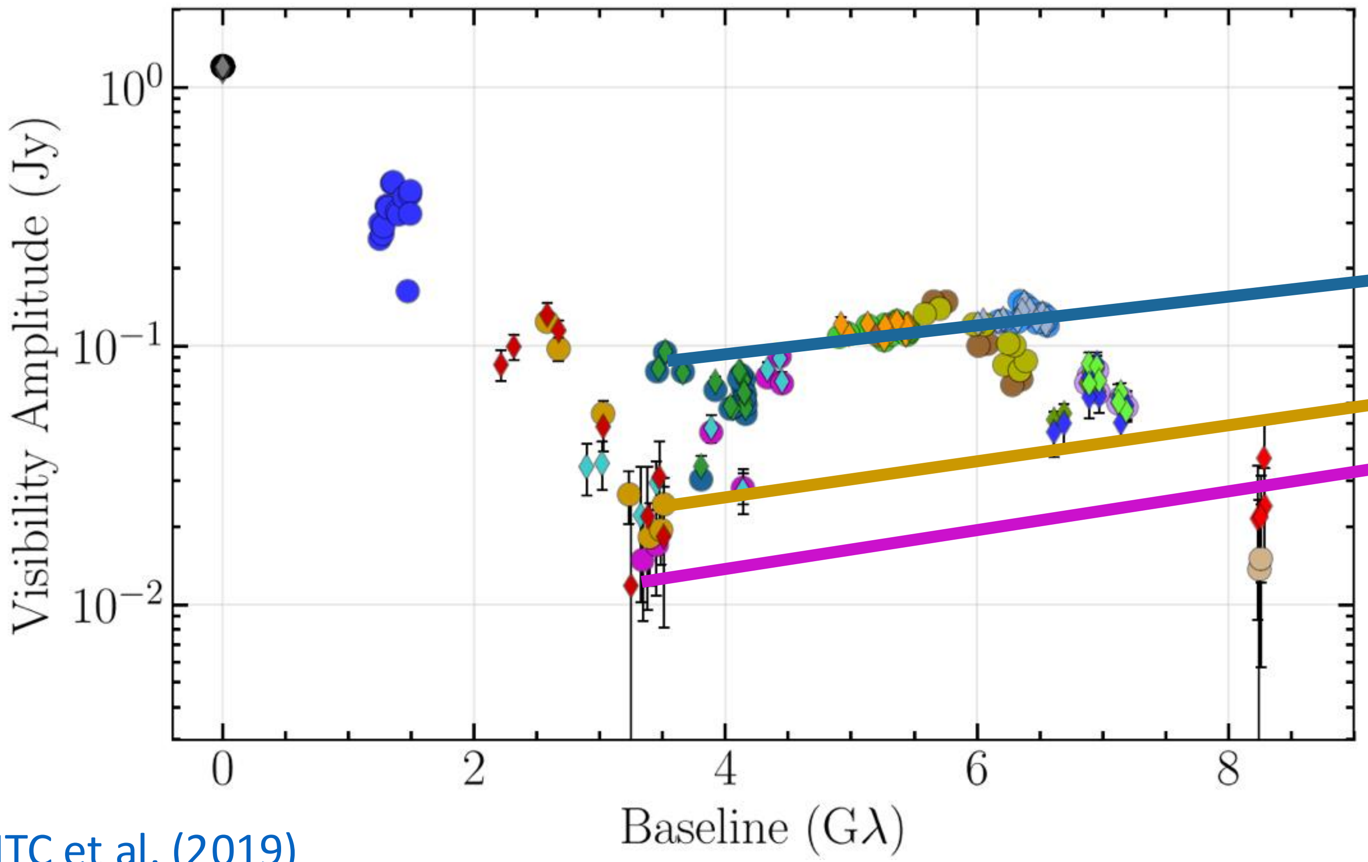


EHTC et al. (2019)

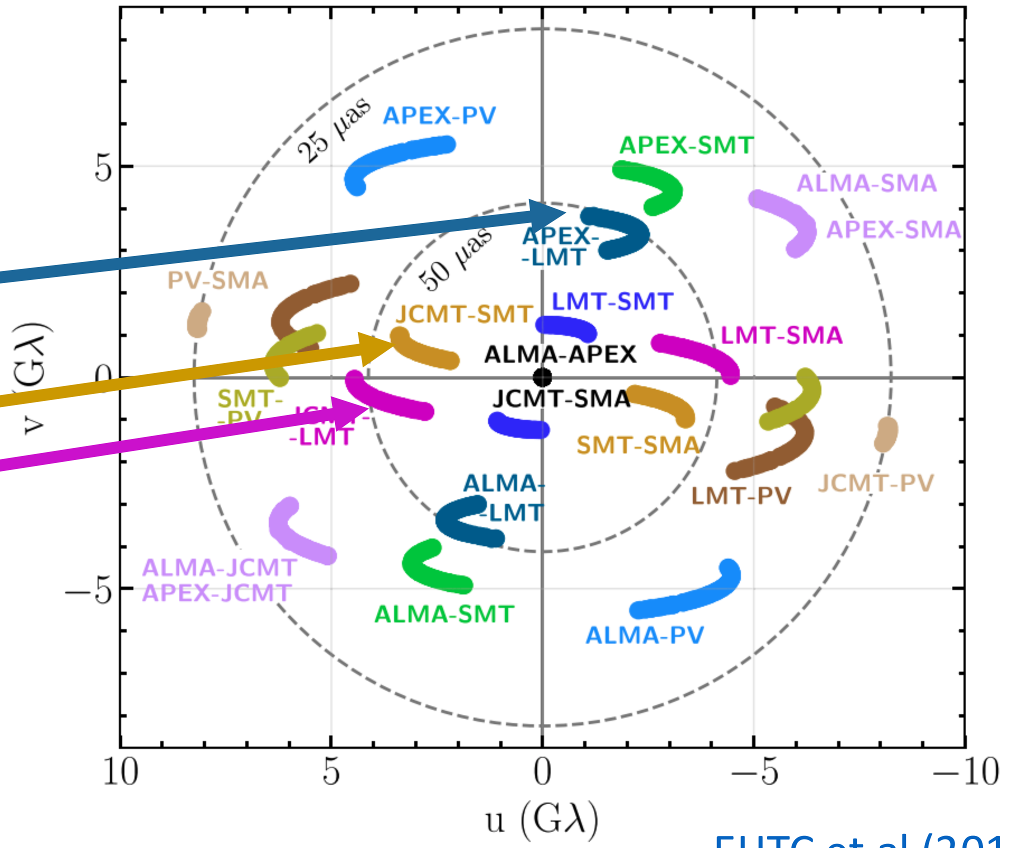


EHTC et al (2019)

# What do the data tell us?

The visibility amplitudes show a clear “bounce,” characteristic of things like double sources

The envelope changes amplitude with orientation, but it never quite goes to zero

- a “double source” at all orientations?

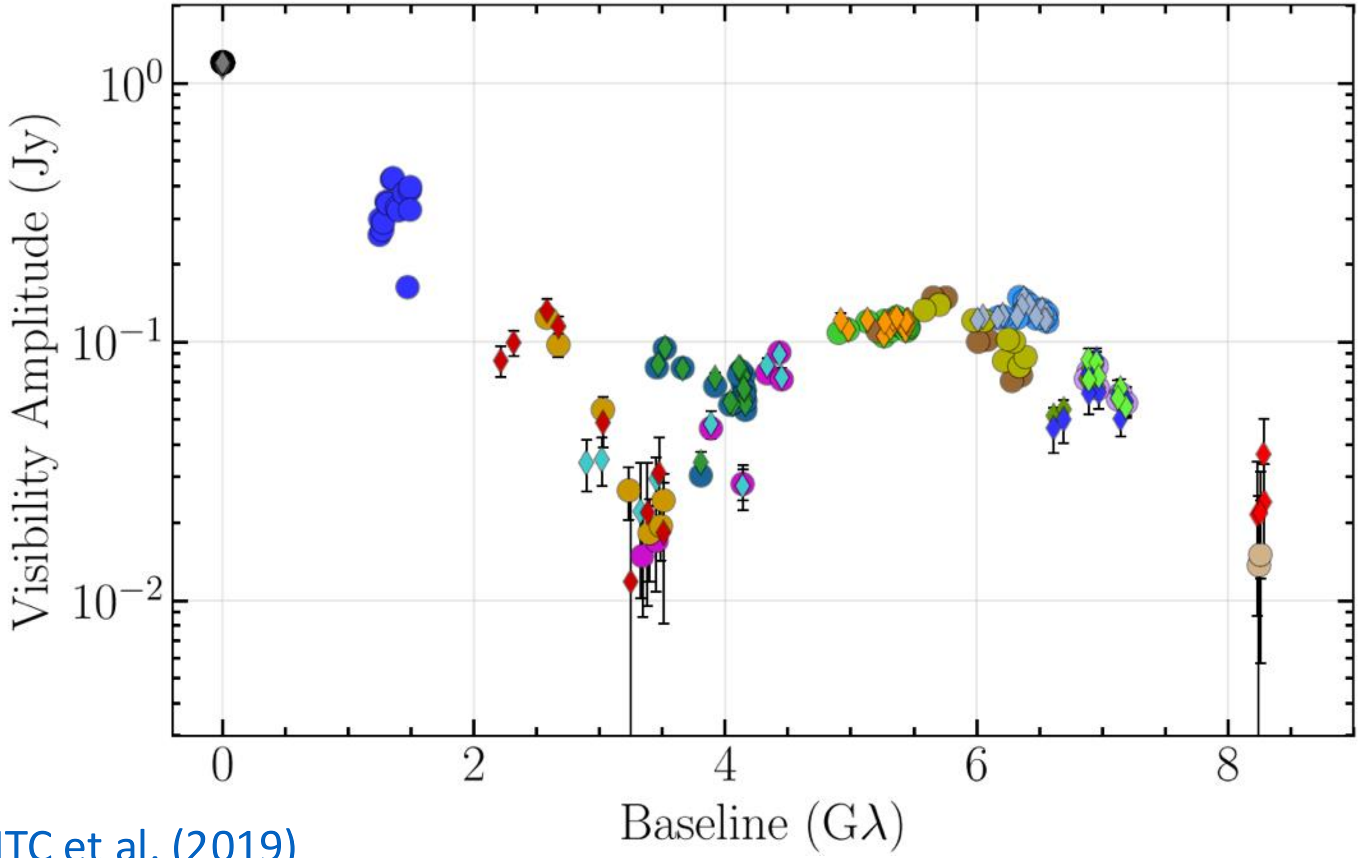


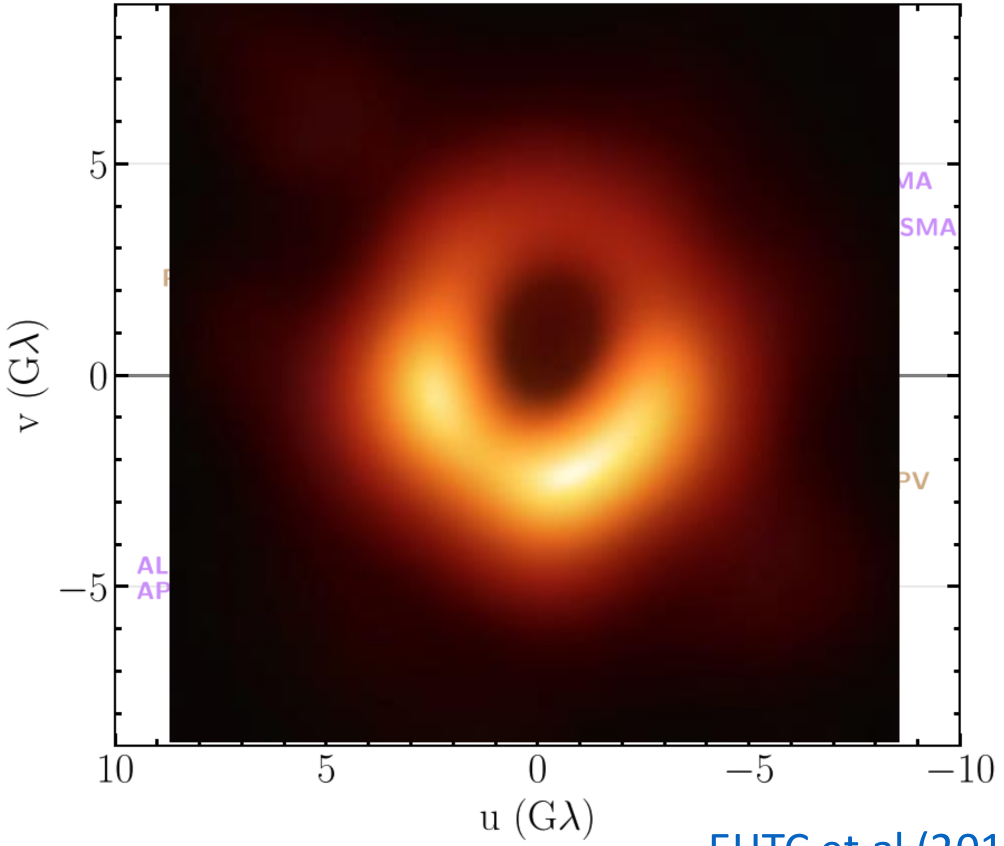


EHTC et al. (2019)

EHTC et al (2019)

# From data to image

The goal of imaging is to solve a particular inverse problem: What is the on-sky source structure corresponding to the observed complex visibilities?

# From data to image

The goal of imaging is to solve a particular inverse problem: What is the on-sky source structure corresponding to the observed complex visibilities?

- no unique solution

# From data to image

The goal of imaging is to solve a particular inverse problem: What is the on-sky source structure corresponding to the observed complex visibilities?

- no unique solution
- complicated by the presence of residual calibration errors
  - phase and amplitude “gains”
  - polarimetric “leakage”

The source structure and remaining calibration quantities must thus be solved as part of the image reconstruction process

# From data to image

The goal of imaging is to solve a particular inverse problem: What is the on-sky source structure corresponding to the observed complex visibilities?

- no unique solution
- complicated by the presence of residual calibration errors
    - phase and amplitude “gains”
    - polarimetric “leakage”

The source structure and remaining calibration quantities must thus be solved as part of the image reconstruction process

- a number of codebases/algorithms are able to carry this procedure out with varying degrees of fidelity, including some that have been developed within the EHT collaboration

Imaging algorithms that have been used in published EHT results include: difmap (Shepherd et al. 1994), LPCAL (Leppänen et al. 1995), polsolve (Martí-Vidal et al. 2021), GPCAL (Park et al. 2021), eht-imaging (Chael et al. 2016, 2018), SMILI (Akiyama et al. 2017a, 2017b), Themis (Broderick et al. 2020), DMC (Pesce 2021), Comrade.jl (Tiede 2022)

# Imaging: building confidence

1. All imaging algorithms are validated using synthetic EHT-like data

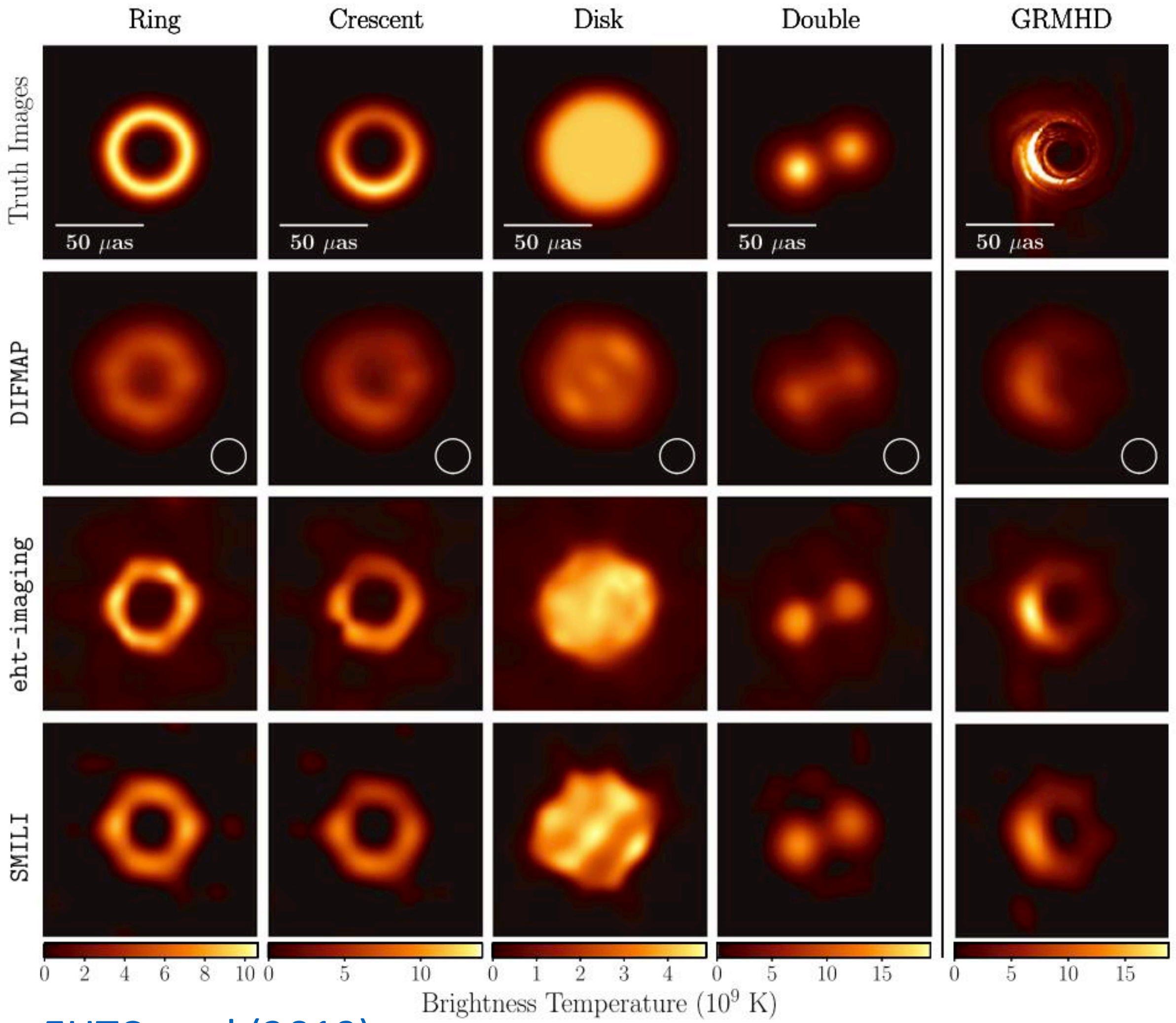


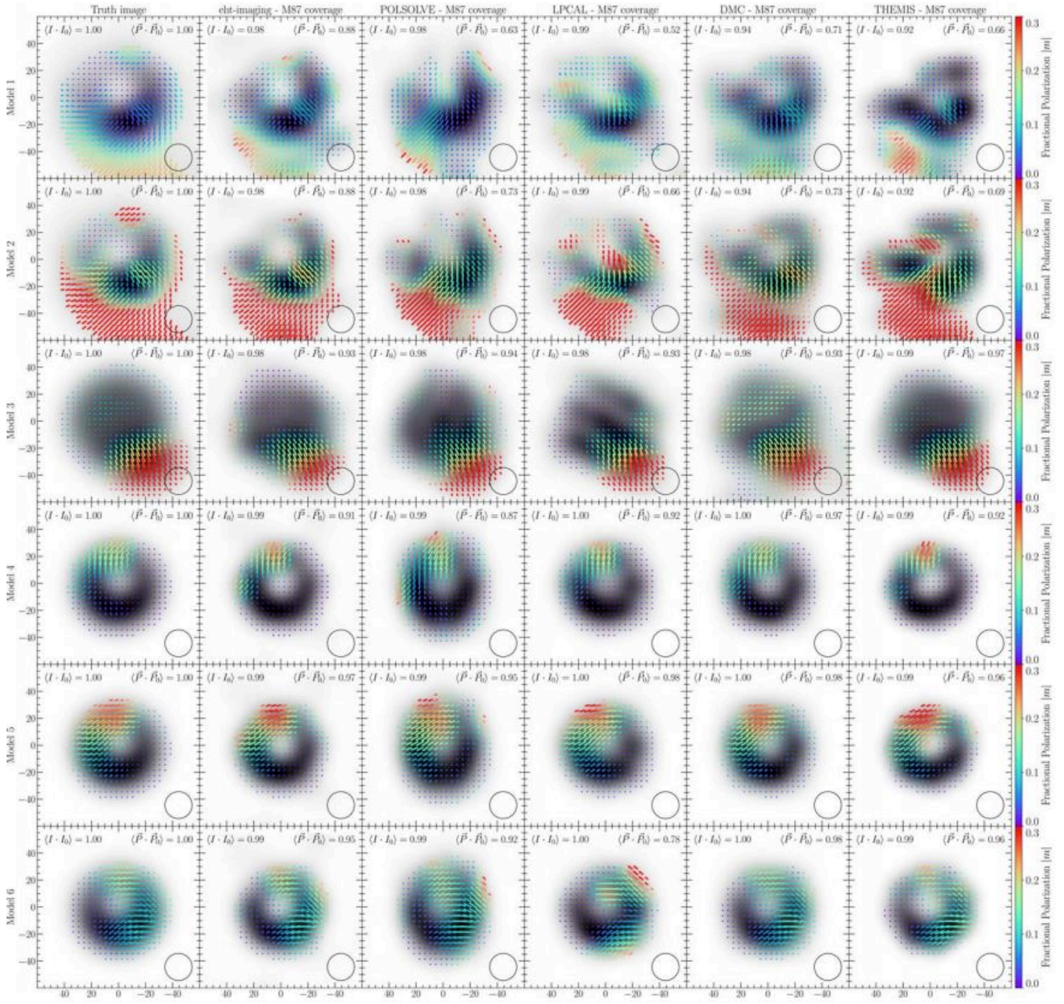


EHTC et al (2019)

EHTC et al. (2021)

# Imaging: building confidence

1. All imaging algorithms are validated using synthetic EHT-like data

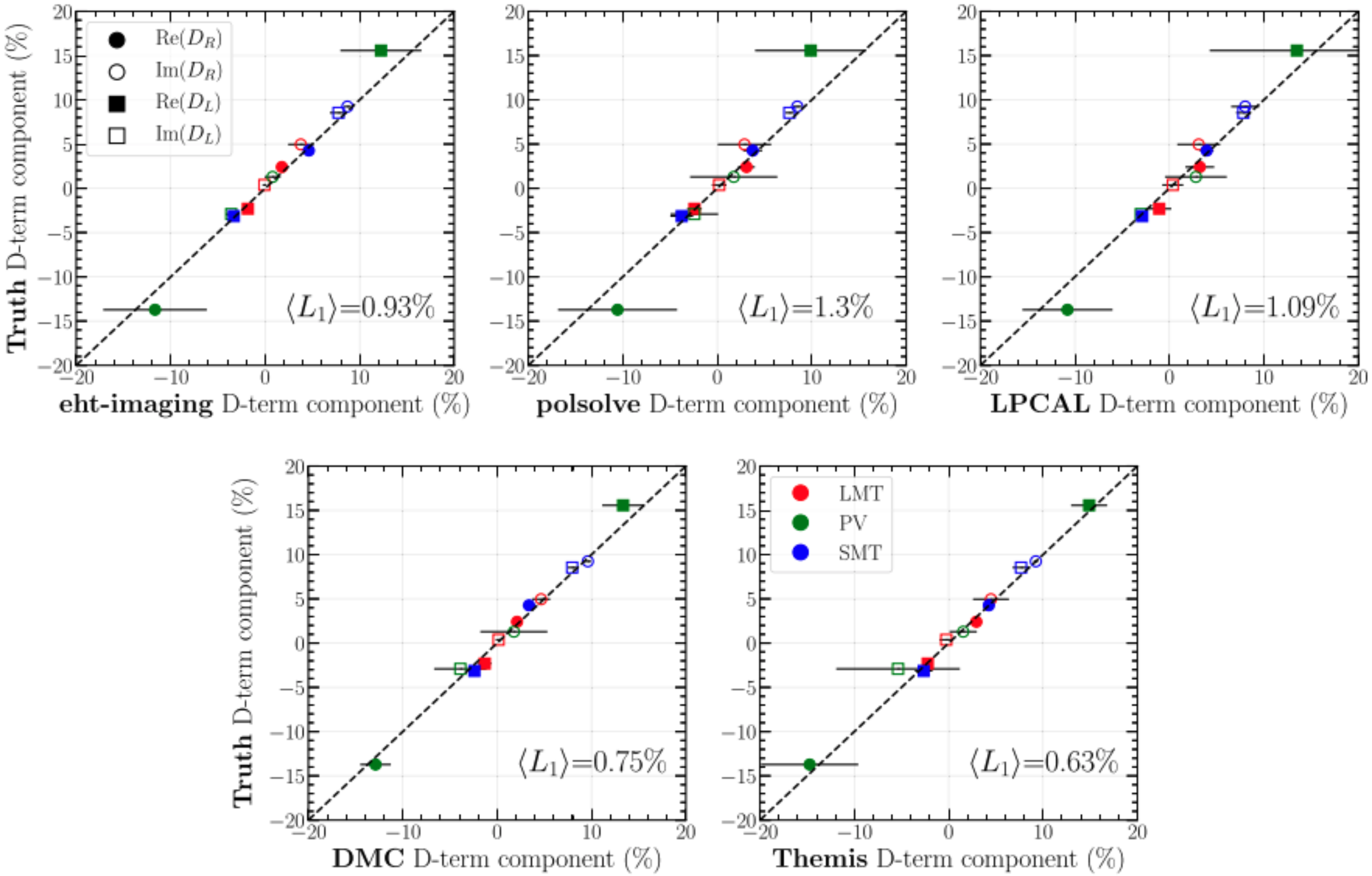


EHTC et al. (2021)

# Imaging: building confidence

1. All imaging algorithms are validated using synthetic EHT-like data
2. The very first EHT imaging results on real data were carried out by four independent teams that were blind to one another's results

The Americas

Harvard-Smithsonian
University of Arizona
U. Concepcion

Global

MIT Haystack
Radboud University
NAOJ

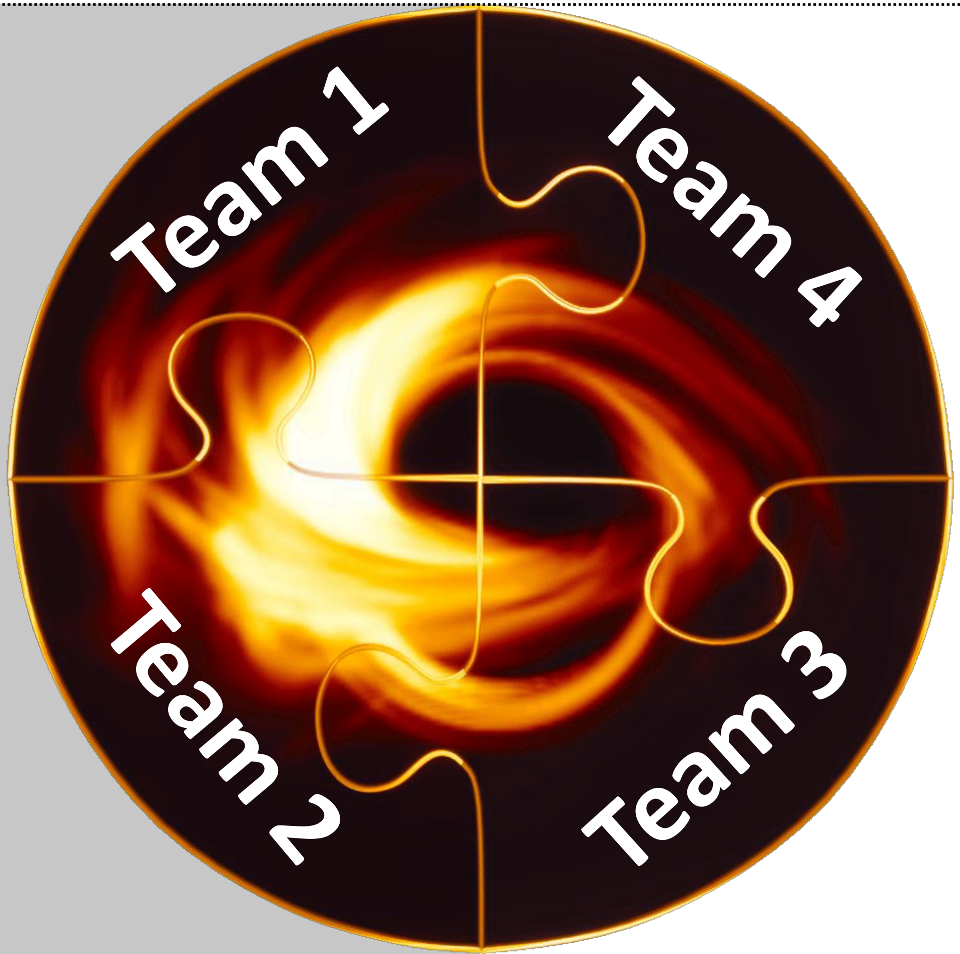


East Asia

ASIAA
KASI
NAOJ

Cross-Atlantic

MPIfR
Boston University
IAA
Aalto

Slide credit: Katie Bouman

# Imaging: building confidence

1. All imaging algorithms are validated using synthetic EHT-like data
2. The very first EHT imaging results on real data were carried out by four independent teams that were blind to one another's results

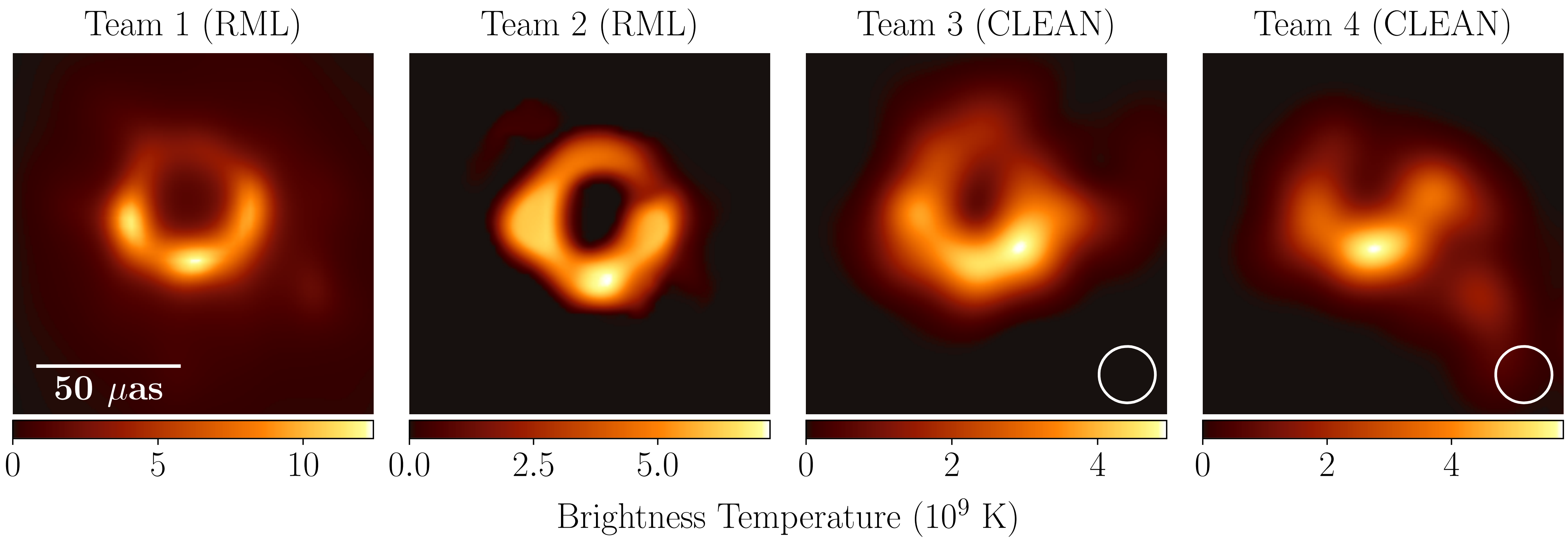


EHTC et al. (2019)

# Imaging: building confidence

1. All imaging algorithms are validated using synthetic EHT-like data
2. The very first EHT imaging results on real data were carried out by four independent teams that were blind to one another's results
3. Extensive hyper-parameter exploration is done following initial imaging

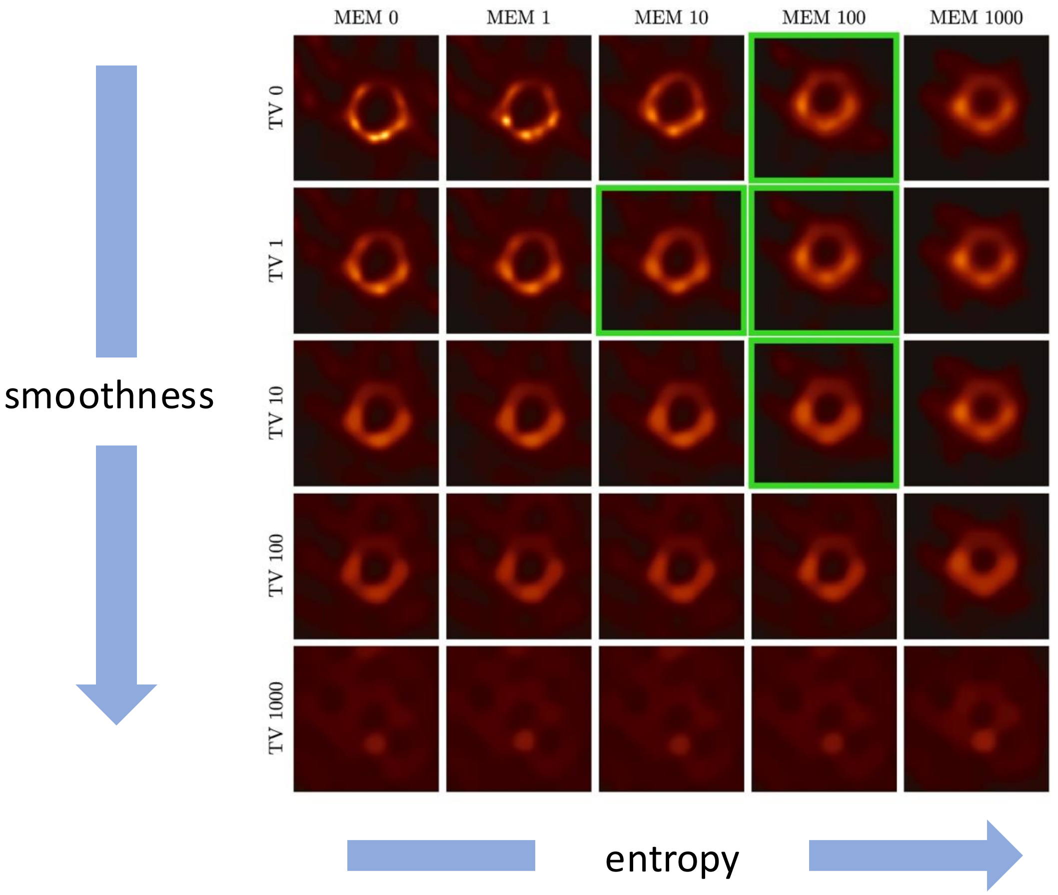


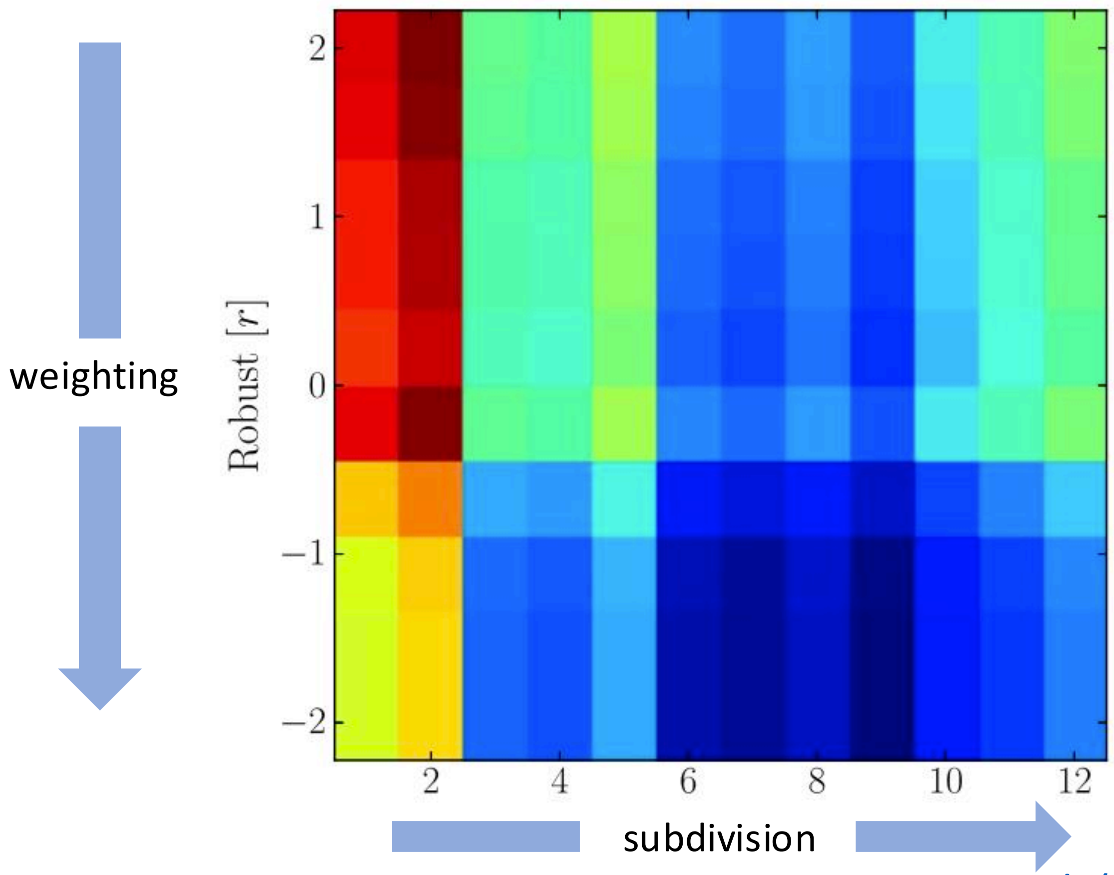


EHTC et al. (2019)

EHTC et al. (2021)

# Imaging: building confidence

1. All imaging algorithms are validated using synthetic EHT-like data
2. The very first EHT imaging results on real data were carried out by four independent teams that were blind to one another's results
3. Extensive hyper-parameter exploration is done following initial imaging
4. Maximally conservative images are constructed by combining the results from all methods

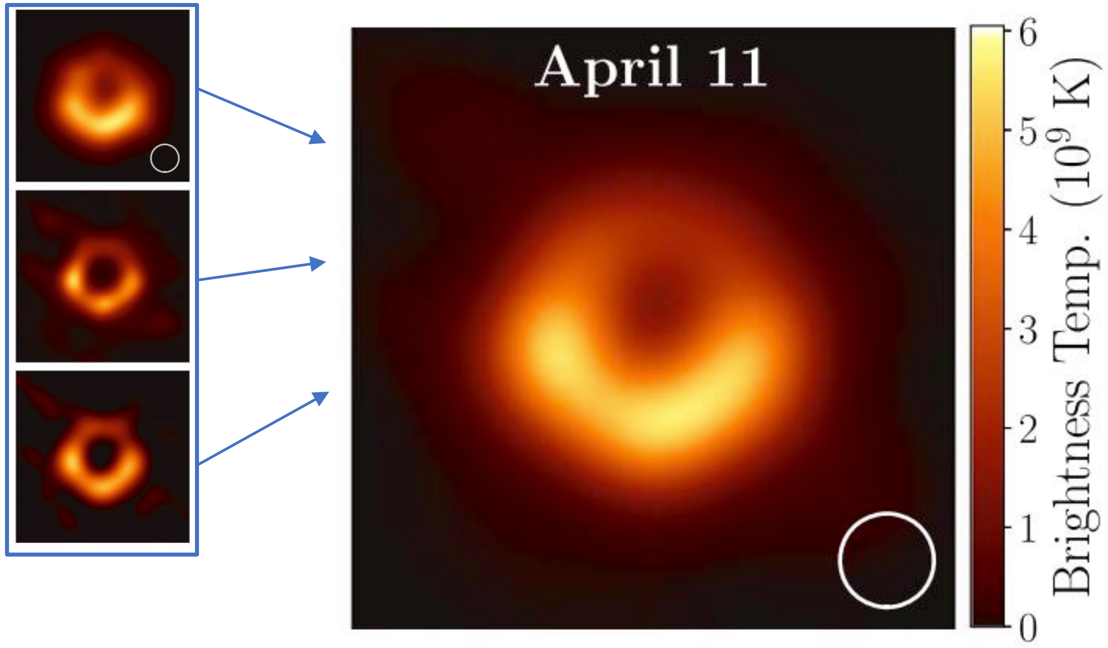


EHTC et al. (2019)

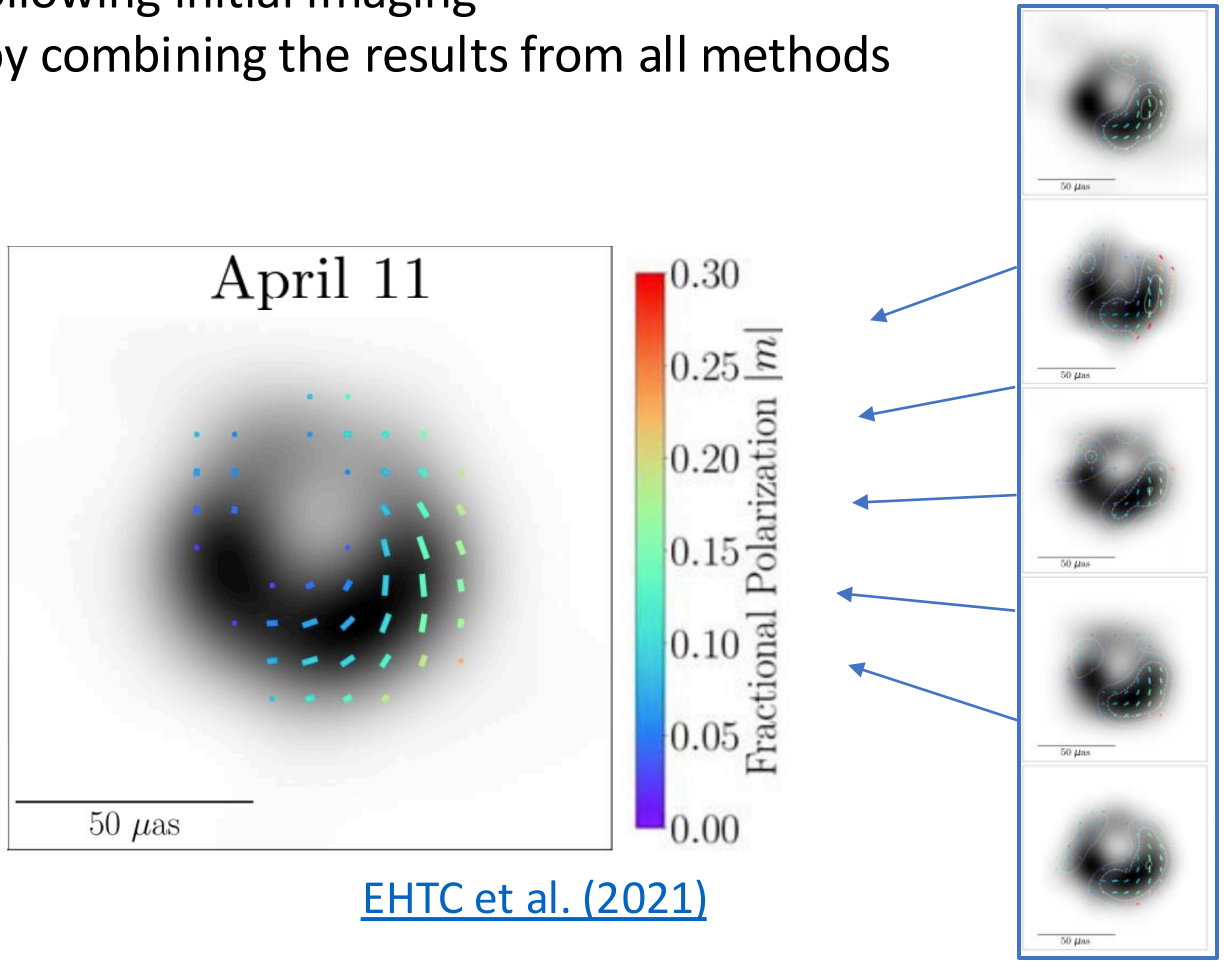


EHTC et al. (2021)

# Imaging: building confidence

1. All imaging algorithms are validated using synthetic EHT-like data
2. The very first EHT imaging results on real data were carried out by four independent teams that were blind to one another's results
3. Extensive hyper-parameter exploration is done following initial imaging
4. Maximally conservative images are constructed by combining the results from all methods
5. Image structures are confirmed across different days and different frequency bands

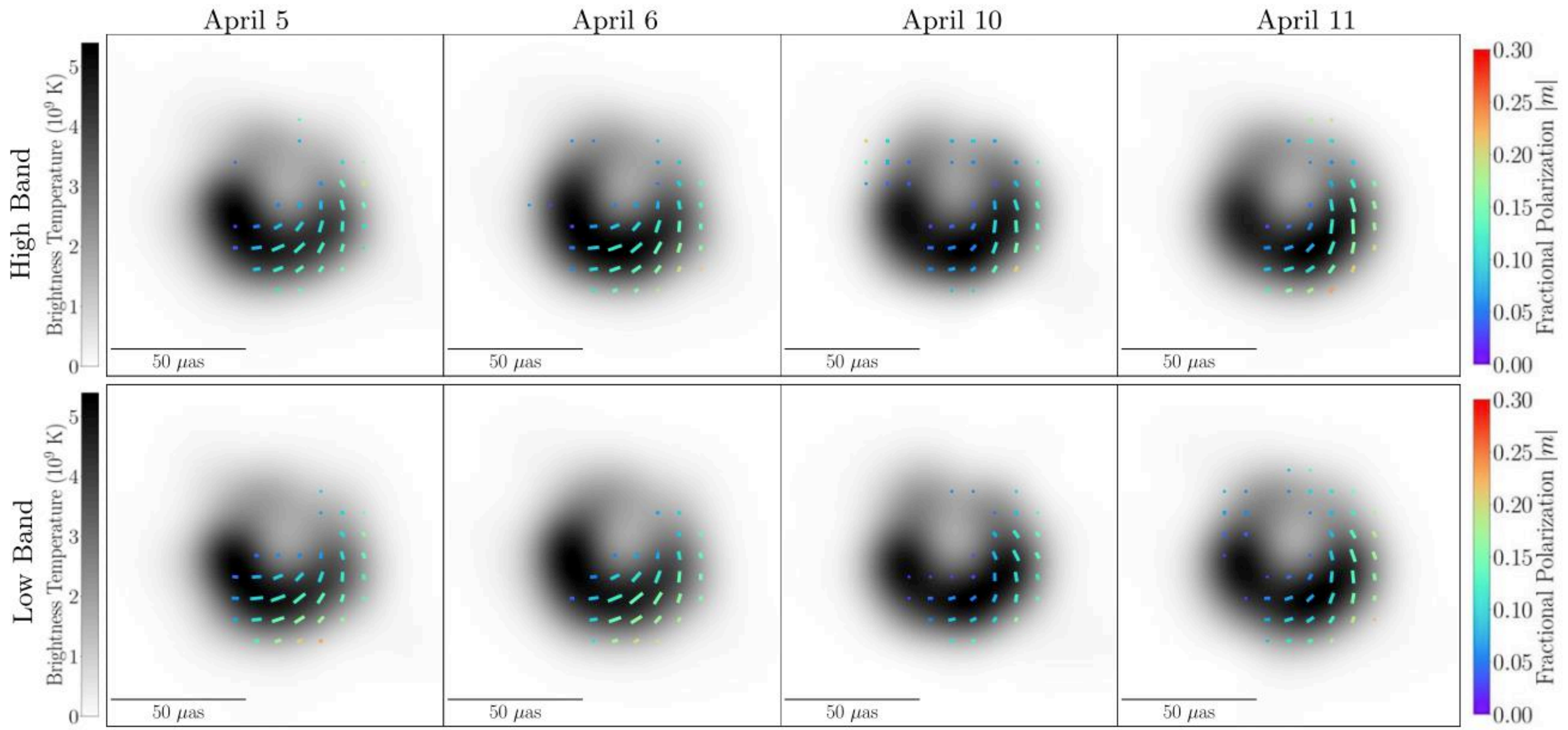


EHTC et al. (2021)

# What do the images tell us?

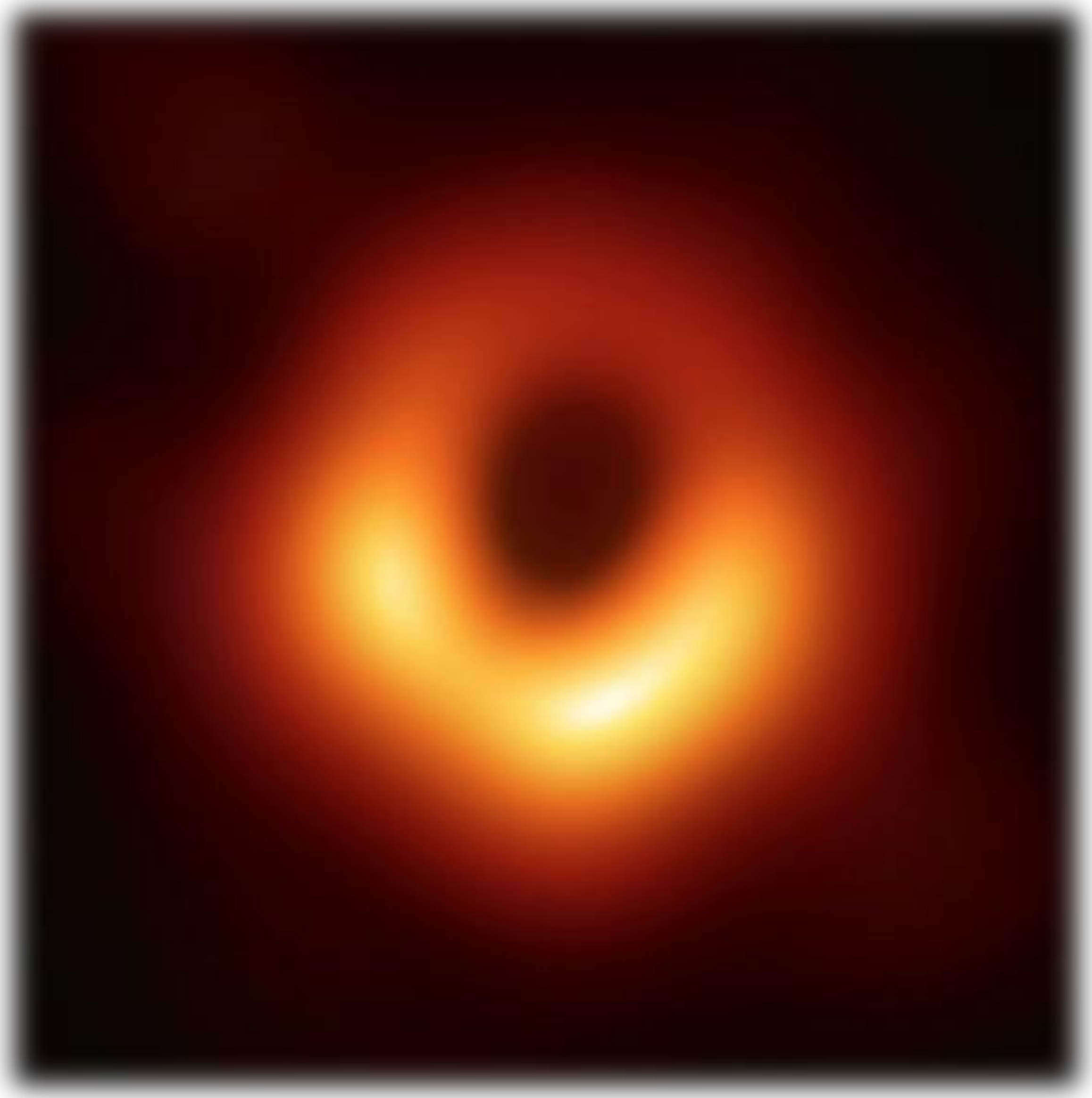

EHTC et al. (2019)

# What do the images tell us?

The diameter of the emission region tells us about the mass of the black hole

- We measure the mass to be 6.5 (±0.7) billion solar masses

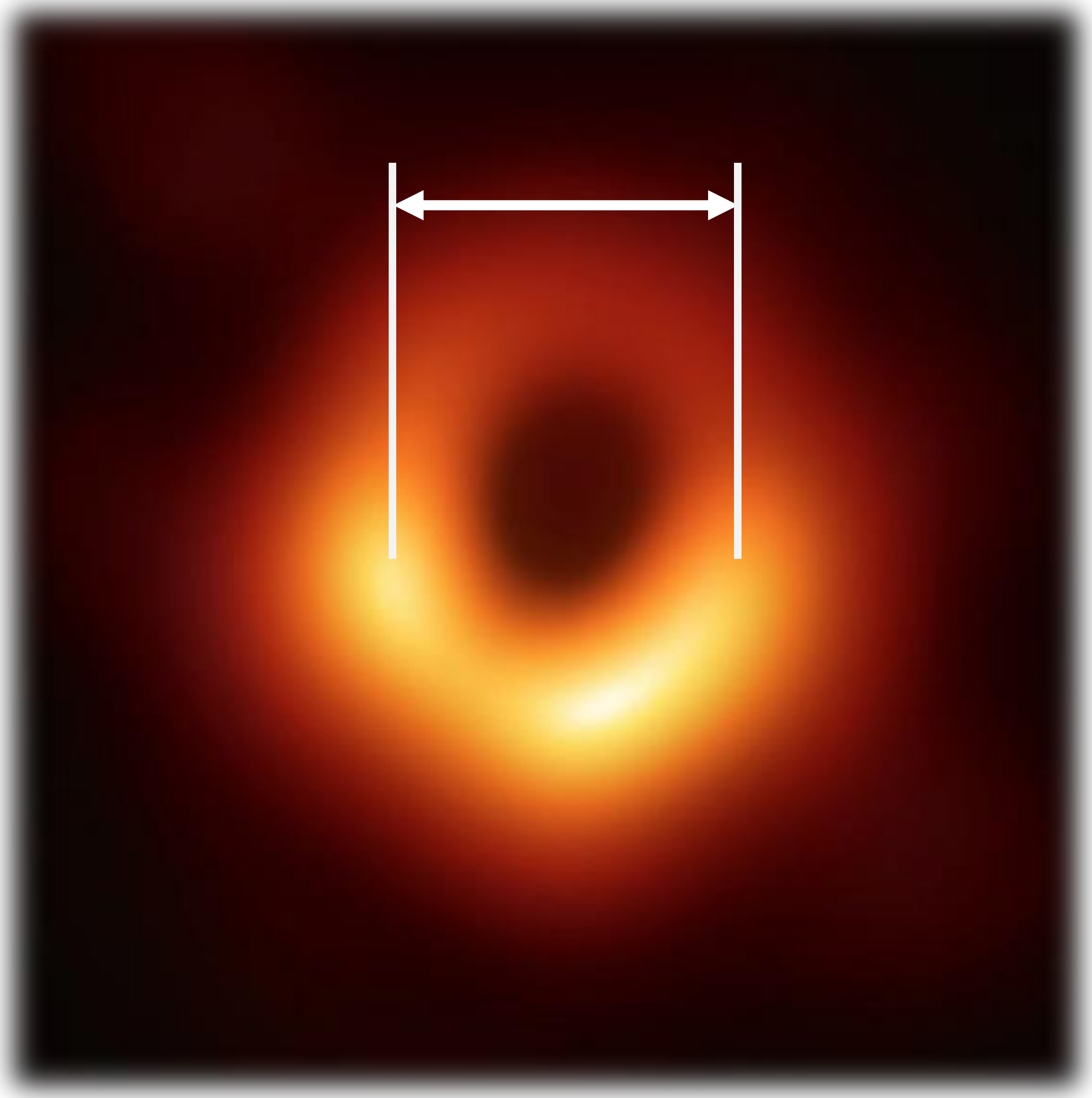

EHTC et al. (2019)

# What do the images tell us?

The diameter of the emission region tells us about the mass of the black hole

- We measure the mass to be 6.5 (±0.7) billion solar masses

The asymmetry of the emission tells us about the black hole’s angular momentum

- Given the large-scale jet axis and the assumption of prograde motion, the black hole spin axis points away from Earth

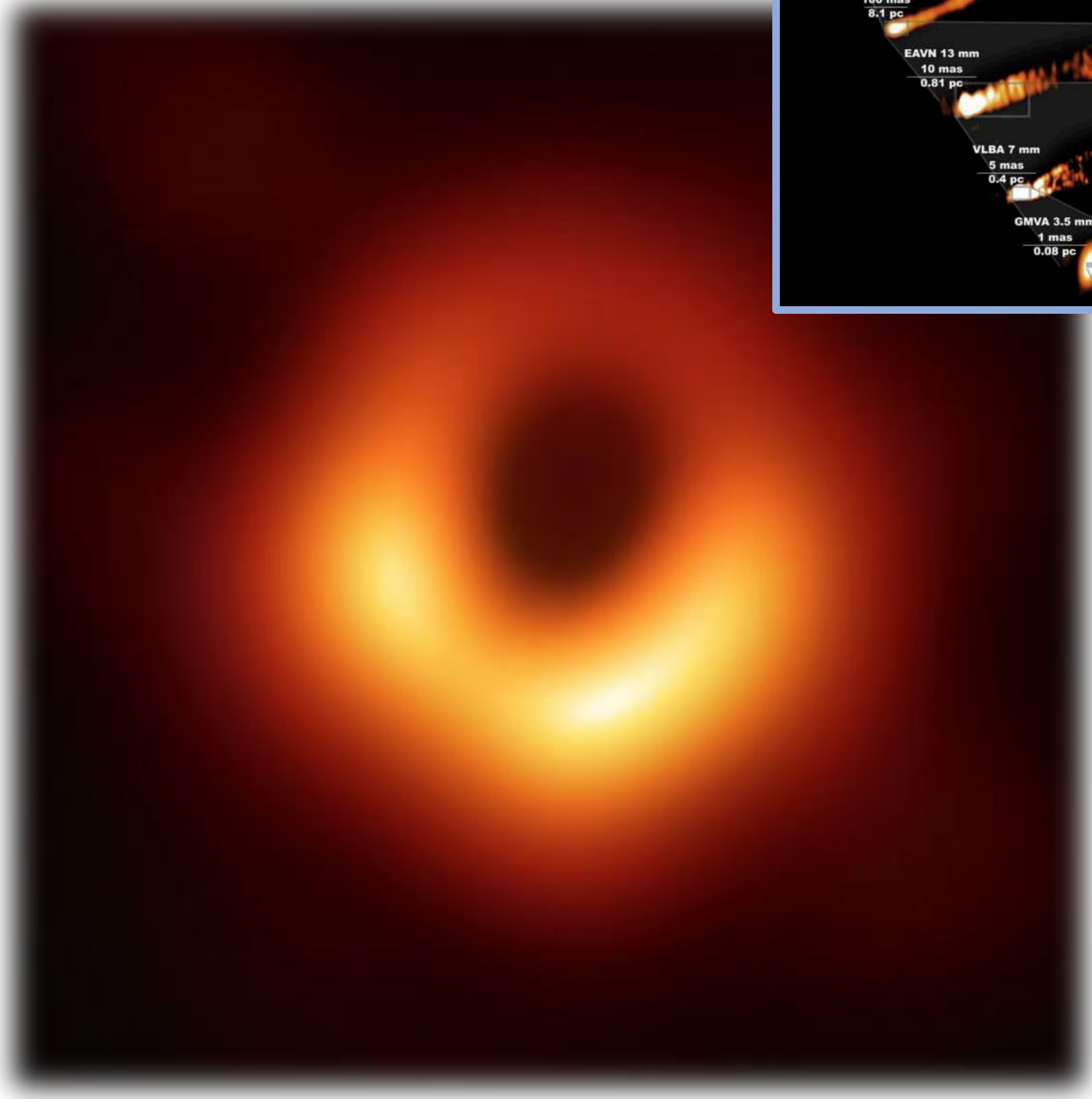

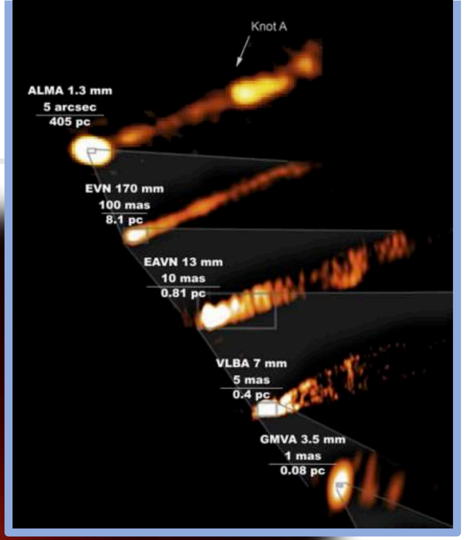


EHTC et al. (2019)

# What do the images tell us?

The primarily azimuthal direction of the polarization pattern tells us about the magnetic field structure

- suggests that there must be a strong poloidal component, and therefore dynamically important magnetic fields

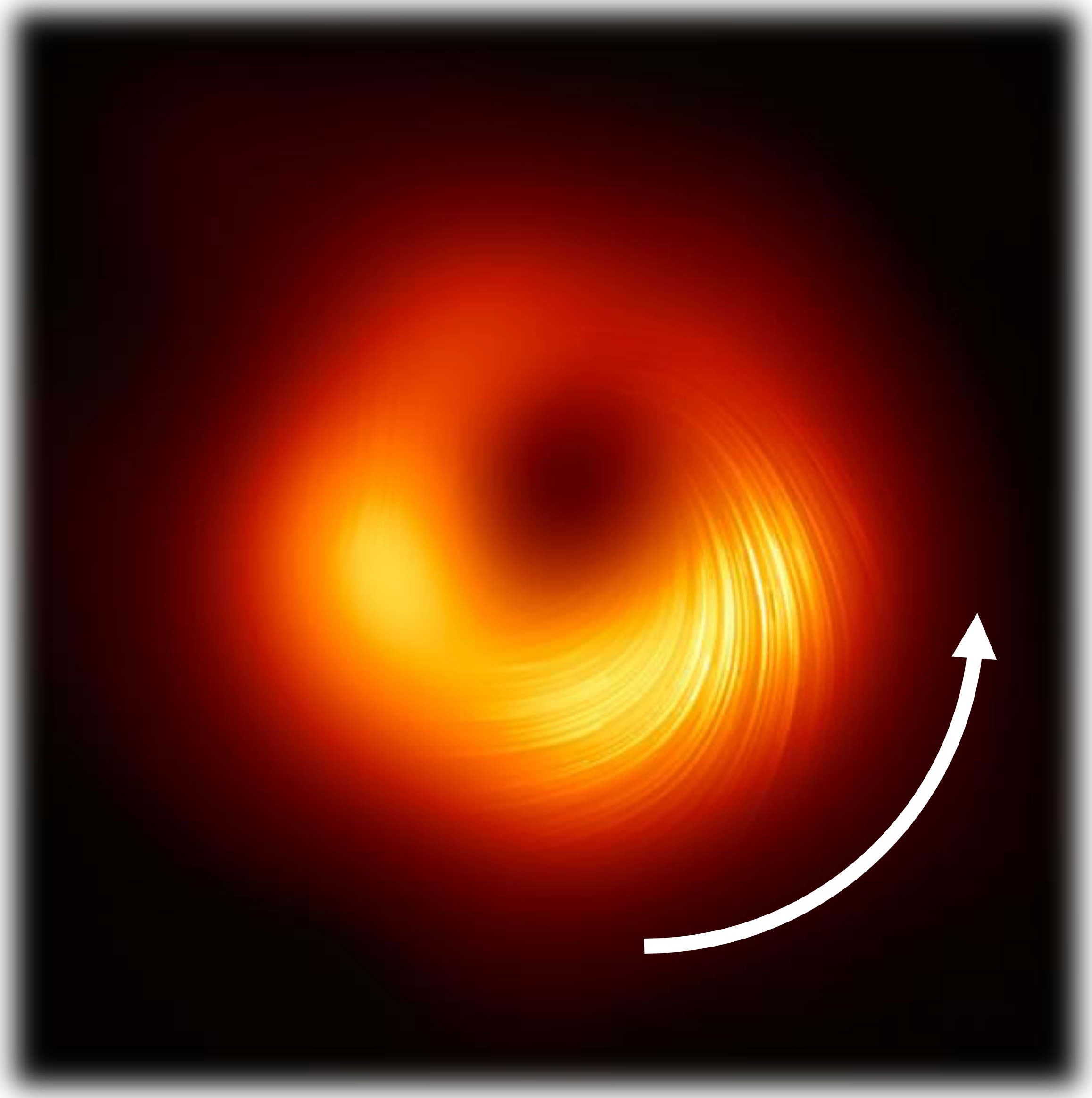

EHTC et al. (2021)

# What do the images tell us?

The primarily azimuthal direction of the polarization pattern tells us about the magnetic field structure

- suggests that there must be a strong poloidal component, and therefore dynamically important magnetic fields

The magnitude of the polarized intensity tells us about the magnitude of internal Faraday rotation

- the magnitude is lower than expected for pure synchrotron, indicating that there is substantial internal Faraday rotation taking place

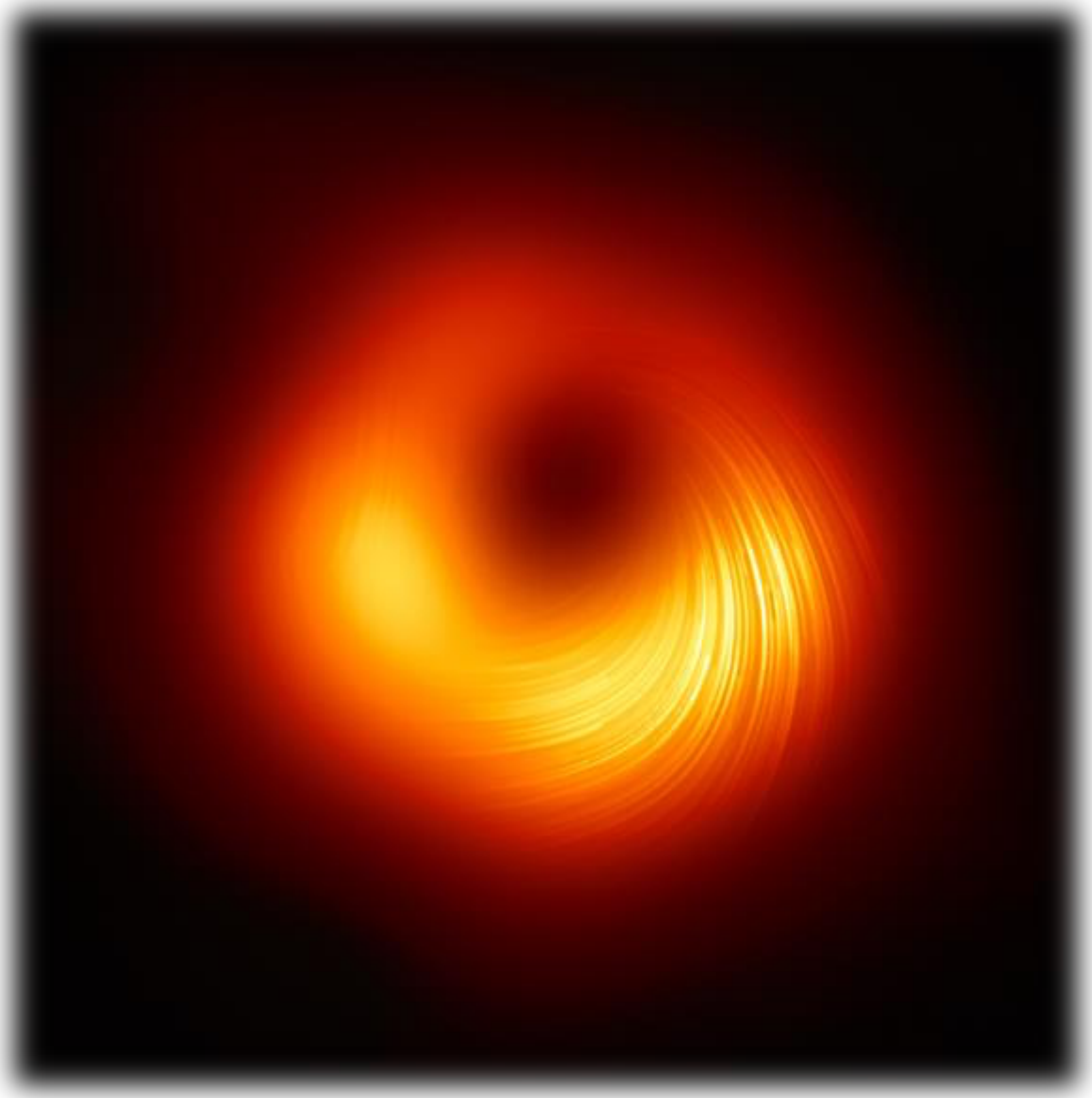

EHTC et al. (2021)

# Looking ahead

# Next-generation radio facilities

The **Square Kilometer Array** (SKA) is a next-generation low-frequency radio telescope being built in Australia and South Africa

- SKA-Low will cover 50 - 350 MHz
- SKA-Mid will cover 350 MHz - 15.4 GHz

Key science goals include:

- early-universe HI mapping
- gravitational tests with pulsars
- discovering FRBs

Total data volumes are expected to be enormous, reaching approximately 700 PB each year

- “big data”

Artist’s impression of SKA-Mid dishes

Image credit: SKAO

# Next-generation radio facilities

The **next-generation Very Large Array** (ngVLA) will be NRAO’s flagship observatory in the next decade

- covering frequencies from 1.2 - 116 GHz

Key science goals include:

- imaging protoplanetary disks
- astrochemistry
- CO measurements across redshift

The ngVLA will have ~10x the collecting area of the VLA, while also spanning baselines as long as those currently covered by the VLBA

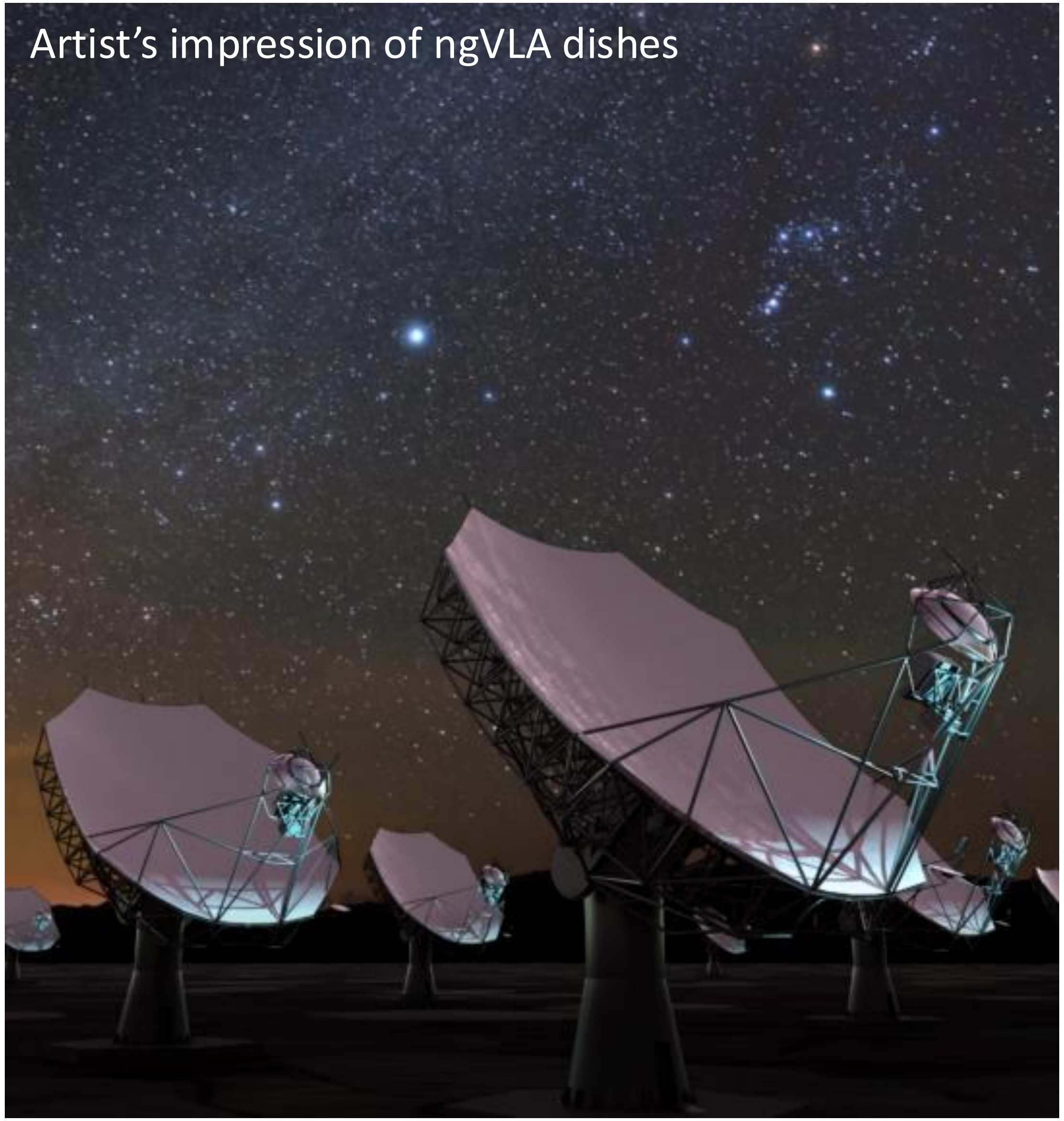

Artist’s impression of ngVLA dishes

Image credit: NRAO

# Next-generation radio facilities

The **next-generation Event Horizon Telescope** (ngEHT) is a project to enhance the EHT
- covering frequencies from 86 - 345 GHz

Key science goals include:
- making movies of near-horizon phenomena
- astrophysical jets
- gravitational physics

The ngEHT will double the sensitivity of the EHT, triple the frequency coverage, and add multiple new stations that collectively expand its short- and long-timescale imaging capabilities

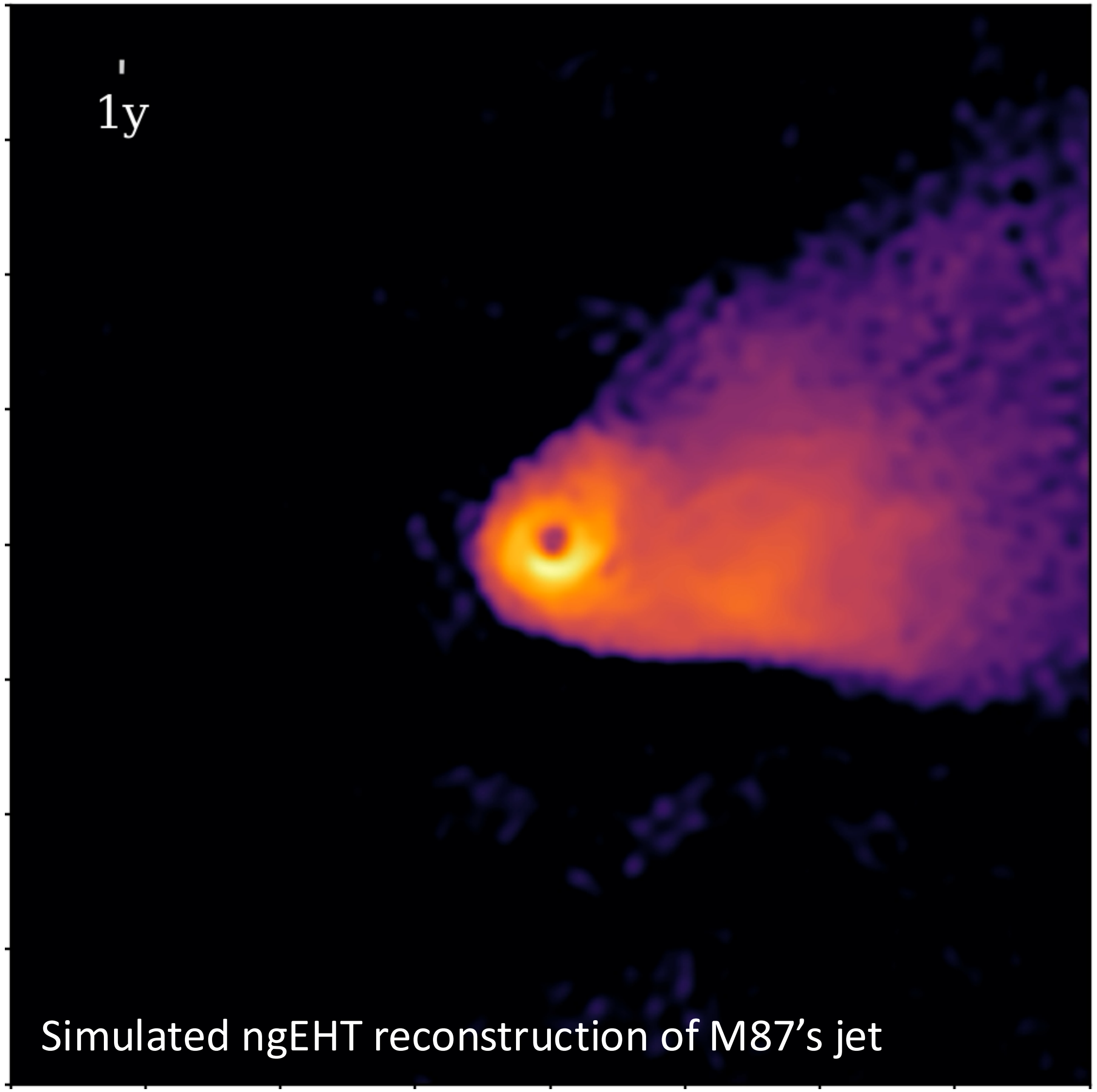

Simulated ngEHT reconstruction of M87's jet

Image credit: ngEHT; L. Blackburn

# Next-generation radio facilities

The **Black Hole Explorer** (BHEX) is a proposed mission to extend the EHT via the addition of a 3.4m radio dish in space

- going out to ~3x Earth-diameter baselines

Key science goals include:

- image the "photon ring" in M87 and Sgr A*
- measure the spin of a black hole
- resolving the shadows of ~dozens of SMBHs

BHEX will achieve the finest angular resolution in the history of astronomy, able to resolve features only a few microarcseconds across

Artist's impression of the BHEX satellite and ground array

Image credit: BHEX; J. Farah

# Summary

$H_2O$ megamasers residing in AGN accretion disks provide unique and valuable tools for measuring the distances to their host galaxies, with implications for cosmology

- The bright, nearby megamaser system in NGC 4258 enables a ~1.5% distance measurement to the host galaxy that is used to anchor distance ladder methods through empirical zero-point calibration

The Megamaser Cosmology Project (MCP) has discovered and determined distances towards megamaser-hosting AGN in the Hubble flow

- constrains $H_0 = 73.9 \pm 3.0$ km/s/Mpc, independent of distance ladders or the CMB

The Event Horizon Telescope was assembled to spatially resolve the event-horizon-scale structure around the largest supermassive black holes in the sky

- it is a VLBI array operating at an observing wavelength of 1.3mm

The EHT produced images of the M87 and Sgr A* black holes, showing the expected gravitational signature of the event horizon on the surrounding emission structure

The next generation of radio astronomical facilities – including the SKA, ngVLA, ngEHT, and BHEX – are being built now